ÉCOLE DE TECHNOLOGIE SUPÉRIEURE
UNIVERSITÉ DU QUÉBEC

A THESIS PRESENTED TO THE
ÉCOLE DE TECHNOLOGIE SUPÉRIEURE

IN FULLFILMENT OF THE THESIS REQUIREMENT
FOR THE DEGREE OF
PHILOSOPHIAE DOCTOR IN ENGINEERING
Ph.D.

BY
PAULO VINICIUS WOLSKI RADTKE

CLASSIFICATION SYSTEMS OPTIMIZATION WITH MULTI-OBJECTIVE EVOLUTIONARY ALGORITHMS

MONTRÉAL, SEPTEMBER 14, 2006

THIS THESIS WAS EVALUATED
BY A COMMITTEE COMPOSED BY :

Mr. Robert Sabourin, thesis supervisor
Département de génie de la production automatisée at École de technologie supérieure

Mr. Tony Wong, thesis co-supervisor
Département de génie de la production automatisée at École de technologie supérieure

Mr. Richard Lepage, president
Département de génie de la production automatisée at École de technologie supérieure

Mr. Mohamed Cheriet, examiner
Département de génie de la production automatisée at École de technologie supérieure

Mr. Marc Parizeau, external examiner
Département de génie électrique et de génie informatique at Université Laval

THIS THESIS WAS DEFENDED IN FRONT OF THE EXAMINATION
COMMITTEE AND THE PUBLIC
ON SEPTEMBER 11, 2006
AT THE ÉCOLE DE TECHNOLOGIE SUPÉRIEURE

CLASSIFICATION SYSTEMS OPTIMIZATION WITH MULTI-OBJECTIVE EVOLUTIONARY ALGORITHMS

Paulo Vinicius Wolski Radtke

ABSTRACT

The optimization of classification systems is a non-trivial task, which is most of the time performed by a human expert. The task usually requires the application of domain knowledge to extract meaningful information for the classification stage. Feature extraction is traditionally a trial and error process, where the expert chooses a set of candidate solutions to investigate their accuracy, and decide if they should be further refined or if a solution is suitable for the classification stage. Once a representation is chosen, its complexity may be reduced through *feature subset selection* (FSS) to reduce classification time. A recent trend is to combine several classifiers into *ensemble of classifiers* (EoC), in order to improve accuracy.

This thesis proposes a feature extraction based approach to optimize classification systems using a *multi-objective genetic algorithm* (MOGA). The approach first optimizes feature sets (representations) using the *Intelligent Feature Extractor* (IFE) methodology, selecting from the resulting set the best representation for a single-classifier based system. After this stage, the selected single classifier can have its complexity reduced through FSS. Another approach is to use the entire IFE result set to optimize an EoC for higher classification accuracy.

Classification systems optimization is challenged by the solution over-fit to the data-set used through the optimization process. This thesis also details a global validation strategy to control over-fit, based on the validation procedure used during classifier training. The global validation strategy is compared to traditional methods with the proposed approach to optimize classification system. Finally, a stopping criterion based on the approximation set improvement is also proposed and tested in the global validation context. The goal is to monitor algorithm improvement and stop the optimization process when it cannot further improve solutions.

An experiment set is performed on isolated handwritten digits with two MOGAs, the *Fast Elitist Non-Dominated Sorting Algorithm* (NSGA-II) and the *Multi-Objective Memetic Algorithm* (MOMA). Both algorithms are compared to verify which is the most appropriate for each optimization stage. Experimental results demonstrate that the approach to optimize classification systems is able to outperform the traditional approach in this problem. Results also confirm both the global validation strategy and the stop criterion. The next experiment set uses the best configuration found with digits to optimize isolated uppercase handwritten letters, demonstrating the approach effectiveness on an unknown problem.

OPTIMISATION DES SYSTÈMES DE CLASSIFICATION AVEC ALGORITHMES ÉVOLUTIFS MULTICRITÈRE

Paulo Vinicius Wolski Radtke

SOMMAIRE

L'optimisation des systèmes de classification est une tâche complexe qui requiert l'intervention d'un spécialiste (expérimentateur). Cette tâche exige une bonne connaissance du domaine d'application afin de réaliser l'extraction de l'information pertinente pour la mise en œuvre du système de classification ou de reconnaissance. L'extraction de caractéristiques est un processus itératif basé sur l'expérience. Normalement plusieurs évaluations de la performance en généralisation du système de reconnaissance, sur une base de données représentative du problème réel, sont requises pour trouver l'espace de représentation adéquat.

Le processus d'extraction de caractéristiques est normalement suivi par une étape de sélection des caractéristiques pertinentes (FSS). L'objectif poursuivi est de réduire la complexité du système de reconnaissance tout en maintenant la performance en généralisation du système. Enfin, si le processus d'extraction de caractéristiques permet la génération de plusieurs représentations du problème, alors il est possible d'obtenir un gain en performance en combinant plusieurs classificateurs basés sur des représentations complémentaires. L'ensemble de classificateurs (EoC) permet éventuellement une meilleure performance en généralisation pour le système de reconnaissance.

Nous proposons dans cette thèse une approche globale pour l'automatisation des tâches d'extraction, de sélection de caractéristiques et de sélection des ensembles de classificateurs basés sur l'optimisation multicritère. L'approche proposée est modulaire et celle-ci permet l'intégration de l'expertise de l'expérimentateur dans le processus d'optimisation. Deux algorithmes génétiques pour l'optimisation multicritère ont été évalués, le *Fast Elitist Non-Dominated sorting Algorithm* (NSGA-II) et le *Multi-Objective Memetic Algorithm* (MOMA). Les algorithmes d'optimisation ont été validés sur un problème difficile, soit la reconnaissance de chiffres manuscrits isolés tirés de la base NIST SD19. Ensuite, notre méthode a été utilisée une seule fois sur un problème de reconnaissance de lettres manuscrites, un problème de reconnaissance provenant du même domaine, pour lequel nous n'avons pas développé une grande expertise. Les résultats expérimentaux sont concluants et ceux-ci ont permis de démontrer que la performance obtenue dépasse celle de l'expérimentateur.

Finalement, une contribution très importante de cette thèse réside dans la mise au point d'une méthode qui permet de visualiser et de contrôler le sur-apprentissage relié aux algorithmes génétiques utilisés pour l'optimisation des systèmes de reconnaissance. Les résultats expérimentaux révèlent que tous les problèmes d'optimisation etudiés (extraction et sélection de caractéristiques de même que la sélection de classificateurs) souffrent éventuellement du problème de sur-apprentissage. À ce jour, cet aspect n'a pas été traité de façon satisfaisante dans la littérature et nous avons proposé une solution efficace pour contribuer à la solution de ce problème d'apprentissage.

OPTIMISATION DES SYSTÈMES DE CLASSIFICATION AVEC ALGORITHMES ÉVOLUTIFS MULTICRITÈRE

Paulo Vinicius Wolski Radtke

RÉSUMÉ

Le processus d'extraction de caractéristiques est un processus qui relève de la science de l'expérimentateur. C'est un processus très coûteux et qui repose également sur l'habileté de l'expérimentateur, à la fois sur son expertise et sur sa connaissance du domaine d'application. Nous avons abordé le processus d'extraction de caractéristiques comme un problème d'optimisation multicritère (MOOP). La méthode proposée est modulaire, ce qui permet de diviser le problème d'optimisation des systèmes de reconnaissance en trois sous-problèmes: l'extraction de caractéristiques, la sélection de caractéristiques pertinentes et enfin la sélection des classificateurs dans les ensembles de classificateurs (EoC).

L'intérêt des algorithmes évolutionnaires pour l'optimisation des systèmes de reconnaissance de formes est qu'ils représentent des algorithmes de recherche stochastiques basés sur l'évolution d'une population de solutions (*eg* de représentations, de classificateurs, etc.). Un avantage immédiat d'avoir une population de solutions est de considérer les *N* meilleures solutions pour la mise en œuvre du système de reconnaissance. Ce type d'approche est habituellement plus robuste et permet une meilleure performance en généralisation sur des données qui n'ont pas été utilisées lors de la conception du système. De plus, les algorithmes évolutionnaires utilisés pour l'optimisation ne requièrent pas une fonction objectif dérivable et la population de solutions permet de s'affranchir des minima locaux.

Un autre avantage des algorithmes d'optimisation multicritère réside dans la facilité d'adaptation de ces algorithmes pour une gamme très grande de problèmes d'optimisation différents. En effet, l'expérimentateur n'est plus obligé de choisir a priori la valeur des coefficients de pondération des objectifs et peut attendre à la fin du processus d'optimisation pour effectuer un choix définitif à partir de l'analyse des solutions optimales qui sont inclus dans *Front de Pareto* (FP). Cette approche réduit au minimum l'intervention humaine dans le processus d'optimisation.

L'objectif principal de cette thèse est de formaliser les processus d'extraction, de sélection de caractéristiques et de génération d'ensembles de classificateurs comme un problème d'optimisation à plusieurs niveaux. Une approche modulaire a donc été proposée où un algorithme d'optimisation multicritère a été utilisé pour résoudre chaque sous-problème.

Le premier chapitre présente l'état de l'art dans les domaines qui touchent de près l'élaboration de cette thèse. En effet, une des difficultés de ce travail de recherche est qu'il se situe à la frontière de plusieurs domaines de recherche : la reconnaissance de formes en général et la reconnaissance de chiffres manuscrits en particulier, les algorithmes d'optimisation évolutionnaires multicritère, l'extraction de caractéristiques pertinentes, la sélection de caractéristiques et enfin la sélection des ensembles de classificateurs.

La méthode globale retenue pour l'optimisation des systèmes de classification est exposée au chapitre deux. L'extraction des caractéristiques repose sur une technique de zonage souvent utilisée dans le domaine de la reconnaissance de caractères manuscrits isolés. Deux opérateurs de division de l'image en différentes configurations de zones sont proposés. Ensuite le lien entre le processus d'extraction et ceux associés à la sélection des caractéristiques et des classificateurs est ensuite présenté.

Une contribution importante est discutée au chapitre trois. Une analyse détaillée du comportement de l'algorithme NSGA-II appliquée à l'optimisation du processus d'extraction de caractéristiques a permis de soulever les lacunes de ce type d'algorithme utilisé pour l'optimisation des systèmes de reconnaissance. Afin de combler ces lacunes, nous avons proposé un algorithme mieux adapté pour optimiser les machines d'apprentissage, soit le *Multi-Objective Memetic Algorithm* (MOMA). Celui-ci combine un MOGA traditionnel avec un algorithme de recherche local pour augmenter la diversité des solutions dans la population. Ce type de méthodes hybrides utilisées pour l'optimisation multicritère permet aux algorithmes évolutionnaires traditionnels de s'affranchir du problème chronique de la convergence prématurée en favorisant à la fois l'exploration et l'exploitation de nouvelles solutions.

Le chapitre quatre propose une méthode innovante pour s'affranchir du problème très important du sur-apprentissage. En effet, il n'y a pas de travaux dans la littérature qui portent spécifiquement sur le problème du sur-apprentissage relié aux algorithmes évolutionnaires utilisés pour l'optimisation de machines d'apprentissage (*eg* des systèmes de classification). Nous avons proposé une méthode de validation globale basée sur un mécanisme d'archivage des meilleures solutions qui permet à tous les algorithmes évolutionnaires de contrôler le sur-apprentissage. Nous avons validé les algorithmes NSGA-II et MOMA sur les problèmes d'extraction de caractéristiques (IFE), de sélection de caractéristiques (FSS) et sur celui de la sélection de classificateurs (EoC) et le tout sur deux problèmes importants, soit la reconnaissance de chiffres manuscrits isolés et sur celui de la reconnaissance des lettres majuscules. Les données proviennent d'une base de données standard – NIST SD19.

Afin de réduire le coût computationnel de la méthode proposée, nous avons présenté au Chapitre 5 un critère d'arrêt basé sur l'évolution des meilleures solutions (le front de Pareto dans le cas du NSGA-II et les solutions localisées à la frontière de l'espace de recherche dans le cas du MOMA) trouvées par les algorithmes évolutionnaires durant l'évolution des populations sur plusieurs générations. Le critère proposé permet d'assurer à l'expérimentateur que les paramètres des algorithmes évolutionnaires sont bien calibrés, ce qui permet à l'algorithme de produire des solutions de meilleure qualité, et également de diminuer de façon substantielle le coût computationnel des processus IFE, FSS et EoC.

Les processus IFE, FSS et EoC ont été évalués au chapitre six sur le problème de la reconnaissance de chiffres manuscrits. Les performances obtenues permettent de confirmer la supériorité de l'approche proposée par rapport à la méthodologie traditionnelle qui repose uniquement sur l'expertise de l'expérimentateur. De plus, nous avons confirmé la nécessité de contrôler le sur-apprentissage pour l'optimisation des trois sous-problèmes IFE, FSS et EoC.

Enfin, nous avons utilisé notre méthode d'optimisation pour l'optimisation d'un système de reconnaissance de lettres manuscrites. En effet, notre hypothèse de départ était de mettre en œuvre une méthodologie qui permet à l'expert expérimentateur de procéder à moindre coût à l'extraction de caractéristiques pertinentes sur un autre problème de reconnaissance pour lequel il n'a pas un grand niveau d'expertise. Notre méthode est modulaire et celle-ci permet à l'expérimentateur d'injecter sa connaissance qu'il a du domaine (ici, la reconnaissance de caractères manuscrits isolés). Les résultats obtenus sont très prometteurs et les performances en généralisation des représentations optimisées par les processus IFE, FSS et EoC sont meilleures que la performance du système de référence conçu par l'expérimentateur.

En résumé, nous avons contribué dans cette thèse à:

- Proposer une approche générique pour optimiser les systèmes de reconnaissance de caractères manuscrits isolés.
- Proposer un MOGA adapté au problème de l'optimisation des systèmes de classification.
- Proposer plusieurs stratégies de validation afin d'éviter le sur-apprentissage associé au processus d'optimisation de systèmes de classification avec MOGAs.
- Proposer et évaluer un critère d'arrêt adapté aux MOGAs. Ce critère d'arrêt est basé sur la convergence des meilleures solutions et il est adapté à la stratégie de validation globale (habituellement, l'exécution des MOGAs est limitée seulement par un nombre maximum de génération et ignore la convergence des solutions pour définir un critère d'arrêt prématuré).
- Évaluer la performance des algorithmes MOGAs dans le contexte de l'optimisation des systèmes de classification.

ACKNOWLEDGMENTS

Writing thesis acknowledgements is a multi-objective NP hard problem. Regardless of how hard we try to solve it, we are unlikely to obtain the global optimum and eventually forget someone in the process. Thus, I would like to say thanks to everyone that contributed directly or indirectly to this thesis. My gratitude to you all cannot be expressed with plain words.

First, I would like to thank my thesis supervisors, Dr. Robert Sabourin and Dr. Tony Wong. I am indebted to their guidance, patience and support in this work. For their comments and invaluable feedback, my thanks to the jury members, Richard Lepage, Mohamed Cheriet and Marc Parizeau.

I also have to thank my parents, Paulo de F. Radtke and Ana R. W. Radtke, for supporting me the last four years, especially through some difficult moments.

I would like to thank the researchers at the *Laboratoire de Vision, d'Imagerie et d'Intelligence Artificielle* during the period I have stayed in Montreal. The laboratory provided me a great environment to work and collaborate with friends. In this regard, I would like to thank two old friends, Luiz Oliveira and Marisa Morita, who helped me a lot when I moved to Montreal and when starting this work.

Special thanks also go to Eulanda M. dos Santos, Guillaume Tremblay, Albert Ko, Jonathan Milgram, Frédéric Grandidier, Youssef Fataicha, Alessandro Koerich, Luis da Costa and Marcelo Kapp. I will not forget your friendship in the short time we have worked together.

I also have to thank the *Pontifical Catholic University of Parana* and the *CAPES - Brazilian Government* (scholarship grant BEX 2234-03/4) for their financial support. This thesis would not have been possible without their support.

Above all, I have to express my sincere gratitude to Melissa Murillo Radtke, my best friend and wife. Gratitude for supporting me since I was a master's student and for enduring with me all the hardships. Above all, for giving me our greatest joy, our son Angelo. I dedicate to them this thesis.

TABLE OF CONTENTS

Page

LIST OF TABLES

LIST OF FIGURES

Page

LIST OF ALGORITHMS

LIST OF ABREVIATIONS AND NOTATIONS

BAB	Branch and bound
DAR	Document analysis recognition
EoC	Ensemble of classifiers
FSS	Feature subset selection
GA	Genetic algorithm
ICR	Intelligent character recognition
IFE	Intelligent feature extraction
LS	Local search algorithm
MA	Memetic algorithm
MLP	Multi-layer Perceptron classifier
MOEA	Multi-objective evolutionary algorithm
MOGA	Multi-objective genetic algorithm
MOMA	Multi-objective memetic algorithm
MOOP	Multi-objective optimization problem
NIST	National Institute of Standards and Technology
NSGA-II	Fast elitist non-dominated sorting genetic algorithm
PD	Projection distance classifier
PR	Pattern recognition
RRT	Record-to-record traveling algorithm
SD	Special database
SFFS	Sequential forward floating search
SFS	Sequential forward search
SPEA2	The Strength Pareto Evolutionary Algorithm 2
SVM	Support vector machines classifier
VEGA	Vector evaluated genetic algorithm
α	Confidence level used in the multiple-comparison test
a	The deviation used by the RRT algorithm

$A(S^l,C)$	The subset of solutions in C that is admissible in S^l
$B(S^l)$	Solution x^i in S^l with the best o_2 value
cg	The coarse grain FSS operator binary vector
$\mathrm{cov}erage$	The coverage function
D	A set of dominated solutions in the NSGA-II auxiliary archive update procedure
d	The divider zoning operator binary vector or a dominated solution in the procedure to update the NSGA-II auxiliary archive
E	The EoC methodology binary vector
F	A feature set in the IFE or the sorted combined population in NSGA-II
f	A single feature (IFE)
fg	The fine grain FSS operator binary vector
g_1	The first group of dividers in the dividers zoning operator
g_2	The second group of dividers in the dividers zoning operator
i	An index or a MOOP candidate solution
ir_t	MOGA average improvement rate at generation t based on improvements in the last w generations
I	An image
$improvement$	The improvement function
j	An index or a MOOP candidate solution
K	A classifier set trained from RS_{IFE}
K^i	The i^{th} classifier in K
k	The number of selected eigenvectors in Ψ_i
L	Binary string length
M	MOMA's mating pool
m	Size of population P
mg	Maximum number of generations the MOGA will run

min_{ir}	Minimum improvement rate threshold
max_{S^l}	Maximum number of solutions stored in each slot S^l
μ_i	The mean vector of the learning samples ω_i
n	Number of neighbors explored by the RRT algorithm
NI	Number of iterations the RRT algorithm searches for neighbor solutions
o_1	MOMA objective function one (integer function)
o_2	MOMA objective function two (optimized for each o_1 value)
ω_i	The observations belonging to class i in the training set
P	The genetic algorithm population
P'	The Pareto-front associated to P
$\hat{P}(C_i \mid x)$	The posterior probability that observation x belongs to class C_i
p	The classifier number in K and the binary string E length in the EoC optimization, or a solution belonging to population P with MOMA
p'	Neighbor to solution p
p_c	Crossover probability
$P_i(x)$	The unknown observation i projection on hyper plane P_i
p_m	Mutation probability
P_S	The decision frontier of population P
Ψ_i	The first k eigenvectors of the covariance matrix of ω_i
R^i	i^{th} frontier rank of population P
Q	The offspring population in the NSGA-II
R_t	The combined population in the NSGA-II
RS_{CG}	The solution set optimized by the coarse grain FSS
RS_{FG}	The solution set optimized by the fine grain FSS
RS_{IFE}	The solution set optimized by the IFE
S	The auxiliary archive
S^l	Slot in S related to o_1 value l

SI	The single best classifier optimized by the IFE
SC	The single classifier optimized by the coarse grain FSS
SE	The EoC optimized by the EoC methodology
SE'	The EoC optimized by the EoC methodology with NSGA-II using RS_{IFE} optimized by MOMA
SF	The single classifier optimized by the fine grain FSS
t	Current iteration/generation during classifier training and genetic optimization
$t_{\max}$	Maximum number of classifier training iterations
t_{stop}	Iteration the classifier training or genetic optimization stops
w	The generation count window used to verify the improvement rate ir_t
$W\left(S^l\right)$	Solution x^i in S^l with the worst o_2 value
x	An unknown observation or a candidate solution to a MOOP
y	A candidate solution to a MOOP
Z	A zoning strategy
z	One zone belonging to a zoning strategy

INTRODUCTION

Multi-objective optimization evolutionary algorithms (MOEAs) are known as powerful search methods for real world optimization problems. One class of MOEAs is target of interest among researchers with motivating results, the *multi-objective optimization genetic algorithms* (MOGAs), based on the working principles of *genetic algorithms* (GAs) [1]. Unlike GAs, which provide a single best solution based on a single objective, MOGAs optimize a solution set regarding the possible trade-offs in the multiple objectives associated to the optimization problem.

One real world optimization problem of interest is found in the *pattern recognition* (PR) domain, which is to automatically determine the representation (feature set) of isolated handwritten characters for classification. This problem comes from the need to automatically process handwritten documents such as forms and bank checks. In order to handle, store and retrieve information, a significant amount of documents is processed daily by computers. In most cases, the information is still acquired by means of expensive human labor, reading and typing the information from handwritten documents to its digital representation. To automate this process and reduce costs and time, the human element can be replaced with an *intelligent character recognizer* (ICR).

ICR combines two research fields, PR and *document analysis recognition* (DAR). Many classification techniques have been proposed over the past years, but the challenge remains to approach the human performance in terms of understanding documents. One aspect embedded in ICR systems is the recognition of isolated handwritten symbols, which is directly related to PR. An isolated handwritten symbol is considered as a handwritten numeral or letter (uppercase or lowercase). It can be said that there are three ways to improve recognition rates on a classification system. The first is to use a discriminative classifier that produces lower error rates than other less performing classifiers. Two classifiers that are well known for their high accuracy are the *Multi-Layer Perceptron* (MLP) neural network [2] and the *Support Vector Machines* (SVM)

[3, 4] classifiers. However, the classifier is limited by the feature set quality, and means to improve accuracy with the same classifier are necessary. The second way to improve classification systems is by defining a discriminative feature set. A discriminative feature set depends on the type of symbols classified. Therefore, a good feature set is problem dependant. The third improvement considered is to aggregate many classifiers to produce better results as an *ensemble of classifiers* (EoC) [5, 6]. The feature extraction and EoC optimization processes can be modeled as an evolutionary optimization problem.

Classification system optimization using evolutionary algorithms is a trend observed recently in the literature, covering feature extraction [7, 8], *feature subset selection* (FSS) [9, 10] and EoC optimization [11, 12, 13, 14, 15]. A population-based approach is preferable to traditional methods based on a single solution for its higher degree of diversity to avoid local optimal solutions. Modeling the problem as a *multi-objective optimization problem* (MOOP) is the most interesting approach, as it eliminates the need for the human expert to choose weighted values for each optimization objective, presenting him instead a choice among various trade-offs for practical applications.

Problem Statement

The task to define the representation of handwritten characters is usually done by a human expert with domain specific knowledge. The representation is determined based on a trial and error process that consumes time and is not guaranteed to produce good results. As the representation depends on the problem domain, it may not be used in other applications if the classification problem changes. Not only the domain change impacts the classification system, but the writing style of a particular region or country as well. Figure 1.a presents digits from the NIST SD-19 database [16], which has north-american writing style, whereas Fig 1.b has handwritten digits from a of Brazilian bank

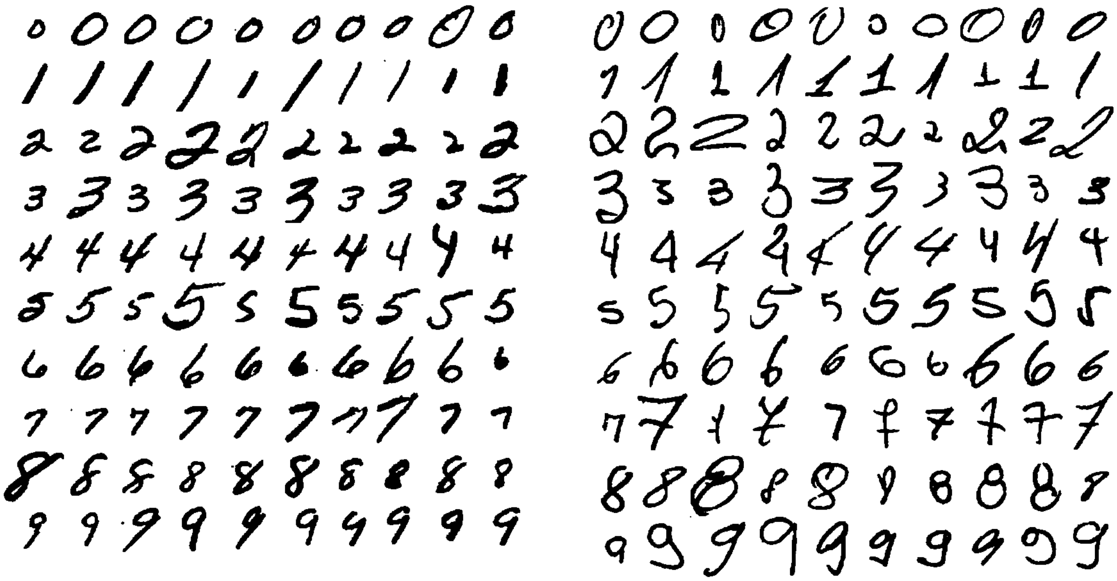

Figure 1 Handwritten digits, NIST SD-19 (a) and Brazilian checks (b) – differences in handwritten styles require different representations for accurate classification

checks database. These issues indicate the need to adapt efficiently pattern recognition systems to several situations and minimize human intervention.

The expert will usually create a set of possible representations based on his knowledge on the problem and choose the best one. It is difficult for a human expert to evaluate a set of possible solutions to create a new set of improved solutions based on previous iterations. On the other hand, evolutionary algorithms are suitable for this kind of problem, as they systematically evolve solutions from an initial set, searching for building blocks that will improve solution quality successively through generations.

When defining a representation, the human expert expects that at least two objectives are attained, high discriminative power and reduced dimensionality. The first is directly related to the recognition rate of a classifier. The second is related to the representation's generalization power, and is related to the dimensionality curse. The power of a classifier comes from the generalization of models to classify unknown observations, but the higher the dimensionality, the less general the models become. Also, smaller representations are faster to extract features and for classification.

The feature extraction problem can be modeled as a MOOP. The representation's discriminative power and dimensionality are translated as objective functions to guide a MOGA to determine automatically an accurate representation to classify isolated handwritten symbols. Two approaches can be used to further improve classification accuracy. The best representation may be submitted to FSS to reduce its cardinality for faster classification, and the resulting set from the feature extraction stage can be used to optimize an EoC for improved accuracy.

Classification systems are based, as the name implies, on classifiers that are responsible for classifying observations for information post-processing. Some classifiers require parameter configuration, and a problem has been that their training procedure is plagued by the over-fitting to the *training* data set – the actual observations used to train the classifier. In this situation, the classifier memorizes the *training* data set, and its power to generalize to unknown observations is poor. This effect is usually avoided with a validation approach based on observations unknown to the training procedure.

Classification accuracy is traditionally used as one objective function when modeling a classification system as a MOOP. The accuracy of the wrapped classifier is evaluated on an *optimization* data set (actual observations), and the optimization algorithm will put pressure on the most accurate solutions according to the objective function trade-offs. This approach transposes the over-fit phenomenon to the optimization process, and the resulting solutions will be specialized to predict the *optimization* data set. Oliveira *et al.* observed the effect in [10] with the feature subset selection problem. Classifier performance on unknown observations is different from the performance observed during the optimization process and a mechanism to avoid this effect during the optimization process is necessary.

Goals of the Research and Contributions

The primary goal is to define a feature extraction based approach to optimize classification systems using MOGAs. This methodology is modeled as a multi-objective optimization problem, thus the result will be a solution set representing the best found optimization objectives trade-offs. The first approach is to choose the most accurate representation, and apply this representation on a handwritten recognition system. At this stage, two different approaches to refine classification systems are possible. First, the selected solution for a single classifier system may have its feature set dimensionality reduced through FSS. The second approach is to use the result set to create an ensemble of classifiers. The block-diagram overview of this system is presented in Fig. 2.

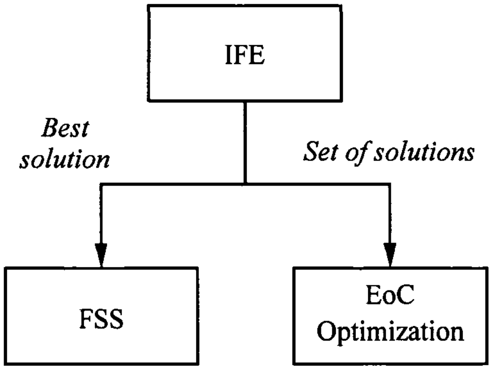

Figure 2 Classification system optimization approach

Part of the classification system optimization approach was the subject of published works in the literature. The *Intelligent Feature Extraction* (IFE) methodology, introduced in [17, 18], is responsible for the feature extraction stage, modeling the human expert knowledge to optimize representations. The EoC optimization employs the solution set produced by the IFE to optimize the classifiers aggregated on an EoC [19, 20].

The second goal is to define a MOGA adapted to specific needs of this class of MOOPs. The most relevant need is the representation diversity provided by the IFE, which impacts directly in the EoC optimization stage. The *Multi-Objective Memetic Algorithm* (MOMA), also introduced in [18], provides means to optimize a diverse set of solutions with the IFE methodology.

The third goal is to propose a strategy to control the over-fit observed when optimizing classification systems. Traditional wrapper-based optimization of classification systems will over-fit candidate solutions to the data set used to optimize solutions, thus a methodology to reduce this effect is mandatory for the proposed approach to optimize classification systems. The *global validation* discussed in this thesis was also presented in [21].

Finally, the last goal is to formulate a stopping criterion for MOGAs, adapted to the proposed approach to optimize classification system and the over-fit control method. Usually, the execution of MOGAs is limited only by a maximum number of generations and ignores the approximation set improvement. In this context, solutions will over-fit and solutions with good generalization power are found in earlier generations. Therefore, the MOGA may be stopped before the maximum set generation number without loss of solution quality. To this effect, a stopping criterion is formulated based on the approximation set improvement rate.

Thus, the contributions of this thesis are fourfold: (1) to propose an approach to optimize classification systems; (2) propose a MOGA adapted to the approach's objective function space; (3) to discuss and compare validation strategies in order to avoid the over-fit associated to the optimization process on MOGAs; and (4) to detail and evaluate a stopping criterion for MOGAs based on the approximation set improvement rate and compatible to the global validation strategy discussed.

Organization

This thesis is organized as follows. First it presents the state-of-the-art in handwritten recognition and MOEAs in Chapter 1. Then it details in Chapter 2 the classification system optimization approach, discussing the IFE, FSS and EoC optimization methodologies. Next, Chapter 3 proposes and details MOMA, a hybrid optimization method adapted to the IFE methodology. Chapter 4 analyzes the over-fit issue observed when optimizing classification systems to propose a strategy to control it. Finally, Chapter 5 presents the stopping criterion for MOGAs and discusses its adaptation to actual MOGAs.

The next two chapters are used to experiment the methodology with actual data-sets. In Chapter 6 a set of experiments is performed with isolated handwritten digits to test the approach to optimize classification systems, comparing both IFE zoning operators (defined in Chapter 2), and verifying the over-fit control strategy and the stopping criterion. These experiments are also used to compare MOGAs performance (MOMA and NSGA-II) and determine which algorithm is more suitable for each stage in the approach to optimize classification systems. These results will be used to determine the best strategy to optimize classifications systems. This strategy is then used to optimize a classification system for isolated handwritten upper-case letters in Chapter 7, concluding the experiments. Finally, the last section discusses the results and goals attained with this thesis.

CHAPTER 1

STATE OF THE ART

This chapter presents the state of the art in the two main research domains discussed in this thesis, handwritten recognition and evolutionary algorithms. Whereas this chapter is divided in two different sections, both sections are equally important, as this thesis focus is the MOGA based optimization of classification systems.

1.1 State of the Art in Handwritting Recognition

This section presents an overview of PR techniques related to this proposition. It first discusses how to represent handwritten characters, and how to improve this representation, so it can be used in the recognition task. Then it presents techniques to reduce the representation size, trying to improve the accuracy of recognition and reduce classification time. The last section discusses the use of ensemble of classifiers.

1.1.1 Character Representation

The main issue in pattern recognition is to compare observations in order to classify models and determine their similarity. The classifier role in a pattern recognition system is to compare unknown observations and measure their similarity to models of known classes. The similarity measure may be a distance, cost or a probability, which is used to decide to which known class the observation belongs to. However, image pixel information has drawbacks and they are not usually applied directly on classifiers. The first aspect is related to the *dimensionality curse*, the higher the dimensionality of the information used in the classifier for learning, the less general the models produced are. The second aspect is that the information in the image is vulnerable to rotation, translation and size changes. This poses a significant problem for handwritten

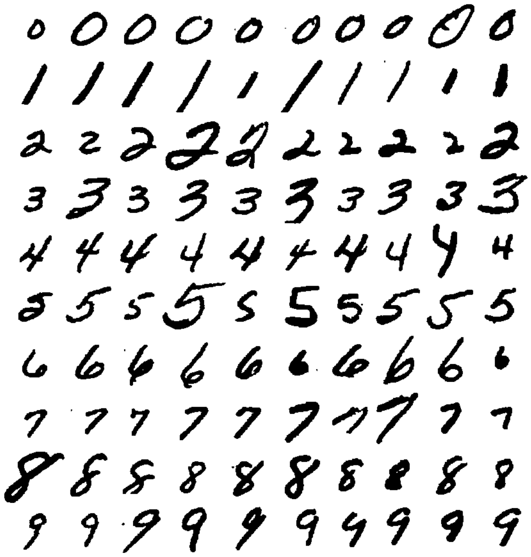

Figure 3 Handwritten digits extracted from NIST-SD19

characters, as humans do not write the same way and it is expected that characters are written in different proportions and inclinations. Figure 3 depicts these problems on actual observations extracted from the NIST-SD19 database.

To overcome these problems we apply mathematical operations to transform the pixel information in the image to other type of information. This process is called *feature extraction.* Features can be extracted in different ways, Trier *et al.* presented in [22] a survey on many feature extraction techniques. Bailey and Srinath presented in [23] a feature extraction methodology based on orthogonal moments, applying it on handwritten digits. Gader discussed in [24] a methodology to extract features using zoning, experimenting also on handwritten digits. Oh and Suen proposed in [25] features based on distance measurements, applying them on handwritten characters. Heutte *et al.* discussed in [26] a feature set based on statistical and structural features, aiming at handwritten characters recognition.

Features may be divided in two groups of interest, *global* and *local* features. Global features are extracted taking into account the whole image, like invariant moments, projections and profiles. Local features are extracted from portions of the image, allowing classifiers to take into account complementary points of view of the symbol structure, such as intersections, concavities, contours, etc. We have special interest in local feature extraction operators, which are suitable for representations involving zoning that place emphasis on specific *foci* of attention.

1.1.2 Zoning

Di Lecce cited in [27] that researchers focused their efforts on the analysis of local characteristics to improve classifier performance with handwritten characters. Figure 3 depicts a typical case on the variability of handwriting between many human writers. Not all digits are written the same way, but they all share structural components that allow human readers to distinguish the symbols. These structural components are placed in specific regions of the image representing the symbol. Such specific regions, the *zones*, are considered as *retinas* around a *focus of attention*, as described by Sabourin *et al.* in [28, 29] and depicted in Fig. 4, where an image is divided in 6 equally sized zones.

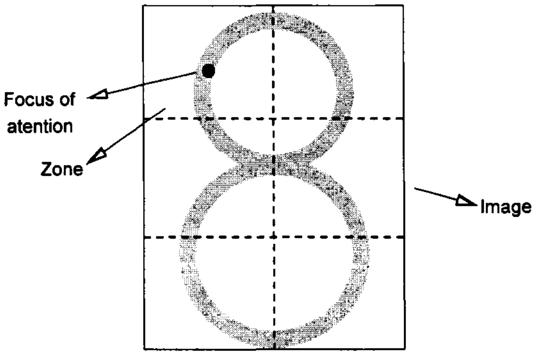

Figure 4 Zoning example

Zoning is defined as the technique to improve symbols recognition through the analysis of local information inside the zones. The difficulty with this technique is that the zoning depends on the recognition problem and relies on human expertise to be defined. Figure 5 depicts three different zoning strategies used in the context of isolated handwritten characters. Oliveira in [30] used the zoning strategy in Fig. 5.a to extract features for handwritten digit recognition, experimenting with the NIST SD-19 database. Shridhar in [31] used the strategy in Fig. 5.b to recognize isolated handwritten characters on a heck reading application. Li and Suen in [32] discussed the impact of *missing parts*, zones where no features are extracted at all, for the recognition of alphanumeric symbols. One of the configurations considered is depicted in Fig. 5.c, where the *X* marked zones are *blind zones*, where no features are extracted. The missing parts might improve character recognition and should be considered for the FSS operation.

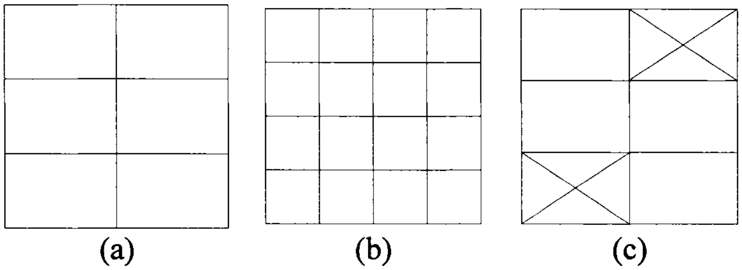

Figure 5 Zoning strategies – strategy (*c*) has *missing parts*, zones that have no feature extracted, marked with an X

The three different zoning strategies in Fig. 5 show that for different problems, different zoning strategies are needed. This indicates the need of efficient and automatic means to determine zoning strategies to adapt pattern recognition systems to different problems. Besides human expertise, some techniques have been proposed in the literature to design zoning strategies automatically. Di Lecce *et al.* presented in [27] a methodology for zoning design on the field of handwritten numerical recognition. Teredesai *et al.* presented in [8] a methodology using genetic programming to define an hierarchical representation based on image partitioning. Lemieux *et al.* describe in [7] a methodology to determine zoning using genetic programming for online recognition of handwritten digits.

1.1.3 Isolated Character Recognition

Methodologies to define the representation of symbols convert raw image data to information that can be used for the recognition task. This task is performed by a classifier, which defines a methodology to learn models and compare them to observations, attempting to classify them. Koerich noted in [33] that neural networks classifiers have been used in many works in the context of character recognition. Gader used in [24] a multi layer Perceptron (MLP) classifier to recognize handwritten characters. However, other classifiers, like support vector machines (SVM), nearest neighbour (NN) and others can be used for this class of problems. Liu *et al.* compared in [34] the performance of many classifiers in the context of handwritten recognition, and it is clear in this work that MLP classifiers are accurate and fast for handwritten recognition, provided there are enough samples to train the network.

1.1.4 Feature Subset Selection

Feature subset selection (FSS) aims to optimize the classification process, eliminating irrelevant features from the representation. Three aspects are changed by FSS. It first reduces the cost to extract features from unknown observations during classification. It also may improve classification accuracy, as correlated features may be eliminated. This is supported by the generalization power of smaller feature sets. The third aspect is that by reducing feature number we have a higher reliability on performance estimates.

Kudo and Sklansky compared in [35] many techniques for FSS, including sequential forward selection (SFS) [36], sequential forward floating selection (SFFS) [37], branch and bound (BAB) [38] and genetic algorithms [39]. This work indicates that GA based techniques are suitable for FSS where a large number of features is considered, where large is a value higher than 50, and the algorithm aims to search for a compromise between dimensionality and classification accuracy. This statement is supported by the search mechanism inherent to GAs, which improves population by searching for good building blocks in an efficient way. Also, GAs can deal with problems with non-monotonic functions to evaluate the feature set quality, as they are based on a random approach for initialization and the building blocks help to avoid local optimal solutions.

If one compares the GA building blocks search mechanism with a sequential algorithm, such as SFS, this GA property for FSS becomes clear. A sequential method usually treats features one by one, like SFS that searches the feature that will better improve the discriminating power of the current set, until it cannot be further improved. The problem is that this does not address feature correlation in a way that given a set P, $|P|=n$, the best feature f selected for the set $P'=P+\{f\}$ is not necessarily a good feature for the set P'', $|P''|=n+2$. Some algorithms include the possibility to solve this problem by allowing the removal of a given number of features after some iterations if this improves the set, like SFFS, which allows this backtrack operation.

However, this is not true for large feature sets. The backtrack operation may not be able to address completely this problem, as the number of features to manipulate at once may be overwhelming to the algorithm. On the other hand, GA is suitable for this kind of manipulation, as mating two different individuals will result in the inclusion and removal of many features at the same time. As this operation is made on many individuals, which are later selected and mated according to their fitness, i.e., how good the feature set they represent, GAs can find better solutions on large problems. This ability to produce subsets that are very different in just one pass allows GAs to perform better than algorithms like SFFS and SBFS.

One choice to be made along the method for FSS is the choice of method to evaluate feature set quality. There are two approches to consider as discussed by Yuan *et al.* in [40], the *filter* and the *wrapper* approaches. On a filter approach, the feature subset selection is made as a preprocessing step, not taking into account the impact of feature removal on the actual classifier. On the other hand, a wrapper approach consider the impact of feature removal on the classifier, so instead of evaluating measures of class separation, a method applying a wrapper approach will use the actual classifier accuracy to evaluate the selected feature subset. The filter approach is less precise than a wrapper approach, which is supported by the direct relation between FSS and classification phases if the employed classifier is the same. The objective in this work is classifier accuracy, which justifies the use of a wrapper approach later.

1.1.5 Ensemble of Classifiers

A recent trend in machine learning has been to combine several learners to improve their overall performance. Thus, classifiers can be combined to improve the classification stage in PR systems. Diettrich discussed in [5] ensemble learning in the context of supervised machine learning. The general learning problem is introduced as a set of points – observations in the context of PR, each described as a feature vector x with a class label y with an assumed function such as $y = f(x)$. The goal of learning is to find in the hypothesis space H an approximation function h to f to assign class labels to new x values. The function h is known as a classifier – a function that assigns class labels to points x. Machine learning search the space of possible functions – called *hypothesis* – to find the best approximation h to the unknown function f.

Thus, learning algorithms that searches for a single hypothesis suffer from three problems illustrated in Fig. 6:

- *Statistical problem*: the number of learning observations is small compared to the complete hypothesis space, hence many hypothesis will have the same accuracy and the learning algorithm must choose one of them. There is no guarantee that the selected classifier will predict correctly data points (Fig. 6.a)

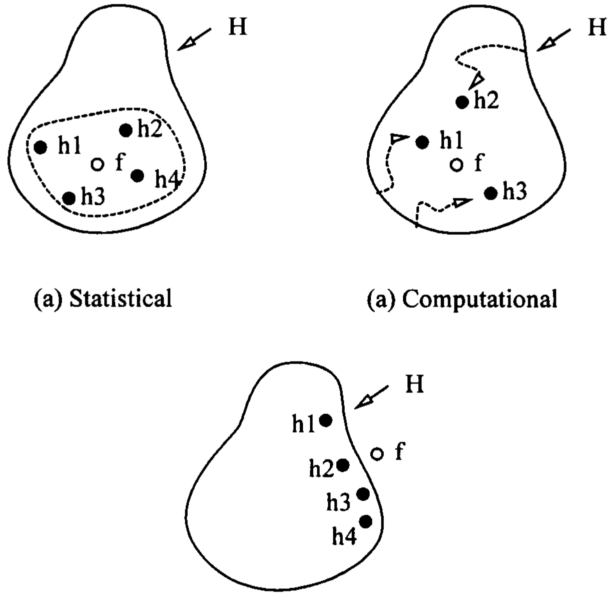

(a) Statistical

(a) Computational

(a) Representational

Figure 6 Problems faced by learning algorithms that searches for a single hypothesis h to the unknown function f [5]

- *Computational problem*: the learning algorithm has no guarantee to find the best hypothesis h in the hypothesis space. A learning algorithm that works searching hypothesis that fit better to the learning data may get stuck on a local optima and produce suboptimal approximation functions (Fig. 6.b).
- *Representational problem*: the hypothesis space does not contain good approximations to the unknown function f (Fig. 6.c).

These problems can be partly avoided with ensemble learning. Instead of searching one good approximation h, the learning algorithm must find an hypothesis set H, where each hypothesis vote for the class one unknown data point belongs to. The combination of these votes determines the class.

An EoC is typically created by running a learning algorithm several times to create a set of classifiers, which are then combined by an aggregation function. Algorithms for creating EoCs will usually fall into one of two main categories. The first category manipulates the training samples for each classifier in the ensemble. Two well-known algorithms for this task are Bagging [41] and Boosting [42]. The second category manipulates the feature set used to train classifiers, which can be performed through FSS [12, 14, 43, 44], or through transformations on the feature set, as in the random subspace approach [12, 14]. The key issue in this process is to generate a set of diverse and fairly accurate classifiers for combination [6].

One trend in the PR literature is the optimization of ensemble of classifiers using genetic optimization to select the most representative combination of hypothesis to increase classification accuracy. Ruta and Gabrys used a GA in [11] to optimize the classifiers aggregated on an EoC, whereas Oliveira *et al.* used a MOGA in [45].

1.1.6 Solution Over-Fit

Classifiers that are trained in several iterations, such as MLP classifiers, suffer from an effect known as over-fit. Due to over-fit, the classifier memorizes the training data set, instead of generalizing for unknown observations. To avoid the phenomena, a validation stage is performed using unknown observations.

The same effect has been observed in the literature when optimizing classification approaches using wrapped classifiers. Thus, solutions in the approximation set are specialized to the optimization data set. Reunanen demonstrated solution over-fit to compare sequential and floating FSS algorithms in [46]. In this context, solutions are evolved based on the accuracy measured over an optimization data set.

Some solutions have been proposed in the literature to avoid the over-fit phenomena during MOGA based classifier optimization. Loughrey and Cunningham discussed an early stoping approach to remove over-fit from solutions optimized by GAs [47] and simulated annealing [48]. Their iterative approach requires two stages. During the first stage, solutions are optimized and validated to determine at which generation solutions start to over-fit to the optimization data set, i.e., the generation where the algorithm has to stop earlier. In order to avoid solution over-fit, the second stage uses this information to optmize solutions until the previously calculated early stopping generation.

Llorà *et al.* used in [49] an approach that analyzed the optimized Pareto-front to determine a *rupture point*. The rupture point divides the Pareto-front in two segments, one over-fitted segment, and another segment where solutions provide higher accuracy on unknown observations. The same approach was also used by Mansilla in [50].

Another known solution to this problem is related to a validation process. Instead of selecting solutions using the traditional approach, i.e. based on the accuracy calculated during the optimization process, a validation data set is used to select solutions in the optimized Pareto-front. This approach was used in [51, 9, 52] and provided better results than selecting solutions using the traditional approach.

1.2 State of the Art in Multi-Objective Genetic Algorithms

Real world optimization problems usually have many objectives to optimize. These objectives are usually conflicting, *i.e.*, improving one objective will decrease the quality of conflicting objectives. The *Min-Ex* problem depicted in (1.1) [53] is a typical unconstrained minimization problem with conflicting objectives, called a ***multi-objective optimization problem*** (MOOP). Minimizing one function maximizes the other. This forces the choice of a compromise between objectives before applying traditional optimization methods. On traditional optimization methods, this compromise is established using a weighted vector, as in (1.2), to create a single objective to direct the optimization process.

$$\begin{array}{ll} \text{Minimize} & f_1(x) = x_1 \\ \text{Minimize} & f_2(x) = \dfrac{1+x_2}{x_1} \\ \text{subject to :} & \begin{cases} 0.1 \le x_1 \le 1 \\ 0 \le x_2 \le 5 \end{cases} \end{array} \tag{1.1}$$

$$f(ev) = w_1 \times f_1(x) + w_2 \times f_2(x) \tag{1.2}$$

This approach is not optimal in the sense that the expert has to choose a specific trade-off, whereas the set of possible trade-offs is unknown. For these optimization problems, the optimal approach is that the algorithm finds the objective function trade-offs, and the expert chooses the best solution based on a requirements analysis. Figure 7 depicts the objective function space for the *Min-Ex* problem, where the bold line indicates the optimal solutions with the best trade-offs. Such trade-offs are generated by a notion of optimality, the *Edgeworth-Pareto optimum* or, simply, *Pareto optimum.* Solutions belonging to the Pareto optimum set are referred as *non-dominated solutions.*

Multi-objective optimization algorithms work according to these principles, searching for a solution set that presents the best possible optimization objectives trade-offs. One specific class of algorithms is targeted in this thesis, the *multi-objective genetic algorithms* (MOGA). These algorithms are based on the working principles of genetic algorithms [1]. Schaffer introduced the *Vector Evaluated Genetic Algorithm* (VEGA) in [54], which many consider to be the first MOGA. This algorithm used a modified GA that selected solutions in turns using one objective function. It was Goldberg in [39] that first hinted the possibility of using the concept of Pareto optimality to solve multi-objective with GAs.

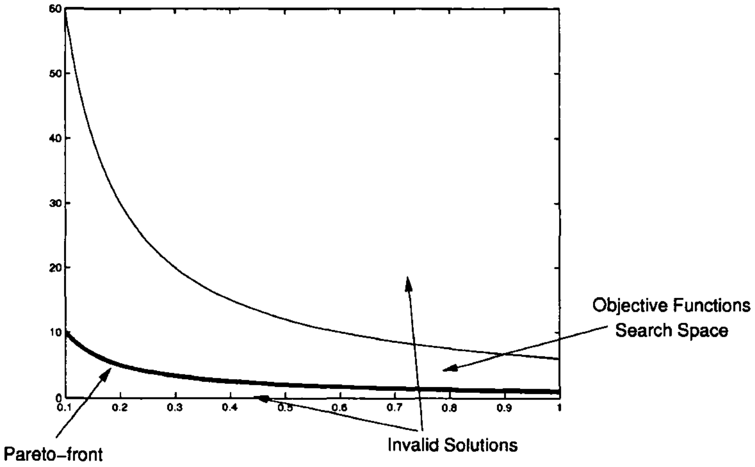

Figure 7 The Min-Ex objective function space

The following sections formalize the concepts behind multi-objective optimization. Next we discuss MOGA algorithms, their parallel counterparts and metrics to evaluate the performance of these algorithms. Coello presented in [55] a historical review on multi-objective optimization. The book by Deb further discusses the subject in [53], focusing on genetic based approaches and related techniques.

1.2.1 Definitions

Multi-objective optimization methods search for a solution set that presents the best trade-off between the optimization objectives. To search for this solution set, a multi-objective optimization algorithm uses the *dominance* concept. For a minimization problem, a solution x_i is said to dominate a solution x_j, $x_i \preceq x_j$, when the following two conditions are met:

- x_i is no worse than x_j for every objective function, or $f_k(x_i) \leq f_k(x_j)$, for $k = 1,2,\ldots,M$.

- x_i is strictly better than x_j for at least one objective function, or $\exists k, k \in \{1,2,\ldots,M\}, f_k(x_i) < f_k(x_j)$.

These conditions indicate that x_i has better objective function values than x_j. If one of the two conditions is broken, these solutions are uncomparable and they provide different objective function trade-offs. In this situation, two solutions are said to non-dominate each other. The following properties are valid for the dominance relation:

- Non-reflexive: a solution can not dominate itself.
- Non-symmetric: if $x_i \preceq x_j$, it is not possible by the dominance definition that $x_j \preceq x_i$.
- Transitive: if $x_i \preceq x_j$ and $x_j \preceq x_k$, it can be said that $x_i \preceq x_k$.

The bold line in Fig. 7 is composed of solutions that are non-dominated between each other, but that dominate the remaining possible solutions. This set is called the *non-dominated set*, or the *Pareto front*. For a specific set P of solutions, the non-dominated set P' is defined as $P' = \{p \mid p \in P \wedge \forall x \in P, x \neq p \rightarrow x \npreceq p\}$. For the solutions in Fig. 8, the non-dominated set is $P' = \{1,2,3,4\}$. The subset P' of a set P is also known as the *approximation set*. Thus, a multi-objective optimization method must optimize the approximation set towards the problem's true Pareto front.

Methods that solve MOOPs must accomplish two specific tasks:

- Find solutions close to the global non-dominated set.
- To evenly cover the global non-dominated set.

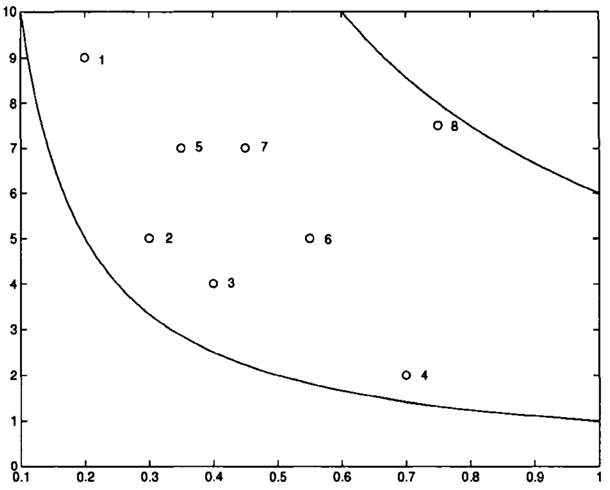

Figure 8 Min-Ex candidate solutions

These two tasks are conflicting, as they require two opposite aspects on search methods: *exploration* and *exploitation*. Exploration searches the entire space for better solutions, trying to get close to the non-dominated set, whereas exploitation search small areas to cover the non-dominated set. The concept of dominance is useful to explore the search space, as a non-dominated set will always be closer to the global non-dominated set. To exploit the non-dominated set, metrics related to the distance between solutions are used. Some well known metrics for this task are the *sharing* [56] (NSGA), the *crowding distance* (NSGA-II) [57] and density estimation [58] (SPEA2).

1.2.2 Multi-Objective Genetic Algorithms

As the name implies, MOGAs are derived from *genetic algorithms* (GA) and follow the same principles. Figure 9 depicts the flowchart of a GA. A population of candidate solutions (individuals) evolve by means of genetic operations during a given number of generations, aiming to increase individuals quality, measured by a *fitness* value.

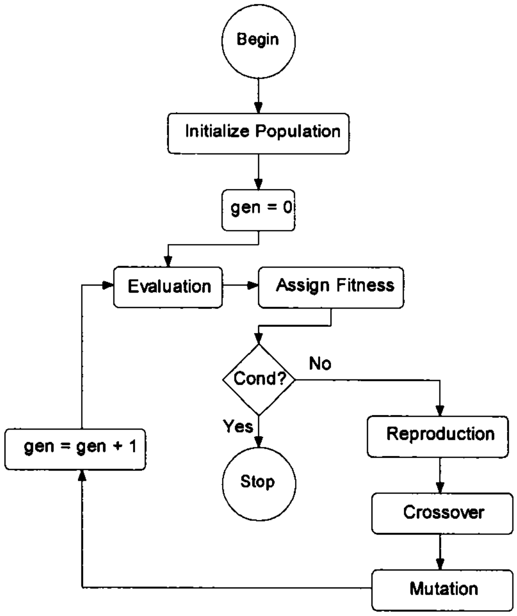

Figure 9 Classical GA flowchart

On each generation, individuals are evaluated and have their fitness assigned. Based on this fitness, individuals are selected to reproduce, exchanging genetic information with a *crossover operator*. To improve population diversity, individuals are often mutated using a *mutation operator*. These two operators create the next generation of individuals, which goes trough the same operations until the maximum number of generations is reached. Spears studied in [59] the role of both operators with single objective GAs. Recently, Ishibuchi and Narukawa compared in [60] the role of both operators in the context of multi-objective optimization, associating crossover to exploitation and mutation to exploration of the objective function space.

MOGAs follow a flowchart similar to Fig. 9, but changing the fitness to a non-dominance based ranking, along with a metric to evenly space solutions in the Pareto-front. Many works have reviewed and compared MOGAS. Deb discussed many algorithms in [53], which was also done by Veldhuizen *et al.* in [61] and Zitzler *et al.* in [62]. The *Fast Elitist Non-Dominated Sorting Genetic Algorithm* (NSGA-II) introduced by Deb *et al.* in [63], which is used as the baseline MOGA for this thesis, is detailed in Appendix 1.

1.2.3 Parallel MOGAs

To speedup the process and improve the solutions quality, studies have been made to use MOGAs in parallel environments. Three primary models are considered, the *master-slave* approach, the *island model* and the *cellular model.* These models employ concepts similar to those of parallel GAs. Cantú-paz presented in [64] a complete study on the issues of parallel GAs, where these three models are further detailed.

The master-slave model approach [65] is suitable to speed up the search on parallel MOGAs. This is due to the fact that the algorithm does not change, it only assign the evaluation of the objective functions to slave nodes, while the genetic operations are made on a master node. Oliveira *et al.* in [30] used a master-slave parallel MOGA for feature subset selection. The parallel cellular model is interesting for machines featuring processor arrays. However, the high cost associated to these machines reduces the interest on this specific research field, which focuses on specific problems that require such processor organization.

The island model, also called *distributed model,* have seen an increase on research effort after the *Beowulf cluster computer* boom. This type of cluster computer is based on inexpensive workstations that are connected through a local network to exchange information and complete a task. Cantú-Paz discussed in [64] the benefits of the island models, posing questions on the differences between their sequential counterparts. He also presented a survey of these algorithms in [66]. Hiroyasu *et al.* discuss in [67, 68] two different approaches for MOGAs based on island models. Zhu and Leung proposed in [69] an asynchronous MOGA with a self-adjustable objective space partitioning. A similar concept is developed by Streichert *et al.* in [70], using clustering to partition ther objective function space.

Our interest lies on the master-slave model, which provides speedup to the optimization process, with no change to the optimization algorithm behavior.

1.2.4 Performance Metrics

Unlike GAs, MOGAs provide a solution set as the optimization process outcome. These solutions are non-dominated, i.e., one solution can not be said to be better than the other. This poses a problem when comparing the solution sets found by two different algorithms, one can not directly compare these solutions. Any metric comparing two different solution sets on MOOPs must address two aspects, the convergence towards the global non-dominated set and its coverage.

Deb in [53] and Knowles in [71] reviewed techniques to evaluate different sets of non-dominated solutions. Zitzler *et al.* recently compared current techniques in [72]. This comparison established a mathematical framework developed for this task, dividing performance metrics in two classes: *unary* and *binary* quality indicators. It was concluded that unary quality indicators are limited, as they assign quality value to approximation sets. Binary quality indicators are more powerful, as they assign a quality value to the comparison of two approximation sets.

Examples of unary quality indicators are the spread [73], and the hypervolume indicator [74]. Examples of binary quality indicators are the coverage [74] and the binary hypervolume indicator, which compares the hypervolume covered by two approximation sets based on the same reference point.

1.2.5 Discussion

This section discussed aspects associated to the research domains related to this thesis. It has been observed that there is a lack of semi-automatic (eg. human centric) methodologies to optimize and adapt classification systems, which encourages the development of the classification system optimization approach covered in Chapter 2. The optimized classification systems will be compared to a high performance baseline representation, detailed in [51].

Over-fit in classification system optimization is an issue which is not often discussed. Most papers in the literature that discuss this phenomena use small data sets, as in [49], where the largest data set has 2048 observations. Thus, analysis with more significant data sets is necessary to better understand this problem and propose an effective solution.

Whereas two discussed papers use early stopping to halt the optimization process [47, 48], they did it as a mean to control over-fit. Instead, over-fit control should be performed by a validation procedure, whereas a stopping criterion has to monitor the optimized approximation set improvement to determine whether the algorithm must stop or continue optimization.

The next chapter discusses an approach to optimize classification systems for isolated handwritten symbols, based on both the pattern recognition and multi-objective optimization techniques discussed in this chapter. The goal of such a system is to optimize classification systems through multi-objective optimization based feature extraction.

CHAPTER 2

CLASSIFICATION SYSTEMS OPTIMIZATION

In order to optimize classification systems, a multi-objective approach based on feature extraction is proposed. This chapter details the approach, first presenting an overview in Section 2.1 that introduces the approach components and roles. Sections 2.2 through 2.4 discusses the feature extraction, feature subset selection (FSS) and ensemble of classifiers (EoC) optimization methodologies. Finally, a discussion in Section 2.6 concludes this chapter.

2.1 System Overview

Traditional image-based *pattern recognition* (PR) usually requires that pixel information be first transformed into an abstract representation (a feature vector) suitable for recognition with classifiers, a process called feature extraction [23, 75, 26, 22, 25]. A relevant classification problem is *intelligent character recognition* (ICR), which is aimed at recognizing handwritten symbols. One ICR application is the offline recognition of isolated handwritten symbols on documents such as forms. Methodologies for extracting features for this problem have been the subject of much research [27, 24, 32].

A methodology that extracts features for PR must select the most appropriate transformations and determine the spatial location of their application on the image. For isolated handwritten symbols, the choice takes into account the *domain context*, which type of symbols will be classified, and the *domain knowledge*, that is, what has been previously done to solve similar problems. Such a process is usually performed by a human expert (the experimenter) in a trial-and-error process specific to high-performance ICR where accuracy improvements of 0.1% are relevant at the classification stage. In high performance ICR, accuracy is around 99% and it is difficult to further improve it, hence these small accuracy improvements are actually large improvements on error rates on character strings. For a n characters string, the actual expected accuracy is $accuracy^n$. Given a 4 character string with a classifier that has 99.1% accuracy for individual characters, the expected accuracy for the 4 characters string is $99.1\%^4 = 96.45\%$. Another consideration is that changes in the domain context manifest themselves not only when changing the PR problem, but the domain context may change in the same classification problem, as illustrated in Fig. 1. To minimize the burden on the human expert (the experimenter) in defining and adapting classifiers, classifier optimization is modeled as an evolutionary MOOP, using the domain knowledge introduced by its user as transformations to extract features and actual data sets to represent the domain context.

Classification systems are modeled in two different two-level processes, as illustrated in Fig. 10. In both processes, the first level uses the *Intelligent Feature Extraction* (IFE) methodology to obtain the representation set RS_{IFE} (Fig. 10.a). The representations in RS_{IFE} are used to train classifiers that are further processed on a second level. The complexity of the best single classifier SI may be reduced through FSS (Fig. 10.b), or all classifiers may be considered for aggregation on an EoC SE for improved accuracy (Fig. 10.c).

Single classifiers and EoCs are both used for classification, but in different situations. A single classifier is faster and suitable for classification systems running on hardware with limited processing resources, such as embedded devices. An EoC demands more processing power and is adequate for high-performance and robust classification systems running on desktop or server computers. Thus, the approach can optimize the classification stage in both situations according to its user needs.

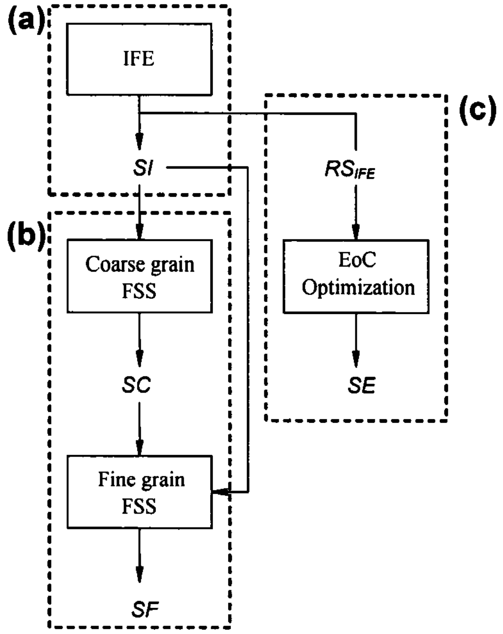

Figure 10 Classification system optimization approach – representations obtained with IFE may be used to further improve accuracy with EoCs, or the complexity of a single classifier may be reduced through FSS

2.2 Intelligent Feature Extraction

Human experts are traditionally responsible for choosing the feature vector used in classification systems. This vector is most often determined using domain knowledge and domain context on a trial-and-error basis. This section details the *Intelligent Feature Extraction* (IFE) methodology, which uses the domain knowledge and domain context in an approach formulated as a MOOP to genetically evolve a candidate solution set. The goal of IFE is to help the human expert define representations (feature vectors) in the context of isolated handwritten symbols, using a wrapper approach with a fast training classifier.

IFE models isolated handwritten symbols as features extracted from specific *foci* of attention on images using *zoning*. This is a strategy known to provide better recognition results than the extraction of features from the whole image [28, 27, 76]. Two operators are used to generate representations with IFE: a *zoning operator* to define foci of attention over images, and a *feature extraction* operator to apply transformations in zones. The choice of transformations for the feature extraction operator constitutes the domain knowledge introduced by the human expert. To obtain representations for specific PR problems, such as digits or uppercase letters, the domain context is introduced in the form of actual observations in the *optimization* data set used to evaluate and compare solutions. Hence, IFE optimizes the zoning operator to the selected feature extraction operator.

The IFE operators are combined to generate a representation such as illustrated in Fig. 11. The zoning operator defines the zoning strategy $Z = \{z^1,\ldots,z^n\}$, where $z^i, 1 \leq i \leq n$ is a zone in the image I and n the total number of zones. Pixels inside the zones in Z are transformed by the feature extraction operator in the representation $F = \{f^1,\ldots,f^n\}$, where $f^i, 1 \leq i \leq n$ is the partial feature vector extracted from z^i. At the end of the optimization process, the resulting representation set $RS_{IFE} = \{F^1,\ldots,F^p\}$ presents the IFE user with a choice among various trade-offs with respect to the optimization objectives, where p is the number of solutions optimized by the IFE.

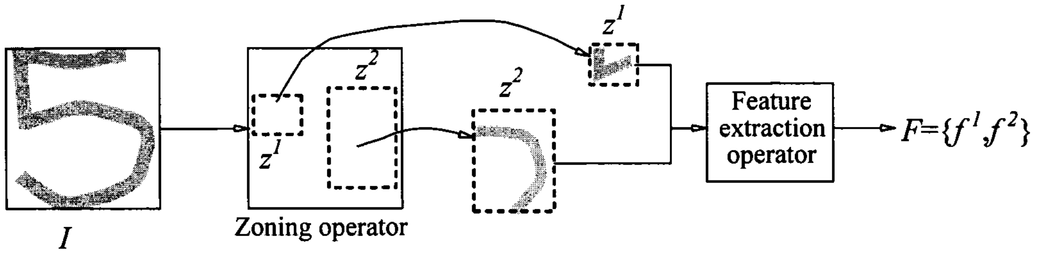

Figure 11 IFE structure – domain knowledge is introduced by the feature extraction operator, and the zoning operator is optimized based on the domain context (actual observations in the *optimization* data set)

The result set RS_{IFE} is used to train a discriminating classifier, creating the classifier set $K = \{K^1,\ldots,K^p\}$, where K^i is the classifier trained with representation F^i. A traditional discriminating classifier used in classification systems is the *multi-layer perceptron* (MLP) [2], which is targeted to train K. The first hypothesis is to select, in K, the most accurate classifier $SI, SI \in K$ for a single classifier system. In this hypothesis, SI can be further optimized to reduce its feature set cardinality through feature subset selection, which is discussed in Section 2.3. The second hypothesis is to use K to optimize an EoC for higher accuracy, an approach discussed in Section 2.4. The remainder of this section discusses the IFE operators chosen for experimentation with isolated handwritten digits and the candidate solution evaluation.

2.2.1 Zoning Operators

The zoning operator is the key element to optimize representations with the IFE. The domain knowledge introduced by the IFE user plays an important role, however, the crucial task to determine the actual *locus* of extraction is performed by the zoning operator. This section discusses two different zoning operators for the IFE. These operators performance will be compared later in Chapter 6.

2.2.1.1 Divider Zoning Operator

A *baseline* representation is considered for reengineering to compare IFE to the traditional human expert approach. This representation is known for its high degree of accuracy on isolated handwritten digits with a MLP classifier [51]. Its zoning strategy, detailed in Fig. 12.b, is defined as a set of three image dividers, producing 6 zones. The *divider zoning operator* expands the baseline zoning concept into a set of 5 horizontal and 5 vertical dividers that can be either *active* or *inactive*. Fig. 12.a details the operator template.

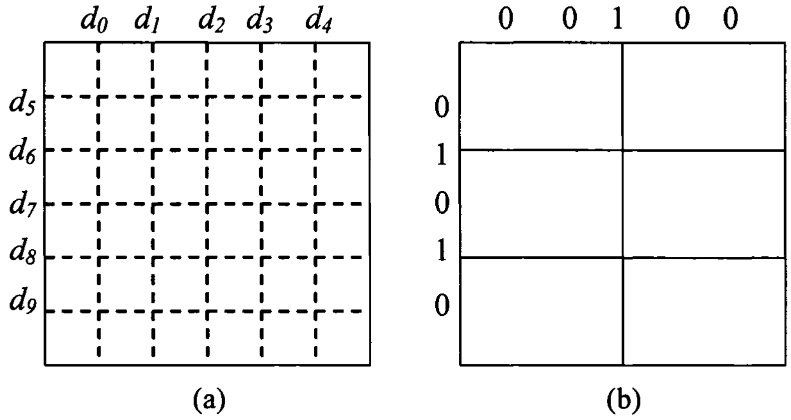

Figure 12 Divider zoning operator – each divider is associated with a bit on a binary string (10 bits), indicating whether or not the divider is active; the baseline representation in (b) is obtained by setting only d_2, d_6 and d_8 as active

The divider zoning operator is genetically represented by a 10-bit binary string. Each bit is associated to a divider's state (1 for active, 0 for inactive), producing zoning strategies with 1 to 36 zones. Figure 13 illustrates an example, relating both the binary coding string and its associated zoning strategy with 4 zones.

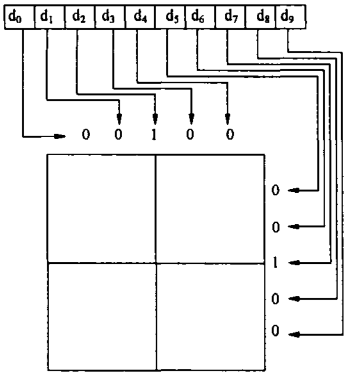

Figure 13 Divider zoning operator example

Genetic operations are performed on the binary string as usual, changing the bits to evolve the current population. Figure 14 illustrates the single point crossover operator on

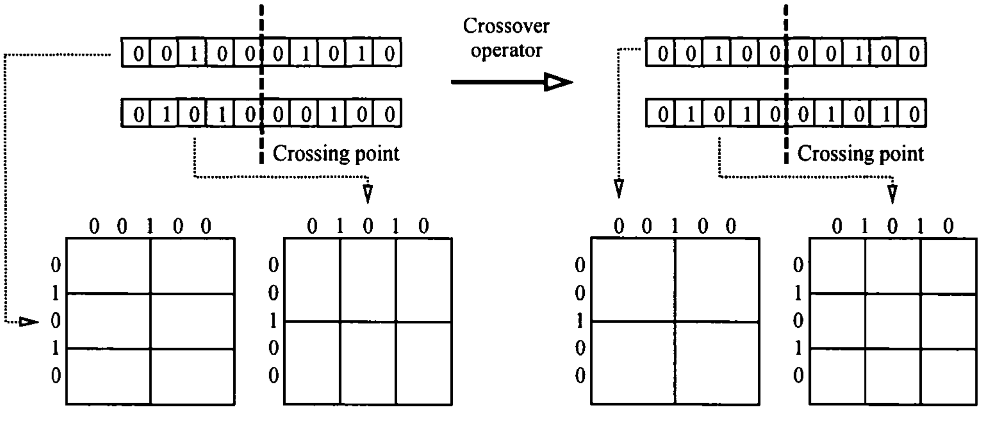

(a) Parents

(b) Offspring

Figure 14 Single point crossover operation example with the divider zoning operator – both parents (a) have bits swapped at the crossing points, producing two offsprings (b) that combine both zoning strategies

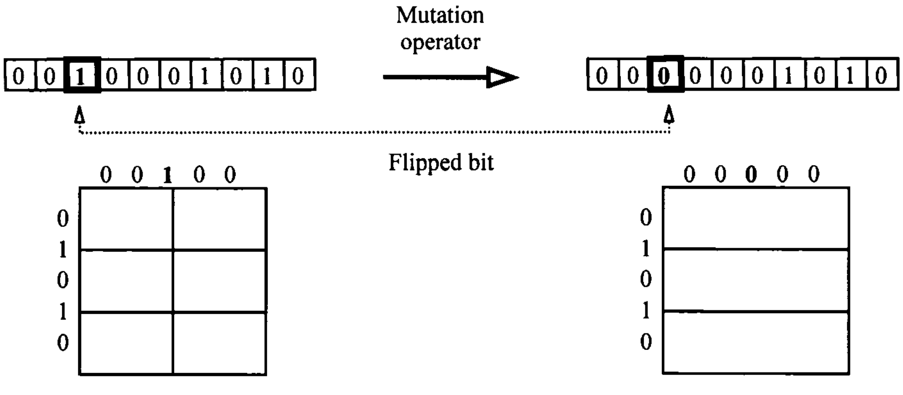

(a) Original solution

(b) Mutated solution

Figure 15 Bitwise mutation operation example with the divider zoning operator – one candidate solution has one bit fliped to create the mutated solution

two candidate solutions, whereas Fig. 15 does the same for the bitwise mutation operator. Both genetic operators will be used during the optimization process.

2.2.1.2 Hierarchical Zoning Operator

This zoning operator defines the zoning strategy based on a set of zoning patterns, depicted in Fig. 16 and associated to an integer number. Each pattern has labeled partitions that can be recursively partitioned with other patterns from the set. This strategy is described as a tree, where a root pattern is further partitioned by leaf patterns associated to its original partitions. Figure 17 illustrates an example of this strategy with one recursion level. Recursion is limited to one level to experiment with the IFE, hence the number of zones that can be defined with this operator range between 1 to 16.

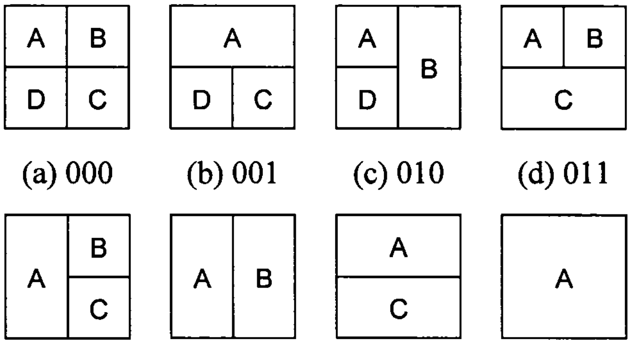

(a) 000 (b) 001 (c) 010 (d) 011

(e) 100 (f) 101 (g) 110 (h) 111

Figure 16 Hierarchical zoning pattern set and associated 3 bits binary strings

The operator is genetically represented by a 15 bits binary string. Each pattern is represented as a 3 bits binary substring, mapping to one of the eight zoning patterns through traditional binary to decimal conversion, where *a* is encoded as 0 and *h* is encoded as 7 (these values are indicated for each zoning pattern in Fig. 16). The complete coding requires a root pattern and 4 leaf patterns, therefore the genetic representation for this operator requires a 15 bits binary string, as demonstrated in Fig. 17.c.

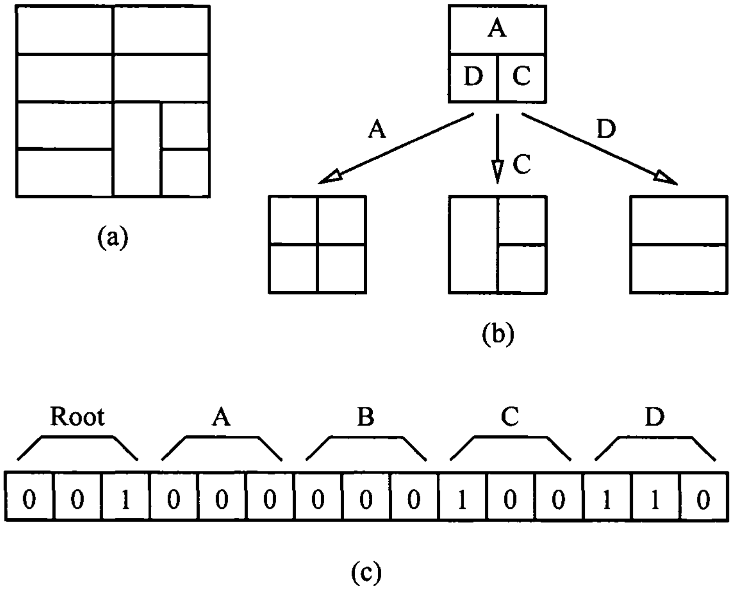

Figure 17 Zoning strategy encoded as *ba#eg* (a), its associated zoning tree (b) and binary string (c)

The example in Fig. 17 has one inactive pattern, as partition *B* does not exist in the root pattern selected. In this case, the encoded value is ignored during feature extraction, however, it is still considered during genetic operations as it can become active at some moment. This operator can produce 5768 different zoning configurations, while keeping a small feature set dimensionality, with a maximum of 16 zones against a maximum of 36 zones provided by the dividers zoning operator.

As with the divider zoning operator, genetic operations are performed as usual over the binary string. Figure 18 illustrates the single point crossover operator on two candidate solutions, whereas Fig. 19 does the same for the bitwise mutation operator. Again, both genetic operators will be used during the optimization process. In both figures, the less significant bit is the leftmost bit in the string.

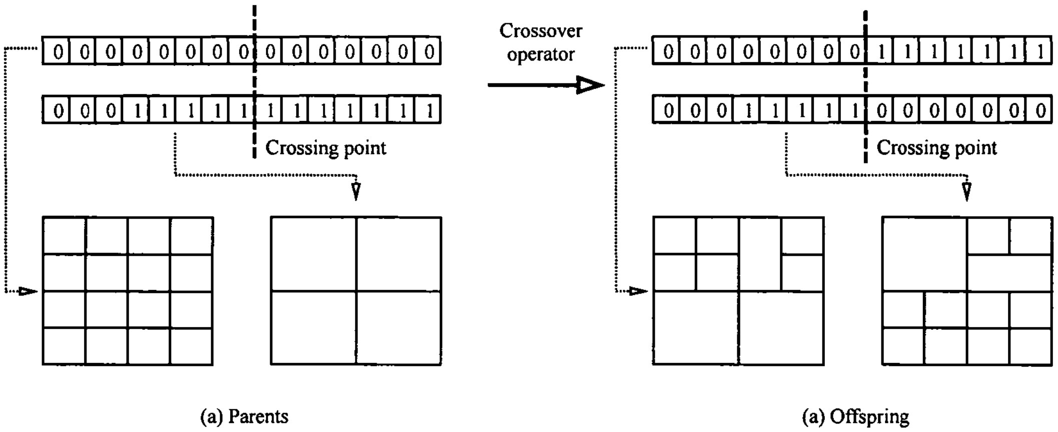

Figure 18 Single point crossover operation example with the hierarchical zoning operator – both parents (a) have bits swapped at the crossing points, producing two offsprings (b) that combine both zoning strategies

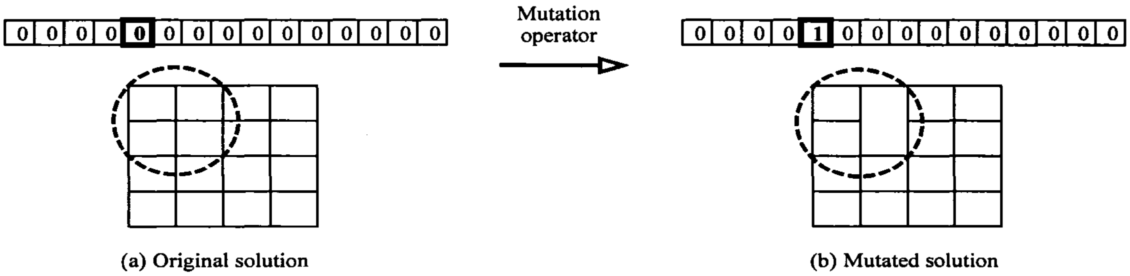

Figure 19 Bitwise mutation operation example with the hierarchical zoning operator – one candidate solution has one bit fliped to create the mutated solution

2.2.2 Feature Extraction Operator

Oliveira *et al.* used and detailed in [51] a mixture of concavities, contour directions and black pixel surface transformations, extracting 22 features per zone (13 for concavities, 8 for contour directions and 1 for surface). To allow a direct comparison between IFE and the baseline representation, the same feature extraction operators (transformations) are used to assess IFE with isolated handwritten digits.

Heutte *et al.* discussed in [26] the concept of concavities transformation. For every white pixel in the image in Fig. 20.a, we search in 4-Freeman directions (Fig. 20.b) for black pixels and determine the directions we reach black pixels and the directions we do not. If we find black pixels in all directions, we search in four auxiliary directions (Fig. 20.c) to confirm that the white pixel is inside a closed contour or not. Pixels that reach only one black pixel are ignored as they are not inside a concavity. For each zone the transformation produces the 13 positions feature vector in Fig. 20.d, where the first line labels the number of directions that black pixels can be reached, the second line labels the directions we find white pixels (for pixels on an open contour) and the last indicates the pixel count associated to that feature. Two examples in Fig. 20.a illustrates the process, pixel x_1 reaches four black pixels but fails to find black pixels in direction S_1, and pixel x_2 reaches three black pixels and misses direction 1.

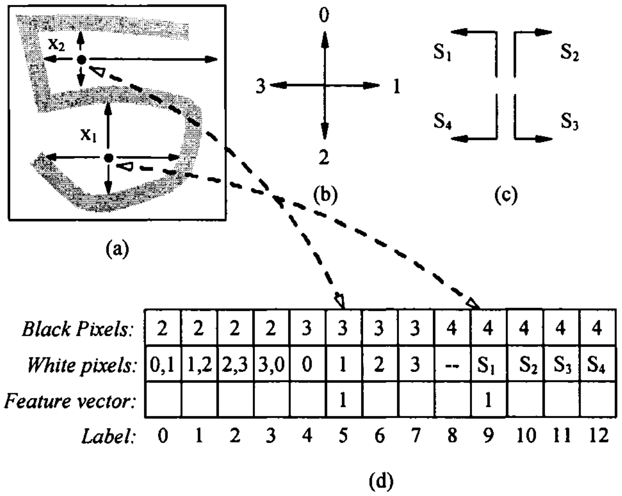

Black Pixels:	2	2	2	2	3	3	3	3	4	4	4	4	4
White pixels:	0,1	1,2	2,3	3,0	0	1	2	3	--	S_1	S_2	S_3	S_4
Feature vector:						1				1			
Label:	0	1	2	3	4	5	6	7	8	9	10	11	12

Figure 20 Concavities transformation, as used in [51]

The contour direction transformation is performed with a histogram of contour directions. For each zone in the image, contour line segments are labeled clockwise and counted regarding the 8-Freeman directions in Fig. 21.b, producing the 8 features vector

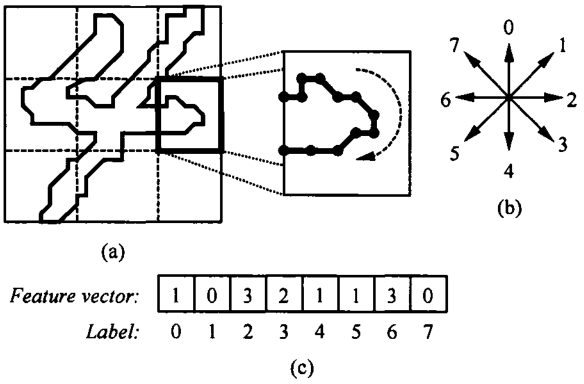

Feature vector:	1	0	3	2	1	1	3	0
Label:	0	1	2	3	4	5	6	7

Figure 21 Contour direction transformation, as used in [51]

in Fig. 21.c. The example in Fig. 21 details the contour count for the highlighted zone in the image. The first line is the direction count in this zone, whereas the second line is the associated Freeman direction.

Finally, the surface transformation simply indicates the number of black pixels in each zone. Thus, the surface transformation produces one feature. For proper comparison between different sized images, all extracted features (concavities, contour and surface) are normalized between 0 and 1 regarding all zones. For each individual feature extracted we calculate its total value on all zones and normalize values in zones in the $[0,1]$ interval.

2.2.3 Candidate Solution Evaluation

Candidate solutions are evaluated with respect to two objective functions, quality and dimensionality. Representation quality is related to classification accuracy, whereas representation dimensionality (feature number) is related to the generalization power associated with the representation. If the dimensionality is too high, the classifier tends to memorize the training set, an effect called the *curse of dimensionality*. Classification processing time is also related to representation dimensionality: the more features associated with the representation, the longer it takes to classify unknown observations. Dimensionality is measured as the representation zone number, given that, for IFE, the same feature vector is extracted from all zones. To evaluate representation quality, two strategies are discussed by John *et al.* in [77], the *filter* and *wrapper* approaches. The filter approach evaluates the representation based on measures over the representation itself, while the wrapper approach evaluates representation performance with actual classification. Chen and Liu indicate in [78] that a wrapper approach is better when the objective is classifier performance. Hence, this approach is the best choice for IFE, as the objectives are to minimize both dimensionality and the classification error rate on the *optimization* data set.

Robust and efficient classification systems require fast and discriminating classifiers. Two common classifiers in these systems are the MLP and *support vector machine* (SVM) [3, 4] classifiers. Both the MLP and SVM classifiers are fast and accurate in classification tasks. However, their training procedure is time-consuming and requires optimization of the configuration parameters. The wrapped classifier needs to be computationally efficient and reasonably accurate to prototype IFE solutions. Kimura *et al.* discussed in [79] the *projection distance* (PD) classifier. Based on hyperplanes to model classes, the PD classifier fairly quickly trains and classifies observations, modeling each class ω_i, a set of learning samples, as a hyperplane. An unknown observation x is projected on the hyperplane with (2.1). The projection $P_i(x)$ is used to calculate the Euclidean distance to the actual observation x. The projection closest to the actual observation determines the class that the observation x belongs to.

$$P_i(x) = (x - \mu_i)\Psi\Psi_i + \mu_i \tag{2.1}$$

On (2.1) we have that Ψ_i are the first k eigenvectors of the covariance matrix Σ_i of ω_i, ordered from the highest to the lowest value of eigenvalues. μ_i is the mean vector of the learning samples ω_i. Based on these working principles, the PD classifier tends to relate the problem classes to compact and well separated clusters that are used for the classification stage, providing higher accuracy than nearest neighbor (NN) classifiers. Also, the PD classifier requires less processing time to train and evaluate IFE solutions than NN or MLP classifiers. Therefore, the PD classifier has been chosen for the wrapper approach used to evaluate IFE representations through the optimization process.

Training a PD classifier requires two data sets, a *training* and a *validation* data set. The *training* data-set is used to create the hyperplane models, whereas the *validation* data set is used to optimize the k value. The PD classifier accuracy on the *validation* data-set is tested for all k values and the highest accuracy is selected to evaluate unknown observations. The process to select k is illustrated in Fig. 22.

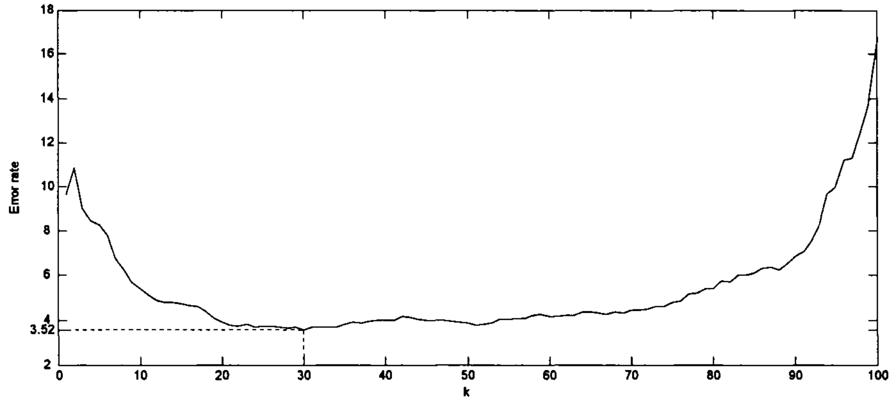

Figure 22 PD clasisfier k values during the training procedure and the associted error rates : the lowest error rate on the *validation* data set is obtained with $k = 30$, yielding a 3.52% error rate

2.3 Feature Subset Selection

Feature subset selection (FSS) [77, 40, 80, 43] aims to optimize the classification process, thereby eliminating irrelevant features from the original representation in order to create a smaller, yet accurate, representation. FSS is primarily used to reduce the computational cost associated with extracting and classifying unknown observations, which is important for embedded devices with limited processing resources. Due to the curse of dimensionality, which favors smaller representations, FSS may also improve classification accuracy by eliminating irrelevant features. The FSS problem is defined as finding a good feature subset regarding some objective function [77]. For the FSS methodology in this section, the objective functions are to minimize classification error and representation cardinality.

Kudo and Sklansky compared FSS techniques in [35], concluding that a GA performs better when the original representation size is large (more than 50 features). Oliveira *et al.* applied a GA-based FSS in [81] using a weighted vector with isolated handwritten digits, postulating that a MOGA could further enhance the results obtained. Their postulate was later confirmed in [10], where the MOGA outperformed the GA on the same problem. The superiority of MOGA in FSS is also confirmed by Emmanouilidis *et al.* [9] using sonar and ionosphere data.

FSS in this chapter is applied on the representation SI obtained with the IFE methodology. The FSS problem is modeled as a MOOP with two different levels (Fig. 10.b). The feature vector extracted for each zone in IFE is a combination of features produced by different transformations (concavities, contour directions and black pixel surface). Thus, a two-level FSS operation is proposed, where a *coarse grain* FSS optimization removes transformations applied on zones in SI (the single classifier optimizaed by the IFE), producing the representation SC. Next, a *fine grain* FSS optimization removes individual features in SC, producing the representation SF. The coarse grain FSS removes large blocks of features, leaving a reduced feature set in *SC* for further processing with the fine grain FSS. The fine grain FSS is similar to traditional FSS approaches and can be applied directly to representation *SI* for comparison purposes.

Li and Suen discussed in [32] the impact of *missing parts* in handwritten recognition, zones with no features extracted. According to the concept of missing parts, the pixel information in some zones of image I are ignored, as illustrated in Fig. 23. It was observed in their experiments that removing entire zones from the feature extraction process improved classification accuracy. This process relates to the FSS process, and therefore it is desirable to emphasize missing parts in solution encoding and its evaluation process.

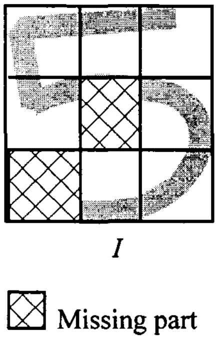

Figure 23 Missing parts example – marked zones are inactive and no features are extracted for classification (the example has 7 active zones)

Candidate solutions in both FSS levels are represented with binary vectors (Fig. 24). Each bit in the coarse grain FSS binary vector *cg* is associated with the state of a transformation applied to a zone (1 if the transformation is applied and 0 otherwise). As for the fine grain FSS, each bit in the binary vector *fg* is associated with the state of an individual feature (1 if the feature is active and 0 otherwise). Missing parts in both FSS levels are obtained when all bits related to a zone are set to 0, eliminating all features

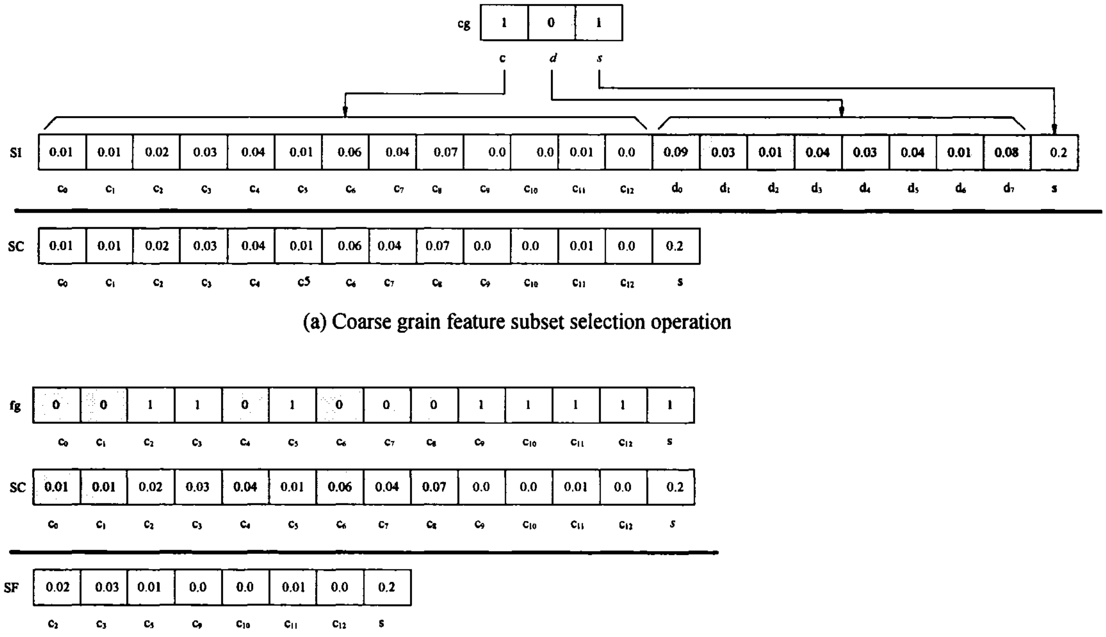
cg 1 0 1
c d s
SI 0.01 0.01 0.02 0.03 0.04 0.01 0.06 0.04 0.07 0.0 0.0 0.01 0.0 0.09 0.03 0.01 0.04 0.03 0.04 0.01 0.08 0.2
c_0 c_1 c_2 c_3 c_4 c_5 c_6 c_7 c_8 c_9 c_{10} c_{11} c_{12} d_0 d_1 d_2 d_3 d_4 d_5 d_6 d_7 s
SC 0.01 0.01 0.02 0.03 0.04 0.01 0.06 0.04 0.07 0.0 0.0 0.01 0.0 0.2
c_0 c_1 c_2 c_3 c_4 c5 c_6 c_7 c_8 c_9 c_{10} c_{11} c_{12} s
fg 0 0 1 1 0 1 0 0 0 1 1 1 1 1
c_0 c_1 c_2 c_3 c_4 c_5 c_6 c_7 c_8 c_9 c_{10} c_{11} c_{12} s
SC 0.01 0.01 0.02 0.03 0.04 0.01 0.06 0.04 0.07 0.0 0.0 0.01 0.0 0.2
c_0 c_1 c_2 c_3 c_4 c_5 c_6 c_7 c_8 c_9 c_{10} c_{11} c_{12} s
SF 0.02 0.03 0.01 0.0 0.0 0.01 0.0 0.2
c_2 c_3 c_5 c_9 c_{10} c_{11} c_{12} s

(a) Coarse grain feature subset selection operation

(b) Fine grain feature subset selection operation

Figure 24 Feature subset selection procedure on an one zone solution *SI* (22 features) : the contour directions transformation has been removed from the feature vector *SI* by the coarse grain FSS, producing the feature vector *SC* (a); individual features in SC are removed with the fine grain FSS to produce the final representation *SF* (b)

extracted. The process is illustrated in Fig. 24 for a theoretical one-zone representation using the concavities (*c*), contour directions (*d*) and black pixel surface (*s*) transformations.

Two objective functions guide the optimization process in both FSS levels, representation cardinality and representation quality. To explicitly emphasize missing parts, representation cardinality is defined in both FSS levels as the active zone number, *i.e.* zones having at least one feature extracted. Representation quality is measured through a wrapped classifier. The MLP classifier is targeted with the IFE experiments, and thus the same classifier is targeted for FSS. Because of the time required to train MLP classifiers, it is not feasible to train actual MLP classifiers to evaluate candidate solutions. Instead, sensitivity analysis [82] is used to estimate the relevance of MLP inputs (features) and classification performance. Given a data set with N observations, the neural network sensitivity S_i to variable i (a feature) is defined in (2.2), where S_{ij} is the calculated sensitivity to observation x_j in (2.3) and $\overline{x}$ is calculated as in (2.4).

$$S_i = \frac{1}{N}\sum_{j=1}^{n} S_{ij} \tag{2.2}$$

$$S_{ij} = SE(\overline{x_i}) - SE(x_{ij}) \tag{2.3}$$

$$\overline{x} = \frac{1}{N}\sum_{j=1}^{n} x_{ij} \tag{2.4}$$

S_i measures the impact on the trained square error (SE) of replacing the MLP input associated to feature i by the calculated average $\overline{x_i}$ for all N training observations. Moody and Utans demonstrated in [82] that MLP inputs are irrelevant if they can be replaced by their average in the *training* data set. Each feature corresponds to an MLP input, thus the MLP classifier is trained once with SI, and features removed in both FSS optimization levels are replaced by their *training* data set average during the optimization process. At the end of the optimization process, candidate solutions are trained with MLP classifiers to obtain the actual performance of reduced representations for selection.

Thus, the objective functions minimized for both FSS levels are the representation error rate and the number of active zones. The result of each FSS optimization level is a solution set RS_{CG} for the coarse grain FSS, and RS_{FG} for the fine grain FSS. In both levels, the most accurate representations $SC, SC \in RS_{CG}$ and $SF, SF \in RS_{FG}$ are selected (Fig. 24.b) for classification (SF) or to continue the FSS procedure (SC).

2.4 EoC Optimization

A recent trend in machine learning has been to combine several learners to improve their overall performance [5]. Thus, classifiers can be combined to improve the classification stage in PR systems. An EoC is typically created by running a learning algorithm several times to create a set of classifiers, which are then combined by an aggregation function. Algorithms for creating EoCs will usually fall into one of two main categories. The first category manipulates the training samples for each classifier in the ensemble. Two well-known algorithms for this task are Bagging [41] and Boosting [42]. The second category manipulates the feature set used to train classifiers, which can be performed through FSS [12, 14, 10, 44], or through transformations on the feature set, as in the random subspace approach [13, 15]. The key issue in this process is to generate a set of diverse and fairly accurate classifiers for combination [6].

Ruta and Gabrys used a GA in [11] to optimize the classifiers aggregated on an EoC. This section details a two-level methodology to create an EoC as a MOOP. The first level creates a classifier set with IFE, and the second level optimizes the classifiers aggregated using a MOGA. As each classifier is trained with a different representation produced by IFE, this approach belongs to the second class of EoC algorithms. The proposed EoC methodology selects which classifiers to aggregate from the set $K = \{K^1, \ldots, K^p\}$, where K^i is the classifier trained with the representation F^i in the IFE result set $RS_{IFE} = \{F^1, \ldots, F^p\}$. This hypothesis assumes that RS_{IFE} generates a set K of p diverse and fairly accurate classifiers. To realize this task as a MOOP, the classifiers in K are associated with a binary string E of p bits, which is optimized to select the best combination of classifiers using a MOGA. The classifier K^i is associated to the i^{th} binary value in E, which indicates whether or not the classifier is active in the EoC.

The optimization process is guided by two objectives, EoC cardinality and EoC quality. Computational effort during classification is related to EoC cardinality: the smaller the EoC, the less computational effort is required to classify observations. Ruta and Gabrys postulated in [11] that combined classifier performance (the wrapper approach) is a reliable and meaningful criterion with which to compare EoCs, and works well with most search algorithms. Thus, EoC quality in this methodology is evaluated with a wrapper approach, using the aggregated classifier output to evaluate accuracy. The goal is to minimize both EoC cardinality and the associated error rate on the *optimization* data set.

Evaluating the EoC error rate requires actual classifier aggregation, which depends on the classifier employed. The normalized continuous values of MLP classifier output are aggregated by their output average [6]. To speed up the process, the MLP outputs are calculated once only, and their actual aggregation is calculated during runtime. PD classifiers are aggregated by majority voting. As with MLP classifiers, PD votes are calculated once only, and the votes are counted during runtime.

2.5 Optimization Algorithm Requirements

To better understand the optimization problem and verify the impact of over-fit, a study was conducted with the IFE using the divider zoning operators and the digits data sets in Table I. Samples in each class are equally distributed in each data set for a more relevant analysis. The wrapped PD classifier is trained with the *learn* data set and the *validation* data set to configure classifier parameters during learning. The *optimization* data set is used with the wrapped classifier to evaluate the objective function associated to representation accuracy (actually, the error rate). In order to verify the generalization power of solutions optimized by the IFE, the *unknown* data set is used to compare the error rates on observations unknown to the optimized solutions.

Figure 25.a partially details the error rates of solutions in the objective function space, where each point relates to a trained PD classifier. Solutions A and C are dominated by solution B in the *optimization* data set objective space (Fig. 25.a). In this context, solution B belong to the Pareto-optimal set. Solutions A and B have the same cardinality, but the later has lower error rate, and solution B outperforms solution C in both feature set cardinality and accuracy. Changing the context to the *unknown* data set to evaluate the error rate in Fig. 25.b, solution B is dominated by solution A, and solution C becomes non-dominated. Both solutions A and C belong to the Pareto-optimal set in the *unknown* data set context. Thus, solution B is over-fitted to the *optimization* data set and does not perform as well on observations unknown to the optimization process.

Table I

Handwritten digits databases extracted from NIST SD19

Database	Size	Origin	Sample range
learn	50000	hsf_0123	1 to 50000
validation	15000	hsf_0123	150001 to 165000
optimization	15000	hsf_0123	165001 to 180000
unknown	15000	hsf_0123	180001 to 195000

Because of the non matching objective function spaces, it is clear that traditional Pareto-based approaches will not always emphasize and explore solutions with good generalization power on unknown observations. This preliminary analysis led to two requirements to be satisfied by an MOGA algorithm to proper optimize classification systems:

1. Allow the optimization of dominated areas in the decision-frontier to find solutions similar to C in Fig. 25.

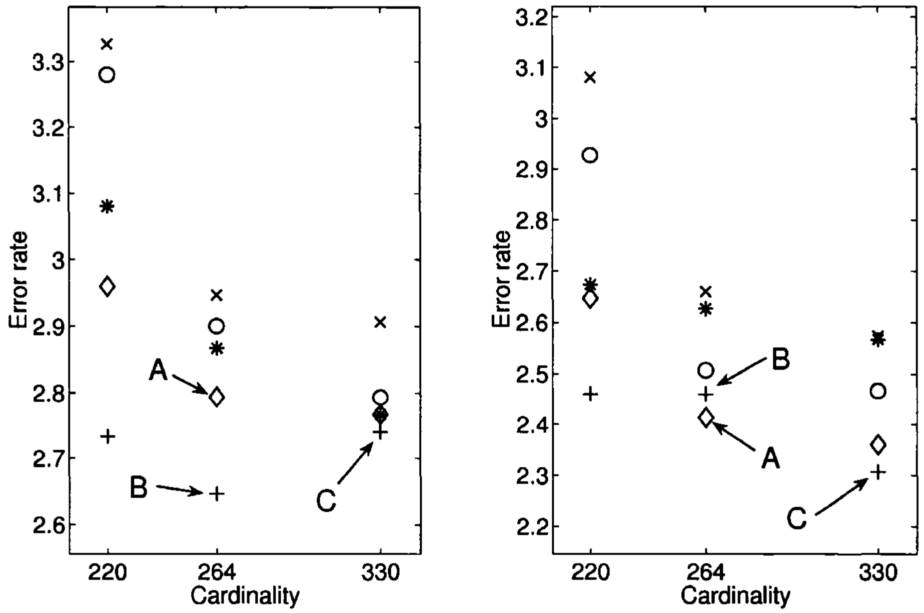

(a) *optimization* data set (b) *unknown* data set

Figure 25 Objective function space associated to different data sets – the *optimization* data set is used to evaluate candidate solutions and guide the optimization process, whereas the *unknown* data set is used to verify the solutions generalization power

2. Archive different levels of accuracy regarding solutions cardinality to keep solutions as A in Fig. 25 for validation.

Both requirements are satisfied by the *Multi-Objective Memetic Algorithm* (MOMA), which is detailed in Chapter 3, the first approach used to solve the over-fit issued verified in this analysis. Later it was observed that MOMA was limited by its configuration parameters and a more robust approach was needed, leading to a complete strategy to control over-fit, which is discussed in Chapter 4.

2.6 Discussion

This chapter detailed an approach to optimize classification systems, based on three methodologies that optimize classification systems for two contexts as MOOPs. The approach can optimize solutions for both single and multiple classifier systems. Most importantly, the approach uses the domain context and the domain knowledge introduced by an human expert to automatically optimize solutions, thus reducing the human intervention in creating and adapting classification systems. This chapter also introduced the over-fit issue, which will be addressed in the following chapters.

The next chapter proposes and discusses a multi-objective optimization algorithm adapted to the issues discussed in Section 2.5. The *Multi-Objective Optimization Memetic Algorithm* (MOMA) provides mechanisms to overcome the limitations associated to traditional Pareto-based approaches when optimizing classification systems.

CHAPTER 3

MULTI-OBJECTIVE OPTIMIZATION MEMETIC ALGORITHM

This chapter details the *Multi-objective Optimization Memetic Algorithm* (MOMA), discussing the motivations to design the algorithm, its concepts and the pseudo-code of each stage of the algorithm. The algorithm is adapted to the IFE and similar methodologies. This algorithm is then tested with the IFE to optimize representations for isolated handwritten digits with several configurations parameters and the results are discused.

MOMA combines a traditional MOGA with a local search algorithm to create a more powerful search mechanism for the IFE, and belong to a class of algorithms known as *memetic algorithms* (MA), which has been the subject of recent research [83, 84, 85, 86]. Jaszkiewicz demonstrates in [87] that hybrid optimization methods outperform methods based solely on genetic operations, hence the interest in developing MOMA, a two-objective optimization algorithm that combine GA with a *local search* (LS) algorithm.

3.1 Algorithm Concepts

Two requirements were defined in Chapter 2 to optimize classifications systems. One is to optimize for each cardinality value the best solution for selection. This set of solutions is called thereafter the *decision front*. Another requirement is to archive for each cardinality value a set of solutions for the selection stage. Thus, an algorithm adapted to this problem must optimize the decision front and archive a set of solutions ranked by decision frontier levels.

To perform this task, objective functions are divided in two categories, *objective function one* (o_1) in the integer domain, that defines the *slots* in the auxiliary archive S, and *objective function two* (o_2), which is optimized for each o_1 value. To archive different levels of performance, each slot S^l is a set of $\max_{S^l}$ solutions, associated to a possible o_1 value. For the approach to optimize classification systems, o_1 is the feature set/EoC cardinality and o_2 is the representation error rate.

The archive is defined as $S=\{S^1,\ldots,S^J\}$, where J is the maximum number of slots. For solution x^i, $o_1(x^i)$ and $o_2(x^i)$ are the solution's values of o_1 and o_2. $B(S^l)=x^b, x^b \in S^l$, such as that $o_2(x^b)=\min(o_2(x^j)), \forall x^j \in S^l$, indicates the solution x^b in S^l with the best o_2 value, whereas $W(S^l)=x^w, x^w \in S^l$, such as that $o_2(x^w)=\max(o_2(x^k)), \forall x^w \in S^l$, indicates the opposite.

The decision frontier set P_S optimized by the MOMA algorithm is defined as $P_S=\bigcup_{l=1}^{J}\{B(S^l)\}$. We indicate that solution x^i is admissible into slot S^l as $x^i\Theta S^l \equiv o_1(x^i)=l$, then $A(S^l,C)=\{c \mid \forall c \in C, c\Theta S^l\}$ denotes the subset of solutions in C that are admissible in S^l.

To optimize the decision frontier as indicated in Fig. 25, solutions are ranked for genetic selection by a *frontier ranking* approach. In the population P, the solution set belonging to the first rank is defined by $R^1=\bigcup_{l=1}^{J}\{B(A(S^l,P))\}$. The solution set belonging to the second rank R^2 is obtained as the first rank of $P \setminus R^1$, and so on.

The decision frontier concept and the archive S are key elements for proper optimization of classification systems using validation at the last generation. Combined, they provide means to select solutions after optimization based on their generalization power on unknown observations. Selecting solutions by the decision frontier allows the optimization of solutions usually discarded by traditional Pareto based approaches. This need is justified to avoid optimization bias as indicated in Fig. 25, where solution C is dominated in the IFE model optimization objective space using the *optimization* data set, but has better generalization power on unknown observations. The same principle justifies the need to store different levels of performance in the slot, solution A in Fig. 25 has better generalization power on unknown observations, but would be discarded from the archive on traditional approaches.

3.2 Algorithm Discussion

The MOMA algorithm is depicted in Fig. 26. It evolves a population P of size m, and archives good solutions found in the slots S, which are updated at the end of each generation. The population P is initialized in two steps. The first creates candidate solutions with a Bernoulli distribution, while the second generates individuals to initialize the slots. For each slot, we choose one random solution that is admissible in the slot and insert it in the population.

During genetic optimization, individuals in the current generation P^t are subjected to frontier ranking. Next a mating pool M is created by tournament selection as indicated in Algorithm 1, followed by traditional crossover and mutation to create the offspring population P^{t+1}. In case of a draw in the tournament selection and both individuals are uncomparable (belong to the same frontier rank), one of the solutions is chosen randomly.

Parks discussed in [88] the effects of genetic overtake due to multiple copies of the same individuals, which degrade the performance of evolutionary algorithms. To avoid

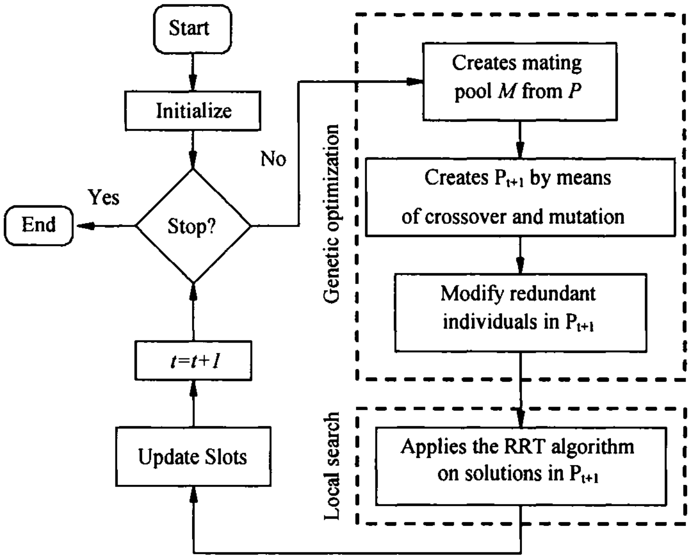
Start
Initialize
Stop?
Yes
No
End
t=t+1
Update Slots
Genetic optimization
Creates mating pool M from P
Creates P_{t+1} by means of crossover and mutation
Modify redundant individuals in P_{t+1}
Local search
Applies the RRT algorithm on solutions in P_{t+1}

Figure 26 MOMA algorithm

Algorithm 1: Tournament selection operator for MOMA

```
Data: Current population $P^t$
Result : Mating pool $M$
repeat
    Select solutions $p, q \in P^t$, such as that both $p$ and $q$ have not yet participated two times in tournaments;
    if $p \rhd q$ then
        $M = M \cup \{p\}$;
    else
        if $p \lhd q$ then
            $M = M \cup \{q\}$;
        else
            Randomly selects individual $r$ from $\{p, q\}$;
            $M = M \cup \{r\}$;
        end
    end
until $|M| = m$;
```

Algorithm 2: Algorithm to insert an individual p into population P^{t+1}

```
Data: Population $P^{t+1}$ and solution $p$
Result : Modified population $P^{t+1}$
if $p \notin P^{t+1}$ then
        $P^{t+1} = P^{t+1} \cup \{p\}$
else
        while $p \in P^{t+1}$ do
                mutate $p$;
        end
        $P^{t+1} = P^{t+1} \cup \{p\}$;
end
```

genetic overtake, redundant individuals are mutated until the population has no redundant individuals as in [11]. To avoid checking every individual against the entire population and to improve algorithm efficiency, individuals are tested for redundancy as they are inserted into P^{t+1}. The algorithm to achieve this taks is described in Algorithm 2. This algorithm tests if $p \notin P^{t+1}$, and if true, p is inserted into P^{t+1}. Otherwise, if $p \in P^{t+1}$, the algorithm mutates p until $p \notin P^{t+1}$ before insertion. To verify that $p \in P^{t+1}$ it is usually enough to verify the binary string equality between p and all candidate solutions in P^{t+1}. It should be noted that the hierarchical zoning operator may produce the same zoning strategy with two different binary strings, thus the test to verify if $p \in P^{t+1}$ should consider for comparison the actual representation associated to solutions when optimizing the IFE with the hierarchical zoning operator.

After genetic optimization, solutions are further improved by a LS algorithm. The algorithm chosen is the *Record-to-Record Travel* (RRT) algorithm [89], an annealing based heuristic. The RRT algorithm improves solutions by searching in its neighborhood for n potential solutions during NI iterations, allowing a decrease in the current performance of $a\%$ to avoid local optimal solutions as indicated in Algorithm 3.

Algorithm 3: Record to record travel (RRT) algorithm used by MOMA to further optimize solutions

```
Data: Population $P$
Result : Modified population $P$
forall $x^i \in P$ do
        $iterations = 0$;
        $p = x^i$;
        $RECORD = o_2(p)$;
        repeat
                Choose a random set of solutions $J$, $|J| = n$, neighbor to $p$;
                Select the best solution $p' \in J$;
                if $o2(p') < RECORD \times (1 + a)$ then
                        $p = p'$;
                        if $o2(p') < RECORD$ then
                                $RECORD = o2(p')$;
                                $x^i = p$;
                        end
                end
                $iterations = iterations + 1$;
        until $iterations = NI$;
end
```

Neighbors to solution x^i must have the same feature set cardinality and similar structure, which is achieved in the IFE model by modifying the zoning operator encoding. For the divider zoning operator, dividers are distributed in two groups, and $g_2 = \{d_5, d_6, d_7, d_8, d_9\}$. To generate a neighbor we select a group to activate one divider and deactivate another. The solution in Fig. 27.a has solutions in Figs. 27.b and 27.c as two possible neighbors. To create a neighbor to the hierarchical zoning operator, the algorithm changes one zoning pattern while keeping the same feature set cardinality. This process is illustrated in Fig. 28, where solution in Fig. 28.a has two neighbors in Figs. 28.b and 28.c. For EoC and fine grain FSS methodologies, two different binary values are swapped in the bit string. The coarse grain FSS follows a similar approach, however, the binary values swapped must belong to the same feature extraction operator.

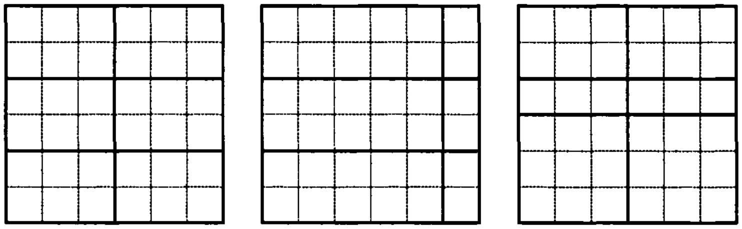

(a) (b) (c)

Figure 27 Divider zoning operator example – zoning strategy (*a*) and two neighbors (*b* and *c*)

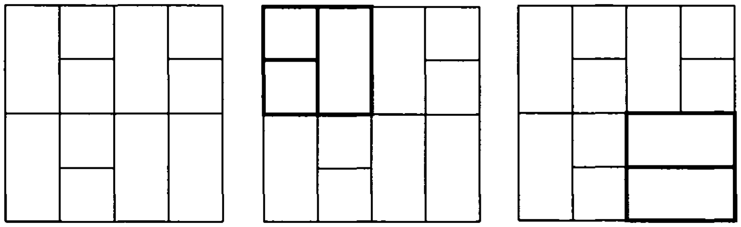

(a) *aeefe* (b) *acefe* (c) *aeege*

Figure 28 Hierarchical zoning operator – zoning strategy (*a*) and two neighbors (*b* and *c*), with associated zoning patterns (the bold letters indicate the zoning pattern replaced to create the neighbor solution)

After the LS, the archive S is updated, storing good solutions from P^{t+1} in the slots as in Algorithm 4. Recall that max_{S^t} is the maximum number of solutions a slot can hold. At this point, the stopping criterion is verified, deciding if the algorithm should continue to the next iteration or stop the optimization process.

3.3 MOMA Validation Tests with the IFE

A model was created to verify MOMA, based on the IFE using the dividers zoning operator. The entire objective function space was calculated (all 1024 possible solutions), evaluating the representations discriminative power on a *wrapper* approach using actual PD classifier performance. The PD classifier details and training procedure are presented in Section 2.2.3. Classifier training and error rate evaluations were made

Algorithm 4: MOMA update slot algorithm

```
Data: Population $P$ and the auxiliary archive $S$
Result : Modified auxiliary archive $S$
forall $x^i \in P$ do
    $l = o_1(x^i)$;
    if $o_2(x^i) < o_2(W(S^l)) \wedge x^i \notin S^l$ then
        $S^l = S^l \cup \{x^i\}$;
        if $|S^l| > \max_{S^l}$ then
            $S^l = S^l \setminus \{W(S^l)\}$;
        end
    end
end
```

with the digits databases in Table II. The disjoint databases are extracted from the NIST-SD19 database, using the digits data sets *hsf_0123* and *hsf_7*. Both the feature set cardinality and the error rate are minimized in these experiments.

PD classifiers were trained using the *learn* data set as the learning examples, and the *validation* data set to configure classifier parameters during learning. Error rate during the IFE optimization is calculated with the trained classifier on the *optimization* data set. To verify the generalization power of solutions optimized by the IFE, the *selection* and *test* databases are used to compare the error rates on unknown observations.

Table II

Handwritten digits databases used to validate MOMA

Database	Size	Origin	Sample range
learn	50000	hsf_0123	1 to 50000
validation	15000	hsf_0123	150001 to 165000
optimization	15000	hsf_0123	165001 to 180000
selection	15000	hsf_0123	180001 to 195000
test	60089	hsf_7	1 to 60089

3.3.1 Algorithmic Parameters

MOMA has a parameter set to configure, both for the genetic optimization and the local search stages. The list bellow indicates parameters that will be verified:

- m : population size
- p_c : crossover probability
- p_m : mutation probability
- n : size of the neighbourhood S for the RRT algorithm
- a : parameter to configure the deviation for the RRT algorithm
- NI : the maximum number of iterations for the RRT algorithm

The MOMA algorithm has another parameter that does not change directly its performance in terms of exploratory power, $\max_{S^l}$, the maximum number of individuals inside each slot. This parameter does not need optimization and is based on user preferences, related to the optimization problem. For instance, $\max_{S^l}$ may be determined based on the number of frontier levels the user wants to archive to optimize an ensemble of classifier later.

3.3.2 Validation and Tests

To test the MOMA algorithm, three test sets were conducted using the IFE . All tests used the *learn* and *validation* databases to train the PD classifier, and the *optimization* data set to evaluate the error rate during the optimization process. The first test verifies that the genetic optimization has convergence properties in this type of problem. This is acheived by disabling the RRT algorithm with $NI = 0$. The second test evaluates MOMA with a neighborhood subset best improvement strategy, while the third test uses a greedy first improvement strategy, where $n = 1$ and $a = 0\%$. These tests are referred as *Test A*, *Test B* and *Test C*, respectively.

The usual genetic operators for the IFE are the single point crossover, where the single point crossover is performed in the chromosome with probability p_c, and the bitwise mutation, which performs the bitwise mutation in the chromosome with probability $p_m = 1/L$, where L is the length in bits of the encoded operator being mutated [90].

A set of values is defined for each algorithmic parameter, using a *fractional design* approach [91] to obtain the 18 configuration sets in Table III. During *Test A* and *Test C*, columns in this table are replaced with specific values to achieve the desired effects.

Table III

Parameter values

#	m	p_c	p_m	a	n	NI
1	32	70%	$1/L$	5%	2	7
2	32	70%	$1/L$	5%	3	5
3	32	70%	$1/L$	5%	4	3
4	32	80%	$1/L$	4%	2	7
5	32	80%	$1/L$	4%	3	5
6	32	80%	$1/L$	4%	4	3
7	32	90%	$1/L$	2%	2	7
8	32	90%	$1/L$	2%	3	5
9	32	90%	$1/L$	2%	4	3
10	64	70%	$1/L$	5%	2	7
11	64	70%	$1/L$	5%	3	5
12	64	70%	$1/L$	5%	4	3
13	64	80%	$1/L$	4%	2	7
14	64	80%	$1/L$	4%	3	5
15	64	80%	$1/L$	4%	4	3
16	64	90%	$1/L$	2%	2	7
17	64	90%	$1/L$	2%	3	5
18	64	90%	$1/L$	2%	4	3

Each configuration set is subjected to 30 replications of 500 generations in each test, and comparisons are made at the generation of convergence. One run is said to have converged when the optimized decision frontier set P_S can no longer be improved. Preliminary experiments indicated that 500 generations far exceed the number of generations required to converge to *Test A*, our worst case scenario. Thus the following metrics are used to compare runs:

- *Unique individual evaluations* – how many unique individuals have been evaluated until the algorithm convergence, which relates to the computational effort.
- *Coverage by the global optimal set* – percentage of individuals in P that are covered by solutions in the global optimal set [72]. A candidate solution x is covered by solution y when, for all objective functions, y has better or equal values than x. The coverage metric is adapted to the decision frontier context. When P_S converges to the optimal set, the coverage is equal to zero.

Both metrics are fair as they hold the same meaning for all three tests. A final test evaluates representations optimized by the MOMA algorithm with the IFE. A result set S is selected, and the error rate of these solutions is evaluated with the *selection* data set and calculate the decision frontier P_S. From this decision frontier a set of solutions is selected for testing to compare with the baseline representation.

3.4 IFE Test Results

The results for the MOMA tests are presented in Figs. 29 to 31. The horizontal axis on the plots relate to configuration sets in Table III. Experiments 1 to 9 represent a smaller population – 32 individuals, while experiments 10 to 18 represent a larger population – 64 individuals. The box plots summarize the values attained in the 30 runs of each configuration set.

The results for *Test A* in Fig. 29.a indicate the convergence property of genetic operations alone, which is capable to optimize an approximation to the global optimal.

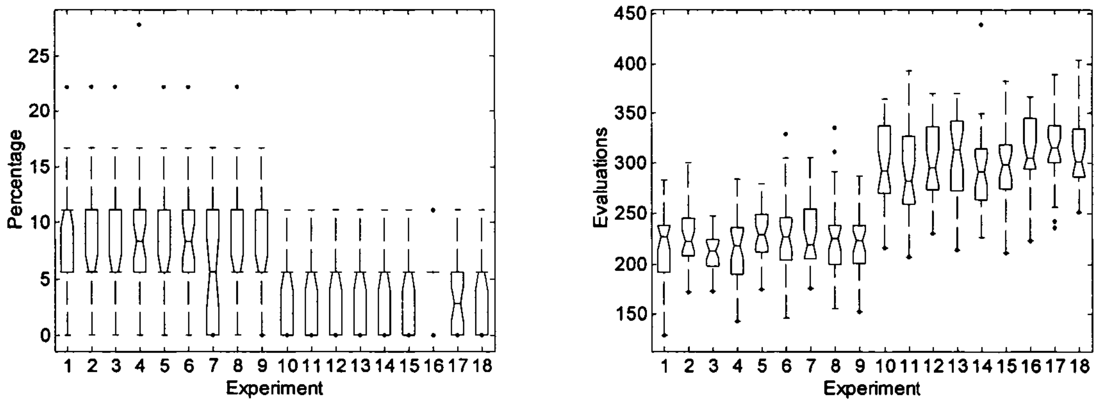

(a)

(b)

Figure 29 MOMA *Test A* results – (*a*) Coverage & (*b*) Unique individual evaluations

The best coverage values where achieved by the larger population, which also explored better the objective space. The exploratory aspect is measured as the number of unique individual evaluations in Fig. 29.b.

To improve convergence and the objective space exploration, *Test B* uses the complete MOMA algorithm. The RRT algorithm improved convergence in all runs but a few outliers in the smaller population converged to the optimal set. Objective space exploration in *Test B* is improved, as the number of unique individual evaluations in Fig. 30 is higher than in *Test A* – Fig. 29.b. This improvement reflects in the convergence toward the global optimal set, which is better than in *Test A*. The LS helps to improve convergence when searching for better solutions, which may also helps the genetic algorithm to better explore the objective space.

In the IFE we are concerned with the error rate evaluation cost. Thus, it is desirable to restrain the number of unique individual evaluations by reducing the strength of the LS. *Test C* modifies the RRT algorithm behavior, using a greedy first improvement strategy where $a = 0\%$ and $n = 1$. The convergence is similar to *Test B* – all runs but a few

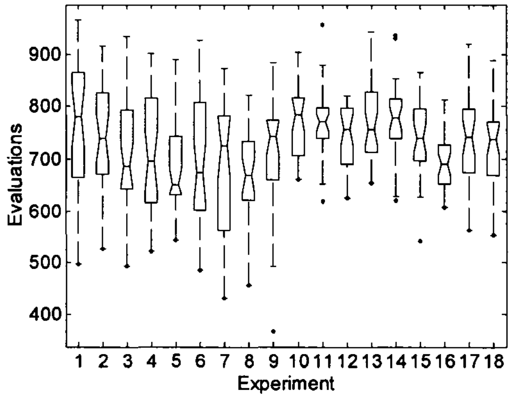

Figure 30 Unique individual evaluations – *Test B*

outliers converged to the optimal set (configuration sets using the smaller population). However, the number of unique individual evaluations in Fig. 31 is lower than in Fig. 30, which suggests that this improvement strategy is more suitable for the IFE problem optimization.

These experimental results demonstrate the effectiveness of the MOMA algorithm with the IFE methodology, reaching solutions that traditional MOGA approaches could not. For better convergence with lower number of unique individual evaluations, the LS with the greedy first improvement strategy is most appropriate. As for the configuration parameters, configuration sets 12, 15 and 18 in Table III differ only on the crossover probability p_c when using the greedy first improvement strategy ($n = 1$ and $a = 0\%$). It should be noted that other parameter sets share the same property. Configuration sets 12, 15 and 18 have good convergence and a low average number of unique individual evaluations. To narrow down the choice, we choose the intermediate crossover probability used ($p_c = 80\%$), thus, configuration set 15 in Table III is chosen to solve the IFE.

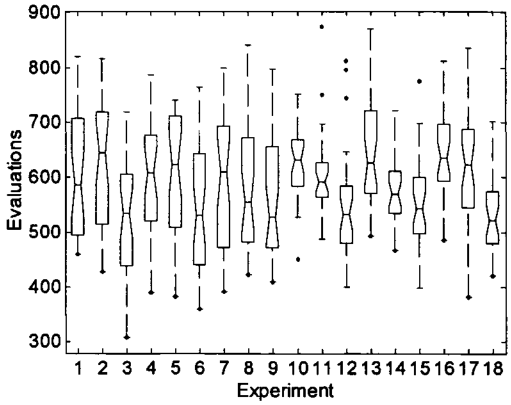

Figure 31 Unique individual evaluations – *Test C*

The final test evaluates a set of solutions optimized by the MOMA algorithm in the IFE model. A random replication from *Test C* is selected and solution error rate is evaluated with the *selection* data set. Solutions a to g are arbitrarily selected from the best decision frontier P_S based on error rates on the *selection* data set. Finally, selected solutions are tested with the *test* data set to compare with the baseline representation. The results are presented in Table IV, where the baseline representation was also trained and evaluated with the PD classifier using the same data sets. The table details the feature set cardinality, the binary string associated to the zoning operator and the error rate in three data sets, *optimization*, *selection* and *test* – e_{opt}, e_{sel} and e_{test}, respectively.

Considering results on the *optimization* data set, which is used during the optimization process, the best solution is f. However, validating solutions at the last generation with the *selection* data set will select solution g. Testing this solution set with the *test* data set, unknown to the optimized solutions, we confirm that this validation step is necessary to correctly select a solution with good generalization power. Solution g is also dominated by solution f and would be discarded by a Pareto-based approach,

Table IV

Representations selected from a random *Test C* replication

Representation	features	Zoning operator	e_{opt}	e_{sel}	e_{test}
Baseline	132	00100 01010	3.53%	3.01%	2.96%
a	110	00000 01111	3.59%	3.05%	3.27%
b	132	00000 11111	3.26%	2.99%	2.93%
c	176	00010 01101	3.15%	2.98%	2.98%
d	198	00101 01010	3.27%	2.99%	2.52%
e	220	00100 01111	2.73%	2.46%	2.44%
f	264	01100 01110	2.65%	2.46%	2.57%
g	330	00110 01111	2.74%	2.31%	2.18%

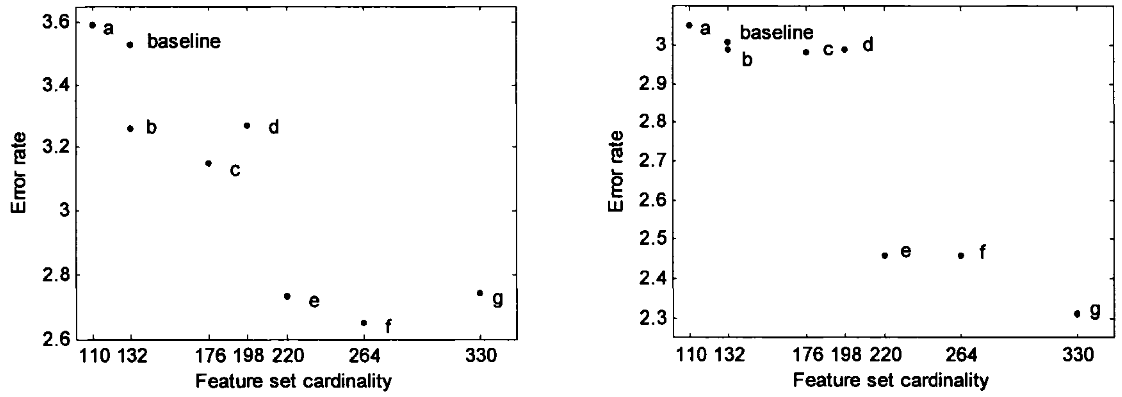

(a) *optimization* data set (b) *selection* data set

Figure 32 Solutions obtained with MOMA (Table IV) in the optimization objective function space and projected in the selection objective function space (the baseline representation is included for comparison purposes, demonstrating that the IFE is capable to optimize solutions that outperform the traditional human based approach)

validating the MOMA algorithm with the IFE methodology. The objective function space associated to these solutions, for both the *optimization* and *selection* data sets, is depicted in Fig. 32.

The zoning strategies associated to solutions in Table IV are illustrated in Fig. 33. This figure demonstrates the zoning strategies diversity for each feature set cardinality.

Whereas some representations share some common building blocks (dividers), they usually are different from one another. This suggests that it is appropriate to use the IFE to create a classifier set for EoC optimization. This claim is confirmed in Chapters 6 and 7, when the IFE result set is actually used to optimize an EoC with both handwritten digits and uppercase letters.

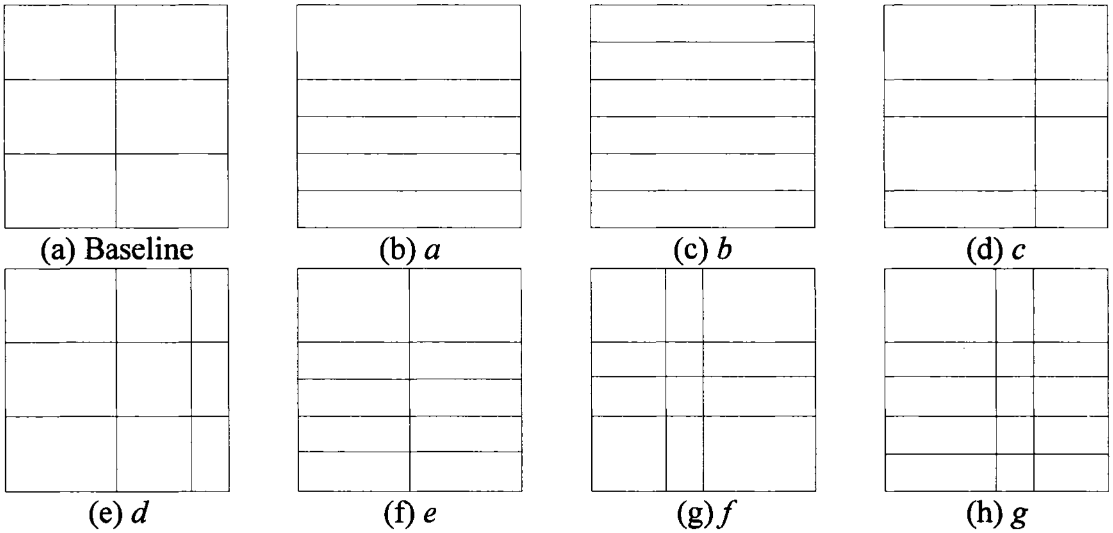
(a) Baseline (b) *a* (c) *b* (d) *c*

(e) *d* (f) *e* (g) *f* (h) *g*

Figure 33 Zoning strategies associated to solutions in Table IV

The results in Table IV demonstrate that the IFE methodology is able to optimize and select solutions that outperform the traditional human expert approach in the domain of unknown observations – the *test* data set. Representation g's error rate is 26.35% lower than the baseline representation on the *test* data set, which justifies the IFE methodology for actual applications. These results also justify MOMA, as solution g, which presents the highest accuracy, is discarded by traditional MOGAs.

3.5 Discussion

This chapter proposed MOMA, based on the requirements defined by the approach to optimize classification systems. A series of tests using the IFE with the divider zoning operator on handwritten digits was used to validate the algorithm and select algorithmic parameters values.

The algorithm is capable of converging to a decision front that features individuals that are not reached by Pareto-based approaches in all tests performed. This allowed the selection of good representations using a set of unknown observations, outperforming the traditional human based approach for feature extraction. Other tests will verify the algorithm performance on the complete approach to optimize classification systems.

The next chapter further discusses the over-fit issue, proposing an strategy to avoid it using a validation strategy similar to the validation strategy used during classifier training. This strategy can be aplied to Pareto-based MOGAs, and its performance will be compared in Chapters 6 and 7 to the strategy to validate solutions at the last generation used by MOMA.

CHAPTER 4

VALIDATION STRATEGIES TO CONTROL SOLUTION OVER-FIT

The challenge to example-based machine learning is the learner over-fit to the *training* data set, which is made up of actual observations used for learning. Example-based optimization of classification systems will transpose the same issue to the optimization process, thus a strategy to overcome solution over-fit to the *optimization* data set is necessary for the IFE, FSS and EoC approaches. The classifier training procedure (e.g. MLP and PD classifiers) is a typical example of learning over-fit, a process of t_{max} iterations where classifier parameters are adjusted based on current accuracy to classify the *training* data set. At each training iteration t, the classifier improves its accuracy. However, after iteration t_{stop}, the classifier starts to memorize the training data set instead of generating a more general model for unknown observations. At this point, it is said that the classifier becomes *over-fitted* to its *training* data set.

Fig. 34 illustrates the ideal classifier training process. On early iterations, the error rate decreases on the *training* data set and on unknown observations. After iteration t_{stop}, the error rate on the *training* data set keeps decreasing, but on observations unknown to the training procedure the error rate will increase. This effect is caused by the over-fit to the *training* data set. Thus, the classifier training problem is to determine the iteration t_{stop} at which the training procedure stops, which is achieved through a validation strategy using a *validation* data set of observations unknown to the training procedure. At each iteration t, the classifier parameters are adjusted as usual and accuracy is evaluated on the *validation* data set. The training iteration t_{stop} is determined as the last iteration during which the classifier improved its accuracy on the *validation* data set.

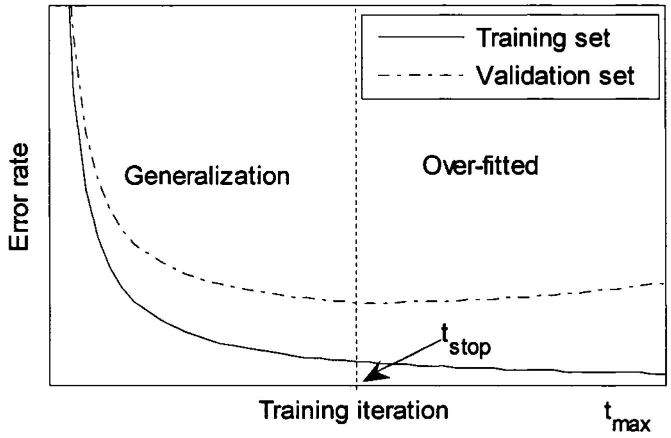

Figure 34 Ideal classifier training error rate curves – the classifier training problem is to determine the iteration at which the classifier training process stops generalizing for unknown observations

Solution over-fit also occurs when classification systems are optimized using a wrapper approach. The optimization process becomes a learning process, searching for solutions based on the wrapped classifier accuracy that is calculated using an *optimization* data set, after the classifier has been trained and validated with a *training* and *validation* data sets. Solutions found at the end of the optimization process might be over-fitted to the *optimization* data set. This effect is observed even where a validation procedure is used to train the wrapped classifier associated with each solution. Thus, a second validation procedure is also needed in the optimization process to select solutions with good generalization power.

Over-fit with IFE is illustrated in Fig. 35, in which a set of solutions explored by a MOGA is detailed where each point is a PD classifier trained with single-split validation. Fig. 35.a is the objective function space associated with *optimization* data set accuracy, which is used to guide the optimization process. To verify a solution's generalization power, a set of unknown observations is used to evaluate accuracy, producing the objective function space in Fig. 35.b. P_2 is the solution with the smallest

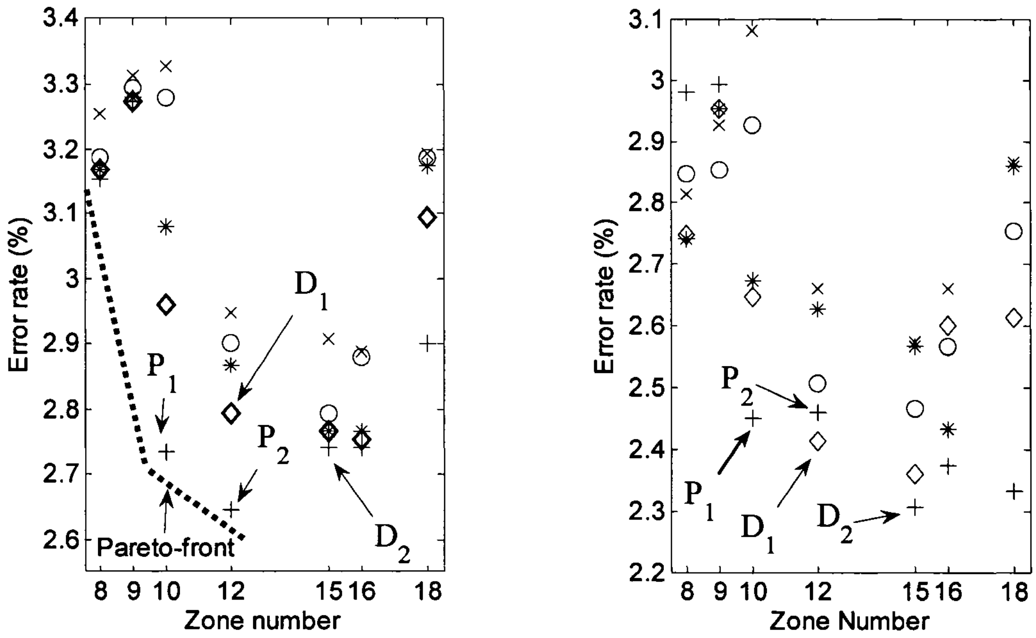

(a) *optimization* data set

(b) Unknown observations

Figure 35 IFE partial objective function spaces – good solutions (classifiers) obtained during the optimization process perform differently on unknown observations : solution P_2 has the smallest error rate on the Pareto front (a), but is dominated with unknown observations by D_1 (b) and generalizes worse than solution P_1, and whereas solution D_2 generalizes best, it is discarded by traditional Pareto-based approaches in (a)

error rate obtained in the Pareto front, but it does not generalize as well as P_1 (also in the Pareto front). One strategy used to overcome this type of over-fit following the optimization process is to validate the Pareto front with a *selection* data set of unknown observations [10, 13, 9], which selects P_1 as the most accurate generalization solution. This strategy produces better results than selecting solutions based solely on the accuracy of the *optimization* data set alone, but it misses D_1 and D_2, dominated solutions discarded by Pareto-based approaches that provide higher generalization power than P_1. The MOMA algorithm introduced in Chapter 3 explores dominated areas in the objective function space and uses an order-preserving strategy, maintaining an auxiliary archive containing a set of solutions for each possible representation cardinality produced by IFE. In this way, MOMA finds and keeps the solutions that generalize best for the validation procedure where D_2 is selected as the most accurate solution.

This validation strategy for MOGAs is performed once the optimization process has been completed at the best approximation set (Pareto front or the MOMA archive). Instead, a more robust validation strategy needs to be performed at each generation, similar to the validation process in classifier training. For a single run with NSGA-II in the proposed EoC methodology, Fig. 36 details all individuals in the population at generation $t = 14$. Fig. 36.a is the objective function space used during the optimization process, and Fig. 36.b is the objective function space used for validation. Points are candidate solutions in the current generation (MLP EoCs). Circles represent solutions in the current Pareto front, and diamonds the current Pareto front obtained in validation. The first conclusion is that, through the generations, non-dominated solutions are not always the best after validation. The second conclusion is that solutions with good generalization power are eliminated by genetic selection, which emphasizes solutions with good performance on the *optimization* data set (memorization). Hence, the most appropriate approach is to validate candidate solutions in all generations during the optimization process with a *selection* data set.

Validating solutions in all generations requires an auxiliary archive in which to store good validated solutions. This approach is demonstrated through the generations in EoC optimization with both NSGA-II and MOMA in Figs. 37 through 40 respectively. The points represent the complete search space covered by the algorithms, and each point is an MLP EoC where individual classifiers were trained with single-split validation. Diamonds are EoCs belonging to the approximation set (Pareto front for NSGA-II and

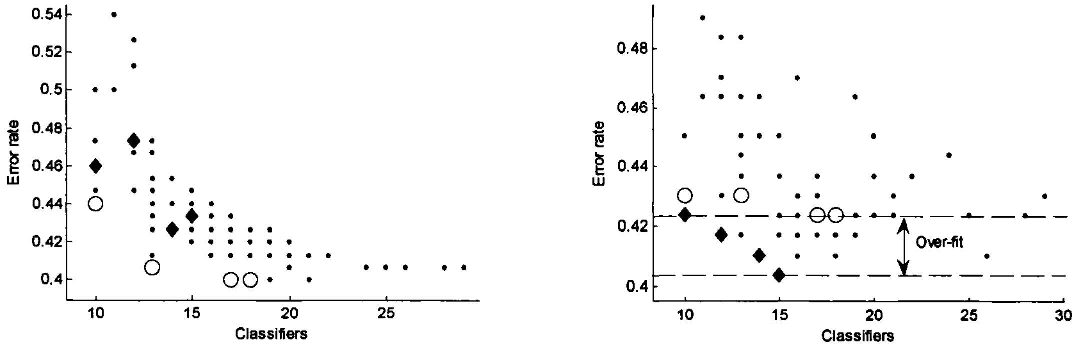

(a) Optimization (b) Validation

Figure 36 MLP EoC solutions as perceived by the optimization and validation processes at generation $t = 14$ with NSGA-II – each point represents a candidate solution, circles represent non-dominated solutions found during the optimization process and diamonds validated non-dominated solutions

the archived decision frontiers for MOMA) at generation t. The four figures details the solution improvement during the optimization process in the first column (a). In Figs. 37 and 39 the second column (b), the same solutions are projected on the *validation* objective function space, demonstrating the over-fit effect. Finally, the second column (b) in Figs. 38 and 40 simulates the improvement in the auxiliary archive obtained by validating the population at each generation t with the *selection* data set.

An algorithmic template for MOGAs using global validation is detailed in Algorithm 5 which requires a disjoint *selection* data set and an auxiliary archive S to store the validated approximation set. An MOGA evolves the population P^t during mg generations. At each generation, the population P^{t+1} is validated and the auxiliary archive S is updated with solutions that have good generalization power. Like the validation strategy used to train classifiers, the validation stage provides no feedback to the MOGA. At the end of the optimization process, the best candidate solutions are stored in S. To present the human expert with a choice of trade-offs,

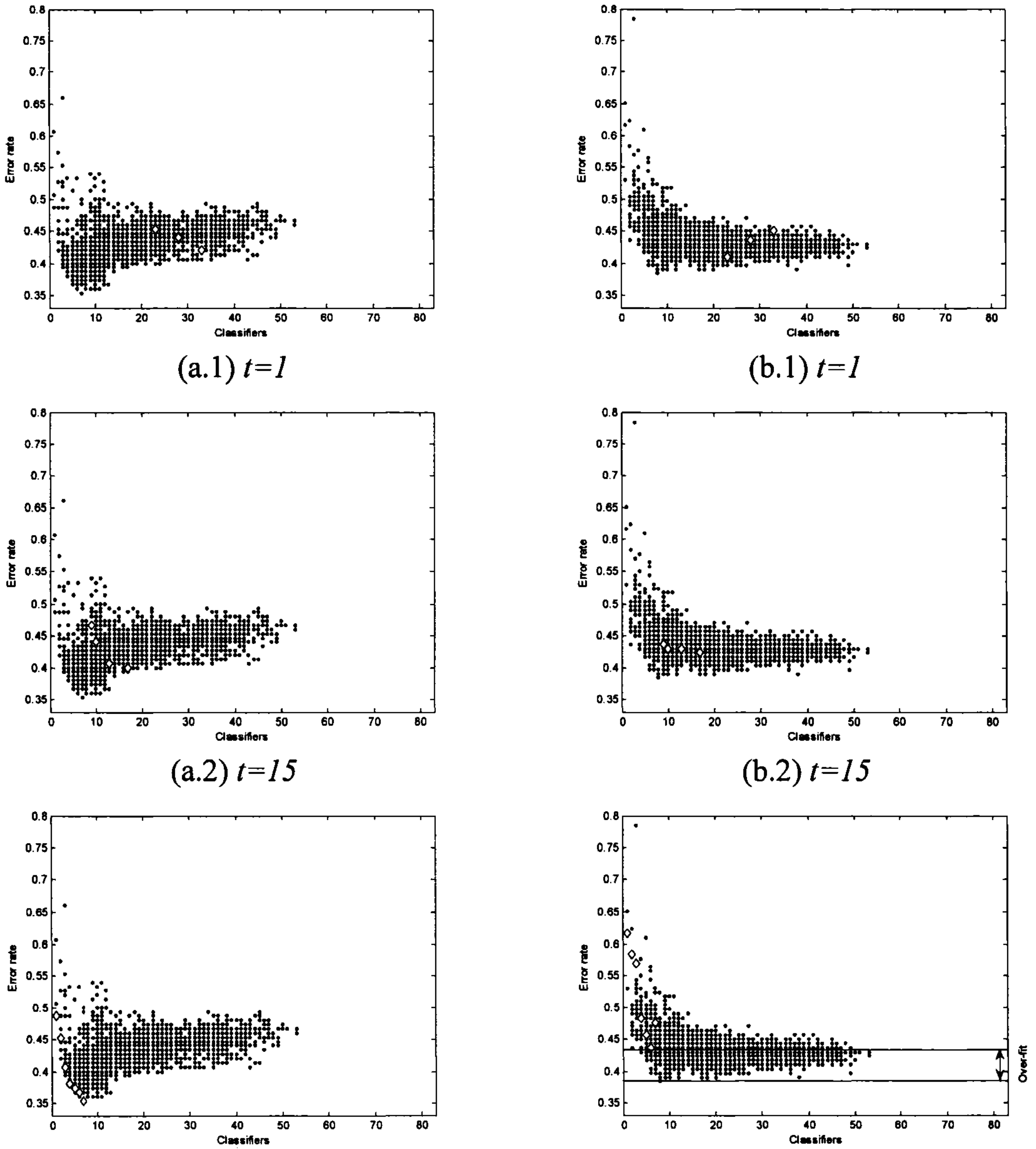

(a.1) *t=1*

(b.1) *t=1*

(a.2) *t=15*

(b.2) *t=15*

(a.3) *t=45*

(b.3) *t=45*

Figure 37 EoC optimization with NSGA-II at generation *t*: (a) Pareto front on the *optimization* data set and (b) Pareto front projected on the *selection* data set; the most accurate solution in (a.3) has an error rate 13.89% higher than the most accurate solution explored in (b.3)

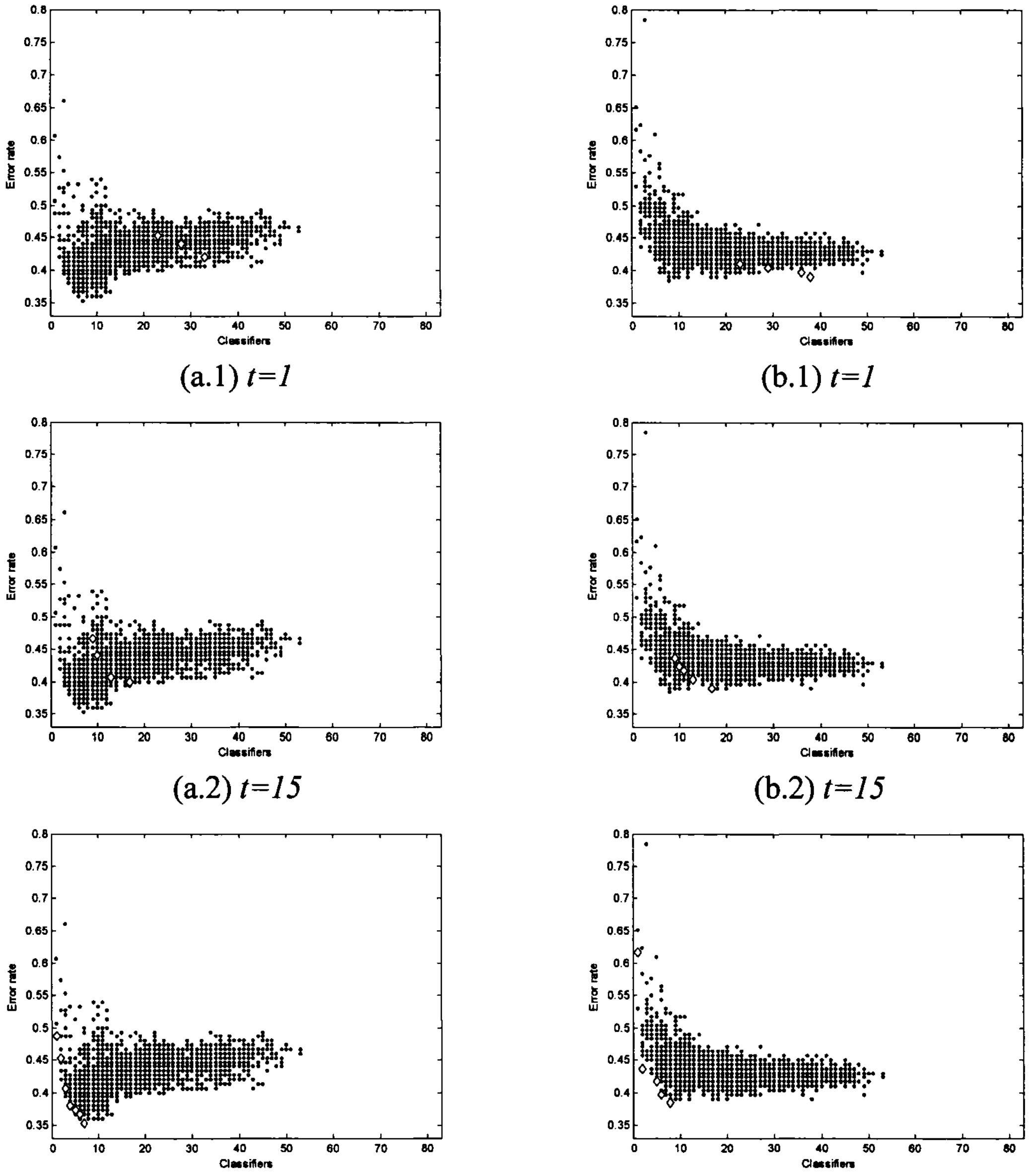

(a.1) *t=1*

(b.1) *t=1*

(a.2) *t=15*

(b.2) *t=15*

(a.3) *t=45*

(b.3) *t=45*

Figure 38 EoC optimization with NSGA-II at generation *t*: (a) Pareto front on the *optimization* data set and (b) the actual Pareto front in the *selection* data set; validating solutions through all generations allows the optimization process to find a good approximation set on generalization

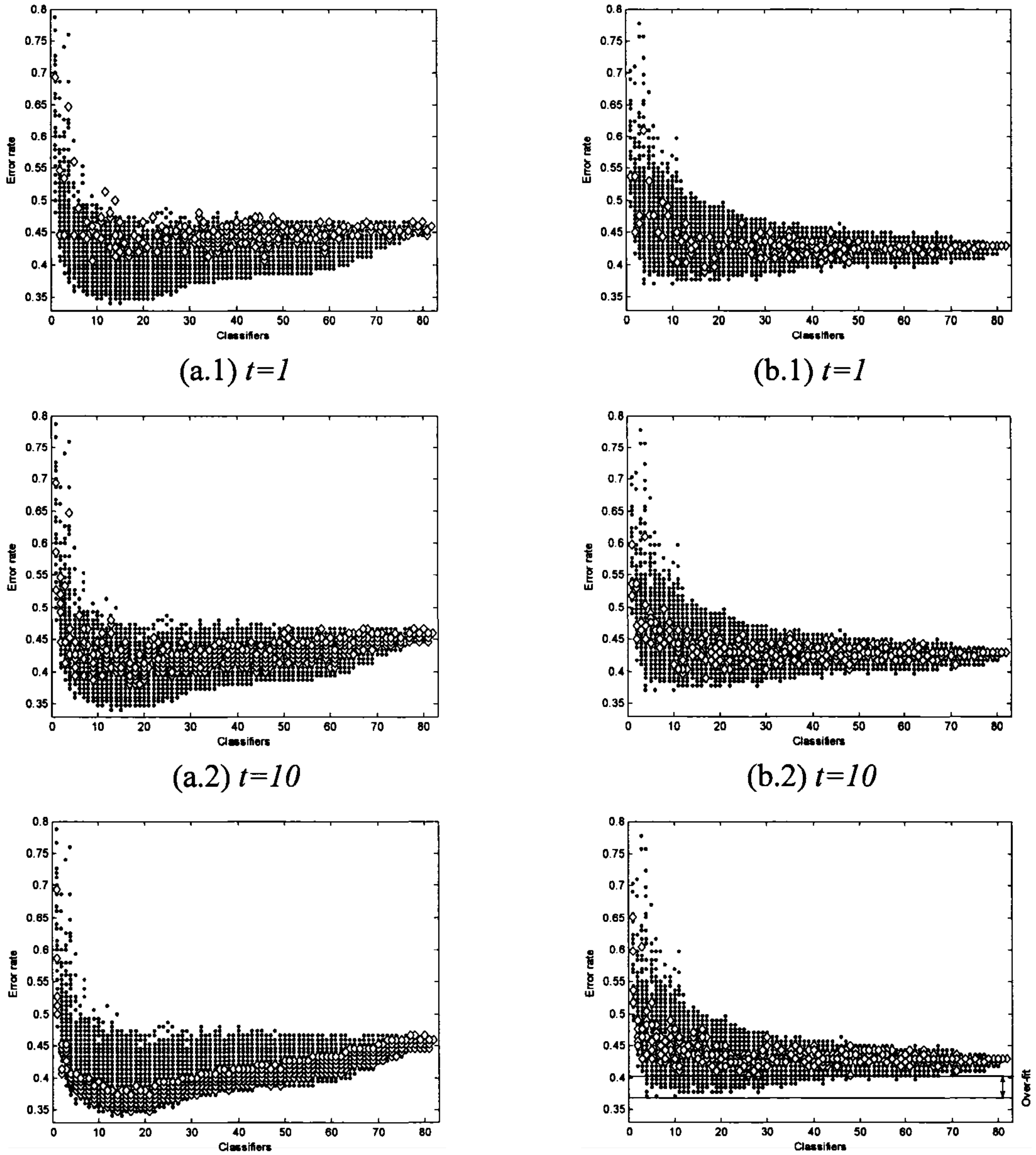

(a.1) *t=1*

(b.1) *t=1*

(a.2) *t=10*

(b.2) *t=10*

(a.3) *t=110*

(b.3) *t=110*

Figure 39 EoC optimization with MOMA at generation *t*: (a) decision frontier on the *optimization* data set and (b) decision frontier projected on the *selection* data set; the most accurate solution in (a.3) has an error rate 9.75% higher than the most accurate solution explored in (c.3)

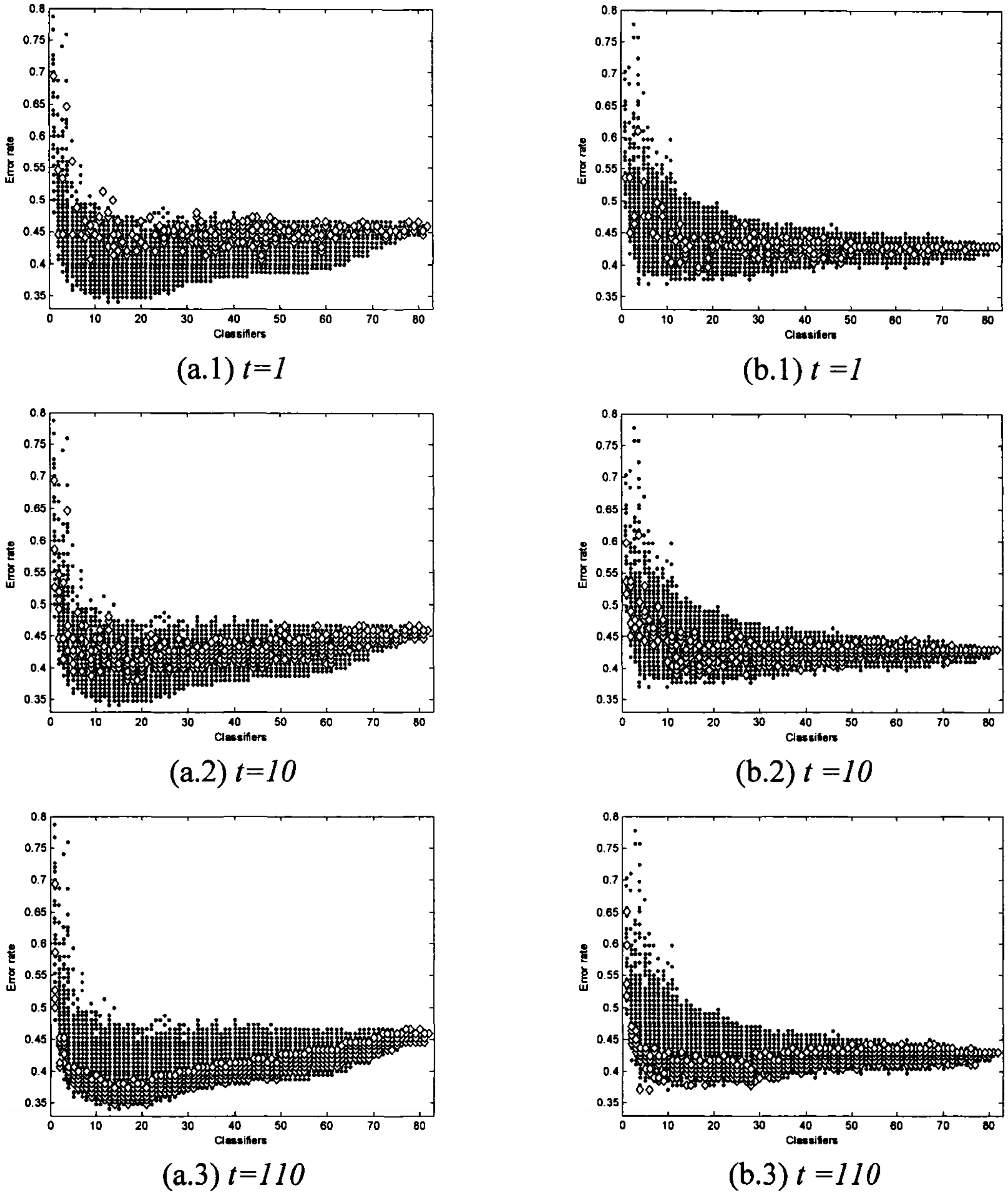

(a.1) *t=1*

(b.1) *t =1*

(a.2) *t=10*

(b.2) *t =10*

(a.3) *t=110*

(b.3) *t =110*

Figure 40 EoC optimization with MOMA at generation t: (a) decision frontier on the *optimization* data set and (b) the actual decision frontier in the *selection* data set; validating solutions through all generations allows the optimization process to find a good approximation set on generalization

Algorithm 5: Template for a MOGA with over-fit control – the population P^{t+1} is validated with the selection data set during mg generations, and the solutions with good generalization power are kept in the auxiliary archive S; in order to avoid over-fitting solutions to the *selection* data set, no feedback is provided to the optimization process from the validation strategy

```
Result : Auxiliary archive $S$
Creates initial population $P^1$ with $m$ individuals
$S = \phi$;
$t = 1$;
while $t < mg$ do
        Evolves $P^{t+1}$ from $P^t$;
        Validates $P^{t+1}$ with the selection data set;
        Update the auxiliary archive $S$ with individuals from $P^{t+1}$ based on the
        validation results;
        $t = t + 1$;
end
```

solutions are inserted and removed from S according to the optimization algorithm used. For a Pareto-based MOGA such as NSGA-II, non-dominated solutions in validation are inserted into S, and dominated solutions are removed if necessary. For MOMA, solutions are inserted according to the decision frontier concept and the maximum number of solutions allowed per cardinality value in the original archive ($\max_{S'}$). Further details on adapting NSGA-II and MOMA are presented in the next section.

4.1 Adapting Optimization Algorithms

Adapting the template in Algorithm 5 to the original NSGA-II produces Algorithm 6. The empty auxiliary archive S is added to the NSGA-II definition, and validated solutions are inserted in S at each generation t according to the auxiliary archive update procedure in Algorithm 7. During this procedure, the *optimization* data set is temporarily replaced by the *selection* data set to evaluate objective functions. Each

Algorithm 6: Modified NSGA-II algorithm – items marked with a star (*) are related to the global validation strategy and are not part of the original algorithm as described in the Appendix 1

```
Result : Auxiliary archive $S$
Creates initial population $P^1$ with $m$ individuals
$S = \phi$; *
$t = 1$;
while $t < mg$ do
        $R^t = P^t \cup Q$;
        $F$ =fast-non-dominated-sort$\left(R^t\right)$;
        while $\left|P^{t+1}\right| + \left|F^i\right| \le m$ do
                $P^{t+1} = P^{t+1} \cup F^i$;
                crowding-distance-assignement$\left(F^i\right)$;
                $i = i + 1$;
        end
        $Sort\left(F^i, \prec_n\right)$;
        $P^{t+1} = P^{t+1} \cup F^i\left[1 : \left(N - \left|P^{t+1}\right|\right)\right]$;
        $Q^{t+1}$=make-new-pop$\left(P^{t+1}\right)$;
        $t = t + 1$;
        Update the auxiliary archive $S$ (Algorithm 7); *
End
```

solution x^i in the current population P^t is tested for insertion in S. If x^i is inserted in S, solutions eventually dominated by x^i in S are checked and eliminated accordingly. At the end of the optimization process the auxiliary archive S contains a Pareto-front of validated solutions. Complete details on NSGA-II can be found in the Appendix 1 and in [63].

Adapting MOMA to the global validation strategy is a simpler process. It is sufficient to temporarily replace the *optimization* data set by the *selection* data set in the original procedure to update the auxiliary archive S already defined in MOMA. The modified auxiliary archive update procedure is indicated in Algorithm 8. The algorithm first

Algorithm 7: Auxiliary archive update procedure for NSGA-II

```
Data : Current population $P^t$ and the auxiliary archive $S$
Result : The modified auxiliary archive $S$
Replaces optimization data set by the selection data set for objective function evaluation;
Calculate objective functions for all solutions in $P^t$;

forall $x^i \in P^t$ do
        if $\nexists x^j, x^j \in P^t \wedge x^j \succ x^i$ then
                $D = \{d \mid xi \succ d \wedge d \in S\}$;
                $S = S \setminus D \cup \{x^i\}$;
        end
end
Restores optimization data set for objective function evaluation;
```

Algorithm 8: Modified auxiliary archive update procedure for MOMA

```
Data: Current population $P^t$ and the auxiliary archive $S$
Result : The modified auxiliary archive $S$
Replaces *optimization* data set by the *selection* data set for objective function evaluation;
forall $x^i \in P^t$ do
        $l = o_1(x^i)$;
        if $o_2(x^i) < o_2(W(S^l)) \wedge x^i \notin S^l$ then
                $S^l = S^l \cup \{x^i\}$;
                if $|S^l| > \max_{S^l}$ then
                        $S^l = S^l \setminus \{W(S^l)\}$;
                end
        end
end
Restores optimization data set for objective function evaluation;
```

replaces the optimization data set by the selection data set. For each solution x^i, the algorithm tests the associated slot S^l for insertion. If x^i is inserted in S^l, the algorithm verifies if it has not exceeded its maximum cardinality ($\max_{S^l}$). If it has exceeded, the algorithm then removes the solution with the worse o_2 value ($W(S^l)$). Finally, the algorithm restores the optimization data set to resume optimization. At the end of the optimization process, the auxiliary archive S will contain the best $\max_{S^l}$ validated fronts. The detailed MOMA and related mathematical definitions are presented in Chapter 3.

4.2 Discussion

This chapter demonstrated that wrapper based classification system optimization is prone to over-fit, similar to the classifier training procedure. It was also demonstrated that a process similar to classifier validation may be applied to these optimization problems to reduce over-fit with a higher success rate than the traditional approach to validate solutions after the optimization process is complete. Thus, a global validation procedure is proposed to the optimization process using a *selection* data set unknown to the wrapped classifier.

The global validation verifies the generalization power of solutions through generations using the *selection* data set, storing good solutions into an auxiliary archive to avoid their loss due to genetic selection pressure towards over-fitted solutions. Once the optimization process is complete, good solutions are found inside the archive despite the fact that the optimization algorithm may discard them through generations.

The global validation will be verified in Chapter 6 during the optimization of classification systems for handwritten digits. Optimization is performed using the approach proposed in Chapter 2, testing the IFE, FSS and EoC approaches. It is expected that global validation is capable of producing solutions at least as accurate as the traditional approach to validate solutions at the last generation in problems where over-fit is not an issue. In problems where over-fit is present, it is expected that the global validation produces better results, as demonstrated with the EoC problems in this chapter. The most accurate approach will be carried out to optimize a classification system for handwritten uppercase letters in Chapter 7 to test the approach on an unknown problem.

CHAPTER 5

STOPPING CRITERION

The execution of MOGAs is usually limited by a maximum number of generations, mg. This approach helps to estimate and limit execution time, but does not take into account the population improvement rate and may allow the optimization algorithm to run in situations in which it cannot improve solutions any further. This section proposes a stopping criterion for MOGAs adapted to the methodologies discussed in this thesis (IFE, EoC and FSS) considering both the maximum number of generations, mg, and the population improvement rate during the optimization process in the context of solution over-fit.

5.1 Concepts

Optimization of classification systems is plagued by candidate solution over-fit to the optimization data set, and the optimization algorithm will improve solutions during more generations than it is actually necessary. This indicates the need for a criterion to stop the optimization process if it has already converged to a good approximation set. The criterion stops the MOGA either if it has reached mg generations or if it has been detected that the algorithm has converged to a good approximation set. To perform this operation the stopping criterion needs means to control the approximation set improvement through generations.

Zitzler and Thiele introduced the coverage metric for Pareto-based approaches in [74]. Given two different approximation sets A and B, $coverage(A, B)$ indicates the fraction of solutions in B that are covered, i.e. weakly dominated, by at least one solution in A. A solution i weakly dominates solution j ($i \succeq j$) if i is not worse than j in all

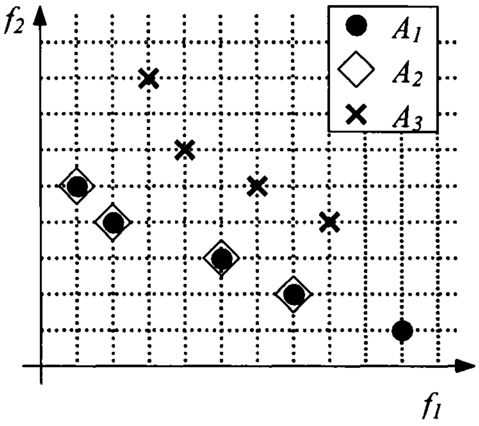

Figure 41 Coverage on three approximation sets (A_1, A_2, A_3) – A_3 is completely covered by A_1 and A_2 (*coverage*(A_1, A_3) = *coverage*(A_2, A_3) = 1), approximation set A_2 covers 80% of set A_1 ($coverage(A_2, A_1) = 0.8$) and A_1 completely covers A_2 ($coverage(A_1, A_2) = 1$)

objective functions. Fig. 41 depicts an example with three different approximation sets. To adapt the coverage metric to the decision frontier used by MOMA, we compare o_2 values in solutions with equal o_1 values. Given solutions i and j, it is said that $i \trianglerighteq j$ (i is weakly better than j) when the two conditions are met:

- $o_1(i) = o_1(j)$, both i and j map to the same slot S^l.
- $o_2(i)$ is not worse than $o_2(j)$. For a minimization problem, $o_2(i) \le o_2(j)$.

The following properties are valid for the weakly better relation:

- Reflexive: a solution i is weakly better than itself ($i \trianglerighteq i$).
- Transitive: if $i \trianglerighteq j$ and $j \trianglerighteq k$, it can be said that $i \trianglerighteq k$.

Thus, $coverage(A,B)$ with MOMA indicates the fraction of solutions in B that have at least one weakly better solution in A.

Later, Zitzler *et al.* demonstrated in [72] a coverage-based comparison method for approximation sets that detects when A is better than B ($A \rhd B$). An approximation set A is better than B when $coverage(A,B)=1$ and $A \neq B$. In Fig. 41, sets A_1 and A_2 are better than A_3, and set A_1 is better than A_2. The coverage metric may also be used to measure the improvement in two consecutive generations, P^t and P^{t+1}. For each generation t, there is a set of best solutions B^t, the current Pareto front for NSGA-II and the decision frontier for MOMA.

Given B^t and B^{t+1}, NSGA-II and MOMA will either improve solutions in the population and $B^{t+1} \rhd B^t$, or no improvement will be achieved and $B^{t+1} = B^t$. When there is solution improvement, set B^t is not able to cover the entire set B^{t+1} and $coverage\left(B^t, B^{t+1}\right) < 1$. If there is no solution improvement ($B^{t+1} = B^t$), then B^t covers the entire set B^{t+1} and $coverage\left(B^t, B^{t+1}\right) = 1$ (the two sets are equal), thus the improvement between two consecutive generations is defined in (5.1), which calculates the fraction of individuals in B^{t+1} that have been improved in comparison to B^t.

$$improvement\left(B^{t+1}, B^t\right) = 1 - coverage\left(B^t, B^{t+1}\right) \tag{5.1}$$

5.2 Stopping MOGAs

To halt the optimization process, we assume that (5.1) is capable to measure the improvement between two consecutive generations. The concept of MOGAs indicates that the population will evolve through generations until it reaches a good approximation set and is unable to further improve solutions. It is desirable to detect this moment and stop the optimization process regardless of the mg value set. Thus, the ideal MOGA optimizes solutions and improve them through generations while $improvement > 0$, until it finally converges. After this generation t_{stop}, the MOGA is unable to improve solutions and $improvement = 0$, as the solution set is no further improved.

However, it was observed on experimental data that both MOMA and NSGA-II will often go through cycles where the algorithm takes some generations to actually improve the approximation set. Hence, measuring the improvement between two consecutive generations is not enough to detect the generation at which the algorithm should stop. For a fair tracking of solution improvement, the improvement rate at generation t (ir^t) is calculated in (5.2) as the average improvement in the last w generations, $1 < w < mg$.

$$ir^t = \frac{\sum_{i=t-w,t>w}^{t-1} improvement\left(B^{i+1}, B^i\right)}{w} \tag{5.2}$$

Choosing an incorrect w value may stop the algorithm before convergence. Fig. 42 demonstrates the effect with two different w values. A low w value (w=10) indicates that the algorithm stopped improving ($ir^t = 0$) earlier, whereas a suitable value (w=41) will let the algorithm explore more solutions and find the true stopping generation.

At the end of each generation $t, t > w$, the ir^t value is evaluated and the optimization process is stopped at generation t_{stop} either if $ir^{t_{stop}} \leq min_{ir}$, a minimum improvement rate threshold, or if $t_{stop} = mg$. The stopping criterion introduces two new parameters to the optimization process, w and min_{cr}. It is desirable to have both good convergence and a good spread of solutions in the approximation set, hence it is adequate to have

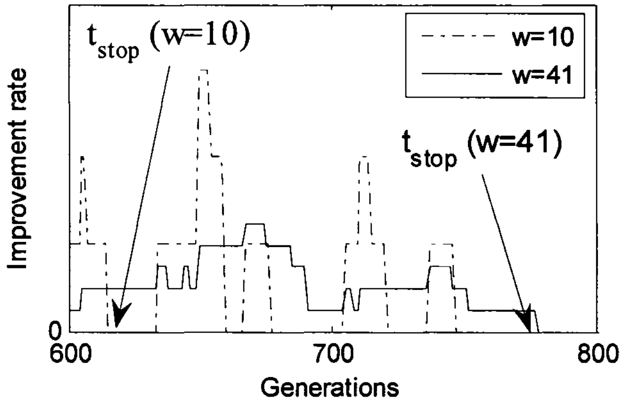

Figure 42 Impromente rate ir^t measured in the last w generations (MLP EoC optimization with MOMA)

$min_{ir} = 0$. The global validation strategy will keep good validated solutions in the auxiliary archive S, hence the optimization algorithm has to stop when it has found a good approximation set that is probably over-fitted to the optimization data set. The w value is expected to be problem-dependent, and it is determined empirically for the IFE and EoC approaches in Chapter 6.

5.3 Discussion

This chapter discussed a stopping criterion for MOGAs, tracking the solution set improvement to determine a generation t^{stop} at which the optimization process is stopped. The stopping criterion is compatible with the global validation strategy discussed in Chapter 4. It is said to be compatible because the optimization algorithms will over-fit solutions to the *optimization* data set, whereas good validated solutions are likely to be found earlier in the optimization process.

The experiments in Chapter 6 will be used to determine a w value related to the binary string length of optimized individuals, in the context of the optimization of a classification system for handwritten digits. This value will be tested on an unknown problem in Chapter 7, using the approach to optimize a classification system for uppercase letters.

The scope of this thesis is limited to the optimization of classification systems, however, the proposed approach may also be used with traditional Pareto-based MOGAs on different problems. Future experiments will verify this possibility, also working with real coded individuals.

CHAPTER 6

VALIDATION EXPERIMENTS ON ISOLATED HANDWRITTEN DIGITS

Once the classification system optimization approach is defined, the next step is to verify the chosen optimization algorithms to each optimization stage. Thus, this section experiments the approach with both zoning operators and optimization algorithms. The goal is to define the most appropriate zoning operator and the most performing algorithm for each optimization stage, in order to reduce processing time while keeping solution quality.

Tests are performed using isolated handwritten digits extracted from the NIST-SD19 database [16], a comprehensive database with more than 300000 handwritten digits samples for optimization and testing. This large database size allows for relevant statistical analysis when comparing optimization algorithms and zoning operators. Complete results for these statistical analysis are detailed in the Appendix 2, whereas this section borrows these test results to present conclusions.

6.1 Experimental Protocol

The tests indicated in Fig. 43 are performed to verify the impact of over-fit and the previously discussed methodology to optimize classification systems. They are performed with both NSGA-II and MOMA for comparison purposes. First, the IFE methodology is solved to obtain the representation set RS_{IFE} (the auxiliary archive S). For NSGA-II, S is a Pareto front, while for MOMA, RS_{IFE} is a set of max_{S^l} fronts. These sets are used to train the classifier sets K_{PD} and K_{MLP} using the PD and MLP classifiers (the PD classifier is included for comparison purposes). For a single classifier system, the most accurate classifiers $SI_{PD} \in K_{PD}$ and $SI_{MLP} \in K_{MLP}$ are selected. EoCs

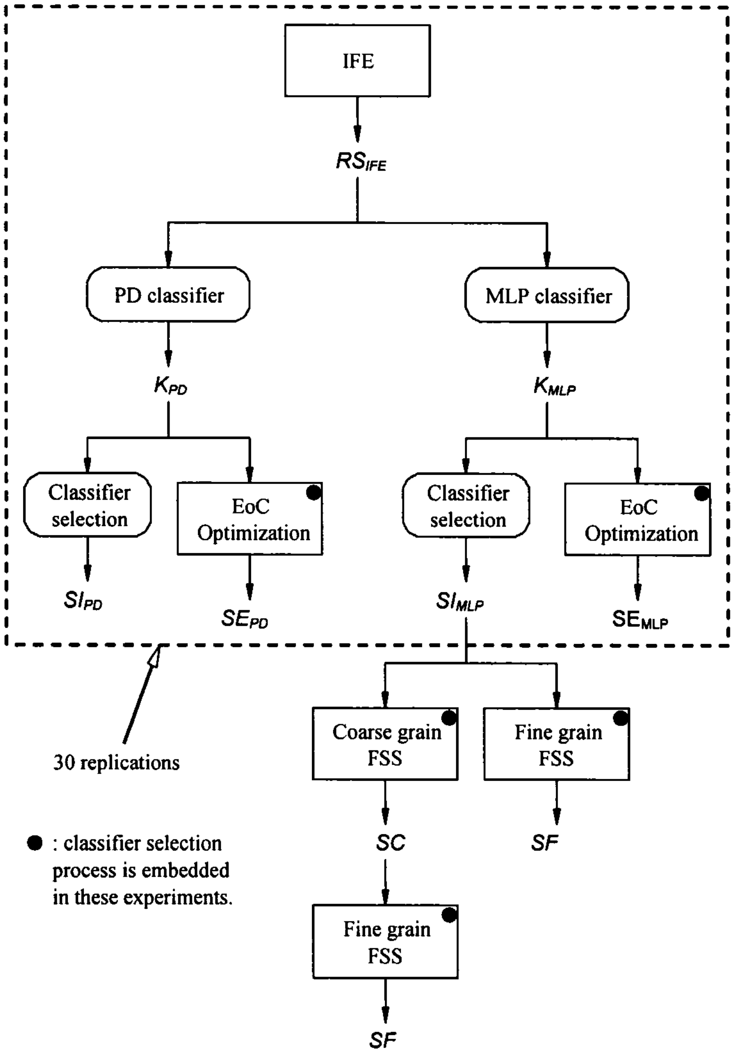

Figure 43 Experimental overview – the classification system optimization approach is tested in two stages, IFE and the EoC methodologies are replicated 30 times for statistical analysis, and experimentation on FSS is performed once, due to the processing time required (the PD classifier is tested only during the first stage, whereas the MLP classifier is tested in both)

are then created with K_{PD} and K_{MLP}, producing SE_{PD} and SE_{MLP}. To further compare NSGA-II and MOMA, an EoC is created with NSGA-II using RS_{IFE} optimized by MOMA, producing SE'_{PD} and SE'_{MLP}. These tests are performed 30 times for meaningful statistical analysis. Then, the FSS approach further refines solution SI_{MLP} with both

NSGA-II and MOMA. Because of the processing time required for each FSS experiment (1 to 3 days), the FSS approach is limited to a single run. Two different FSS scenarios are analyzed: the traditional FSS approach optimizes SI_{MLP} directly with the fine grain FSS to obtain SF'; then, both FSS levels are applied on SI_{MLP} to obtain SC and SF. The two scenarios are compared to determine whether or not the two-level FSS approach is better than traditional MOGA-based FSS.

To demonstrate solution over-fit related to the MOGA optimization process, the experiments are analyzed in three situations. First, no validation strategy is used and solutions are selected based only on the *optimization* data set accuracy. Next, candidate solutions are validated in the last generation with the *selection* data set. Finally, solutions are validated in all generations with the global validation strategy using the *selection* data set. The three approaches are compared to demonstrate which produces the best results.

The disjoint data sets in Table V are used in the experiments, which are isolated handwritten digits extracted from NIST-SD19. Except for $test_a$ and $test_b$, observations for each class are uniformly distributed in each data set. MLP hidden nodes are optimized as feature set cardinality fractions in the set $f = \{0.4, 0.45, 0.50, 0.55, 0.6\}$. MLP classifier training is performed with the *training* data set, while the PD classifier is trained with the smaller *training'* data set, to implement a computationally efficient wrapper approach for IFE. The remaining data sets are used with both classifiers. The *validation* data set is used to adjust the classifier parameters (MLP hidden nodes and PD hyper planes). The wrapper approach is performed with the *optimization* data set, and the *selection* data set is used to validate candidate solutions (global validation and validation at the last generation). Solutions are compared with $test_a$ and $test_b$, data sets

Table V

Handwritten digits data sets extracted from NIST-SD19

Database	Size	Origin	Sample range
training	150000	hsf_0123	1 to 150000
training'	50000	hsf_0123	1 to 50000
validation	15000	hsf_0123	150001 to 165000
optimization	15000	hsf_0123	165001 to 180000
selection	15000	hsf_0123	180001 to 195000
$test_a$	60089	hsf_7	1 to 60089
$test_b$	58646	hsf_4	1 to 58646

unknown to the resulting solutions. It is known that $test_b$ is more difficult to classify than $test_a$ [16], hence the robustness of the resulting solutions are tested on two different levels of classification complexity.

Rejection strategies are applied on the best solutions obtained in each optimization stage. The experimental data are also used to empirically determine the w value and validate the stopping criterion with the global validation strategy. The 30 replications with the IFE and EoC methodologies are divided into two groups. The first group of 10 random replications is used to empirically estimate the w values and to relate w to the binary string length. The second group, with the 20 remaining replications, is then used to validate the stopping criterion. For each replication, the criterion is verified if the validated solutions are the same as they are when the traditional maximum generation number (mg) approach is used. The FSS experimental data are used to further validate the relation between w and the binary string length (L).

The parameters used with MOMA are the following: crossover probability is set to $p_c = 80\%$, and mutation is set to $p_m = 1/L$, where L is the length of the mutated binary string [90]. The maximum number of generations is set to $mg = 1000$ for all experiments to study the impact of the w value, and the local search will look for $n = 1$

neighbors during $NI=3$ iterations, with deviation $a=0\%$. Each slot in the archive S is allowed to store $max_{S^l}=5$ solutions. These parameters were determined empirically in Chapter 3. The same parameters ($p_c=80\%, p_m=1/L$ and $mg=1000$) are used for NSGA-II. Population size depends on the optimization problem. To optimize the zoning operator, the population size is $m=64$, while to optimize FSS, we use $m=100$ to keep processing time reasonable. For the EoC optimization, $m=166$ is used with RS_{IFE} optimized by MOMA (m is twice $|RS_{IFE}|$), and $m=32$ for RS_{IFE} optimized by NSGA-II. Individual initialization is performed in two steps for both optimization algorithms. The first step creates one individual for each possible cardinality value. For IFE and FSS optimization, one individual associated to each possible zone number is added, while for EoC optimization, one individual is added for each possible EoC cardinality. The second step completes the population with individuals initialized with a Bernoulli distribution.

Experiments are conducted on a Beowulf cluster with 25 nodes using Athlon XP 2500+ processors with 1GB of PC-2700 DDR RAM (333MHz FSB). The optimization algorithms were implemented using LAM MPI v6.5 in master-slave mode with a simple load balance. PD vote and MLP output calculations were performed once in parallel using a load balance strategy, and results were stored in files to be loaded into memory for the EOC optimization process.

All tests replicated 30 times were subjected to a multiple comparison test. A Kruskal-Wallis nonparametric test is used to test the equality of mean values, using bootstrap to create the confidence intervals from the 30 observations in each sample. The conclusions presented regarding the validation strategies and the algorithm comparison were obtained with a confidence level of 95% ($\alpha=0.05$). Further details on these tests are found in the Appendix 2.

6.2 Divider Zoning Experimental Results

This section presents and discusses results obtained for handwritten digits using the divider zoning operator, and is divided in four subsections. The first details results for the IFE and EoC optimization, followed by a subsection that presents results for the FSS optimization. The third subsection verifies the proposed stopping criterion on the experimental data. Finally, the last subsection presents conclusions related to the results obtained with the divider zoning operator on handwritten digits.

6.2.1 IFE and EoC Experimental Results

The first stage optimizes the IFE and EoC methodologies in 30 replications using the divider zoning operator. For each run, the most accurate solution is selected according to the validation strategy used. Figs. 44 and 45 detail the error rate dispersion obtained in these experiments for the PD and MLP classifiers respectively. Mean values and standard deviations for these experiments are detailed in Tables VI and VII. In both tables, *validation* indicates the validation strategy used, *zones* the solution zone number, *HN* the number of nodes in the MLP hidden layer (MLP classifier results only), $|S|$ the solution cardinality in features or aggregated classifiers, and e_{test_a} and e_{test_b} the error rates in the $test_a$ and $test_b$ data sets. The baseline representation is included in both tables for reference.

In terms of validation strategies, the statistical tests in Appendix 2 indicate that the results obtained have an order relation between the validation approaches tested. Using no validation is worse than using validation at the last generation, which in turn is worse than using the global validation strategy. Mean error rate values in Tables VI and VII are lower with the global validation strategy, which is also observed in Figs. 44 and 45.

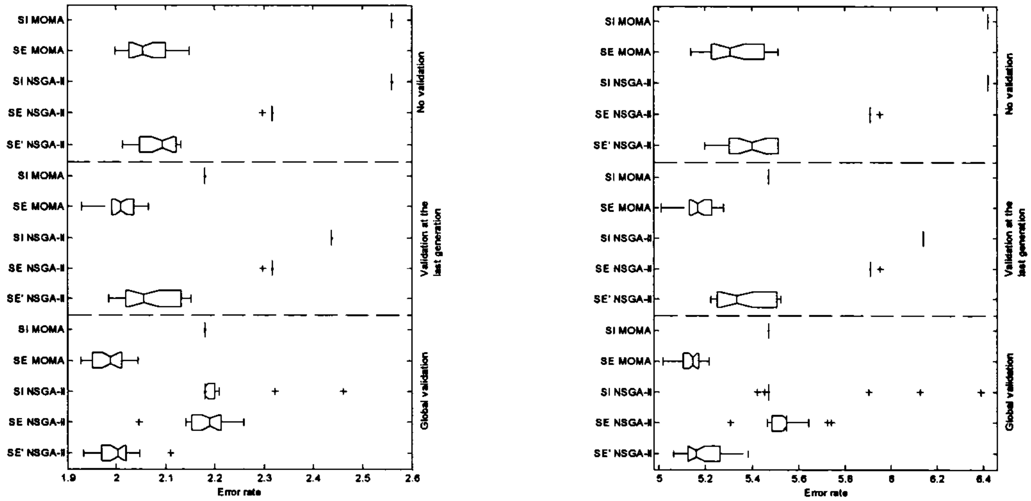

(a) *test*$_a$ (b) *test*$_b$

Figure 44 PD error rate dispersion on 30 replications with the divider zoning operator – each solution set relates to one validation strategy tested: no validation, the traditional validation at the last generation and global validation

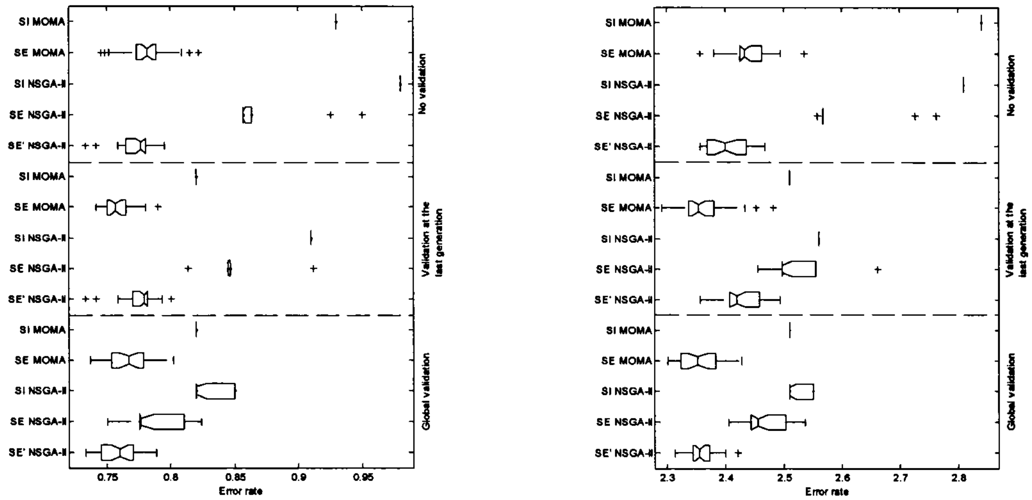

(a) *test*$_a$ (b) *test*$_b$

Figure 45 MLP error rate dispersion on 30 replications with the divider zoning operator – each solution set relates to one validation strategy tested: no validation, the traditional validation at the last generation and global validation

Table VI

PD optimization results with the divider zoning operator – mean values on 30 replications and standard deviation values (shown in parenthesis)

Validation	Solution	MOMA				NSGA-II			
		Zones	$\lvert S \rvert$	e_{test_a}	e_{test_b}	Zones	$\lvert S \rvert$	e_{test_a}	e_{test_b}
	Baseline	6	132	2.96%	6.83%	6	132	2.96%	6.83%
None	SI_{PD}	12	264	2.57% (0)	6.42% (0)	12	264	2.57% (0)	6.42% (0)
	SE_{PD}	-	16.67	2.07% (0.043)	5.32% (0.121)	-	7	2.31% (0.007)	5.92% (0.015)
	SE'_{PD}	-	-	-	-	-	12.47	2.08% (0.042)	5.40% (0.112)
Last	SI_{PD}	15	330	2.18% (0)	5.47% (0)	10	220	2.44% (0)	6.14% (0)
	SE_{PD}	-	22.5	2.01% (0.032)	5.17% (0.069)	-	7	2.31% (0.07)	5.91% (0.014)
	SE'_{PD}	-	-	-	-	-	11.47	2.07% (0.058)	5.37% (0.114)
Global	SI_{PD}	15	330	2.18% (0)	5.47% (0)	15.77	346.85	2.22% (0.0001)	5.55% (0.02)
	SE_{PD}	-	22.33	1.98% (0.033)	5.14% (0.056)	-	7.4	2.18% (0.063)	5.53% (0.122)
	SE'_{PD}	-	-	-	-	-	24.67	2.00% (0.040)	5.19% (0.087)

Whereas these conclusions are valid for the general case, in three specific situations the differences among validation strategies are not significant. Using MOMA with IFE produces the same results with validation at the last generation or the global validation. The same is observed when creating MLP EoCs with MOMA. Finally, creating EoCs with NSGA-II will produce similar results with no validation or validation at the last generation. The effect observed with MOMA is related to its auxiliary archive strategy, which keeps a solution set of $max_{S'}$ solutions for each possible cardinality value, and partially removes the over-fit with the validation at the last generation. The exception observed with NSGA-II is not relevant, as the global validation strategy is better. The experimental results associated to the tests in Appendix 2 indicate that the global validation strategy is better for both the IFE and EoC methodologies, as the impact of over-fit on solutions is not known *a priori*.

Table VII

MLP optimization results with the divider zoning operator – mean values on 30 replications and standard deviation values (shown in parenthesis)

Validation	Solution	MOMA					NSGA-II				
		Zones	HN	$\|S\|$	e_{test_a}	e_{test_b}	Zones	HN	$\|S\|$	e_{test_a}	e_{test_b}
	Baseline	6	60	132	0.91%	2.89%	6	60	132	0.91%	2.89%
None	SI_{MLP}	8	97	176	0.93% (0)	2.84% (0)	6	70	132	0.98% (0)	2.81% (0)
	SE_{MLP}	-	-	10.07	0.78% (0.017)	2.44% (0.037)	-	-	4.73	0.88% (0.037)	2.61% (0.081)
	SE'_{MLP}	-	-	-	-	-	-	-	6.8	0.77% (0.015)	2.41% (0.037)
Last	SI_{MLP}	15	132	330	0.82% (0)	2.51% (0)	12	132	264	0.91% (0)	2.56% (0)
	SE_{MLP}	-	-	16.23	0.76% (0.012)	2.37% (0.042)	-	-	4.77	0.85% (0.015)	2.52% (0.040)
	SE'_{MLP}	-	-	-	-	-	-	-	4.9	0.77% (0.016)	2.42% (0.034)
Global	SI_{MLP}	15	132	330	0.82% (0)	2.51% (0)	13.67	129.32	300.6	0.83% (0.013)	2.52% (0.018)
	SE_{MLP}	-	-	10.33	0.77% (0.017)	2.35% (0.030)	-	-	4.5	0.79% (0.023)	2.47% (0.040)
	SE'_{MLP}	-	-	-	-	-	-	-	14.13	0.76% (0.016)	2.36% (0.022)

Optimization algorithms are compared based on the results obtained with the global validation strategy. MOMA and NSGA-II performs similarly with both classifiers to optimize IFE (solutions SI_{PD} and SI_{MLP}), selecting the zoning representation with 15 active zones depicted in Fig. 46. MOMA has no error rate dispersion with either classifier, while NSGA-II may produce suboptimal solutions. This result is no surprise, as MOMA was designed for the IFE methodology. Another motivation for choosing MOMA at the IFE level is to create a more diverse RS_{IFE} set. In the 30 experimental replications, the RS_{IFE} cardinality is $|RS_{IFE}| = 82$ when $max_{S'} = 5$ with MOMA, whereas with NSGA-II the cardinality is only $|RS_{IFE}| = 10$. MOMA also offers

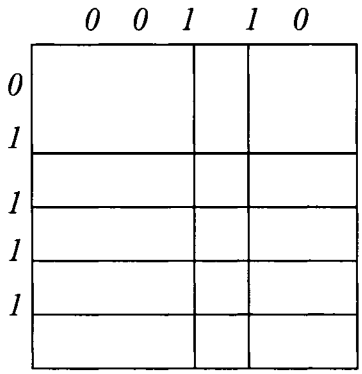

Figure 46 Solution SI_{PD} / SI_{MLP} (15 active zones) selected with the global validation strategy in the IFE optimization with the divider zoning operator

higher lateral diversity due to the decision frontier, and its RS_{IFE} set comprises individuals with up to 36 active zones, while the RS_{IFE} produced by NSGA-II contains individuals with at most 15 active zones. Classifier diversity is a key issue in optimizing EoCs, and this is reflected on results in Tables VI and VII, where SE_{PD} and SE_{MLP} optimized by NSGA-II are worse than SE'_{PD} and SE'_{MLP} optimized by NSGA-II with RS_{IFE} optimized by MOMA.

Comparing the EoCs optimized with the global validation and using the RS_{IFE} obtained by MOMA, there is no significant difference between MOMA and NSGA-II. Mean error rates in Tables VI and VII are comparable according to tests performed in Appendix 2. NSGA-II is less processor-intensive than MOMA, however, and thus it is preferable to use NSGA-II to optimize EoCs with the RS_{IFE} obtained by MOMA.

Mean error rates in Tables VI and VII also demonstrate the accuracy improvement over the baseline representation defined by a human expert. For a single PD classifier, the IFE methodology reduced error rates by 26.35% on $test_a$ and 19.91% on $test_b$. For a PD EoC obtained by NSGA-II, error rates on $test_a$ are reduced by 32.43% based on mean values and by 24.01% on $test_b$. While improvements are proportionally higher on $test_a$, numerically they are more significant on $test_b$, where the EoC can correctly recognize 1.64% (962) more observations. This is an important improvement, as $test_b$ is more difficult to classify than $test_a$. For a single MLP classifier, the IFE methodology reduced error rates by 9.89% on $test_a$ and by 13.15% on $test_b$. For an MLP EoC obtained with NSGA-II, improvements based on mean values are 16.48% on $test_a$ and 18.33% on $test_b$. Again, improvements on $test_b$ are numerically higher, as the EoC can correctly recognize 0.53% (311) more observations in $test_b$.

These experimental results indicate that the global validation strategy is the best approach for both the IFE and EoC methodologies. It was also observed that it is better to use MOMA to optimize the IFE in order to obtain a diverse set RS_{IFE} to optimize EoCs using the NSGA-II. Selecting the best solutions with this configuration produces the results in Tables VIII and IX. As indicated by mean values previously discussed in Tables VI and VII, EoC cardinality is lower for the MLP EoC. Both tables details classification accuracy with zero rejection ($e_{\max}$) and with three fixed error rates using rejection. Each classifier requires different rejection strategies, which are detailed in the Appendix 3.

Figures 47 and 48 demonstrate the error-rejection curve for solutions in Tables VIII and IX. Given these results, we observe that solutions produced by the IFE and EoC optimization approaches outperform the baseline representation not only with zero rejection, but with rejection as well. Classification systems optimized with both the PD and MLP classifiers are more robust than the original baseline representation, yielding higher accuracies. We observe that the PD EoC accuracy is boosted when using rejection rates higher than 0%, which does not happen with the MLP EoC. This effect

Table VIII

IFE and EoC best results obtained in 30 replications with the PD classifier (handwriten digits using the divider zoning operator) – accuracies measured with and without rejection

Solution	Zones	$\|S\|$	$test_a$				$test_b$			
			$e_{\max}$	1.5%	1%	0.5%	$e_{\max}$	3%	2%	1%
Baseline	6	132	97.04%	92.67%	85.15%	63.78%	93.17%	85.31%	77.69%	61.64%
SI_{PD}	15	330	97.82%	96.05%	90.15%	68.96%	94.53%	88.57%	81.64%	67.71%
SE_{PD}	-	23	98.05%	97.62%	96.96%	95.35%	94.94%	93.03%	90.87%	86.47%

Table IX

IFE and EoC best results obtained in 30 replications with the MLP classifier (handwriten digits and using the divider zoning operator) – accuracies measured with and without rejection

Solution	Zones	$\|S\|$	$test_a$				$test_b$			
			$e_{\max}$	0.5%	0.25%	0.1%	$e_{\max}$	1.5%	1%	0.5%
Baseline	6	132	99.09%	98.22%	96.72%	93.46%	97.11%	94.64%	92.90%	88.01%
SI_{MLP}	15	330	99.18%	98.54%	97.10%	94.41%	97.49%	96.14%	94.65%	91.26%
SE_{MLP}	-	11	99.27%	98.88%	98.07%	95.45%	97.67%	96.65%	95.27%	92.19%

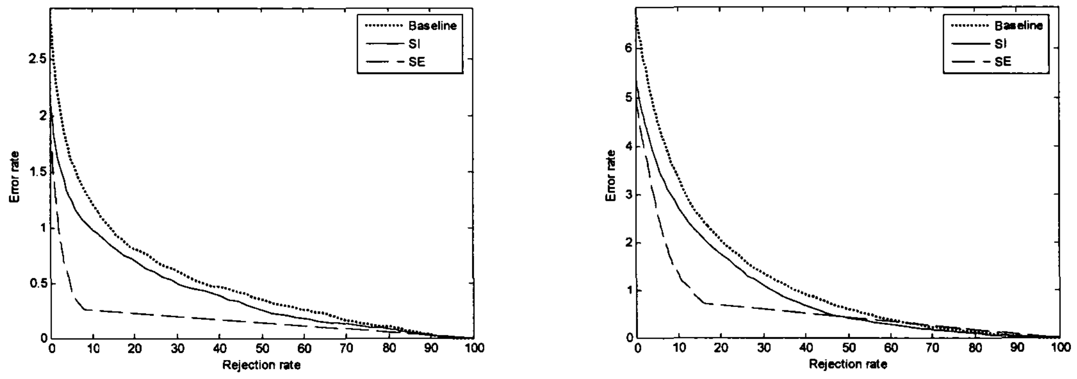

(a) $test_a$ (b) $test_b$

Figure 47 PD classifier rejection rate curves of solutions in Table VIII (IFE with divider zoning operator)

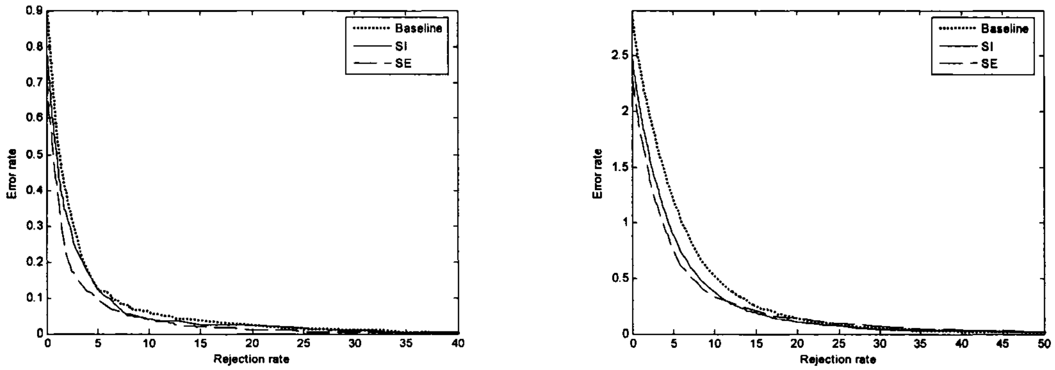

(a) $test_a$ (b) $test_b$

Figure 48 MLP classifier rejection rate curves of solutions in Table IX (IFE with divider zoning operator)

relates to the model-based approach used by PD, which is less discriminating than an MLP classifier.

The EoCs in Tables VIII and IX combine multiple classifiers to predict unknown observations. The individual classifiers for each EoC SE are detailed in Figs. 49 and 50, for the PD and MLP classifiers respectively, where $|S|$ indicates the zone number associated to the zoning representation. It is interesting to observe that not only accurate classifiers compose each EoC, as classifiers with lower accuracies contribute positively to the overall EoC. This confirms the claim that classifier diversity is a key issue for EoC optimization. Also, the PD EoC includes the representation SI optimized by MOMA and the baseline representation (Figs. 49.e and 49.l), whereas the MLP EoC does not include any of them.

6.2.2 FSS Experimental Results

The next experiment reduces the SI_{MLP} complexity through FSS. The goal is to reduce representation complexity while keeping the accuracy comparable to that of the original

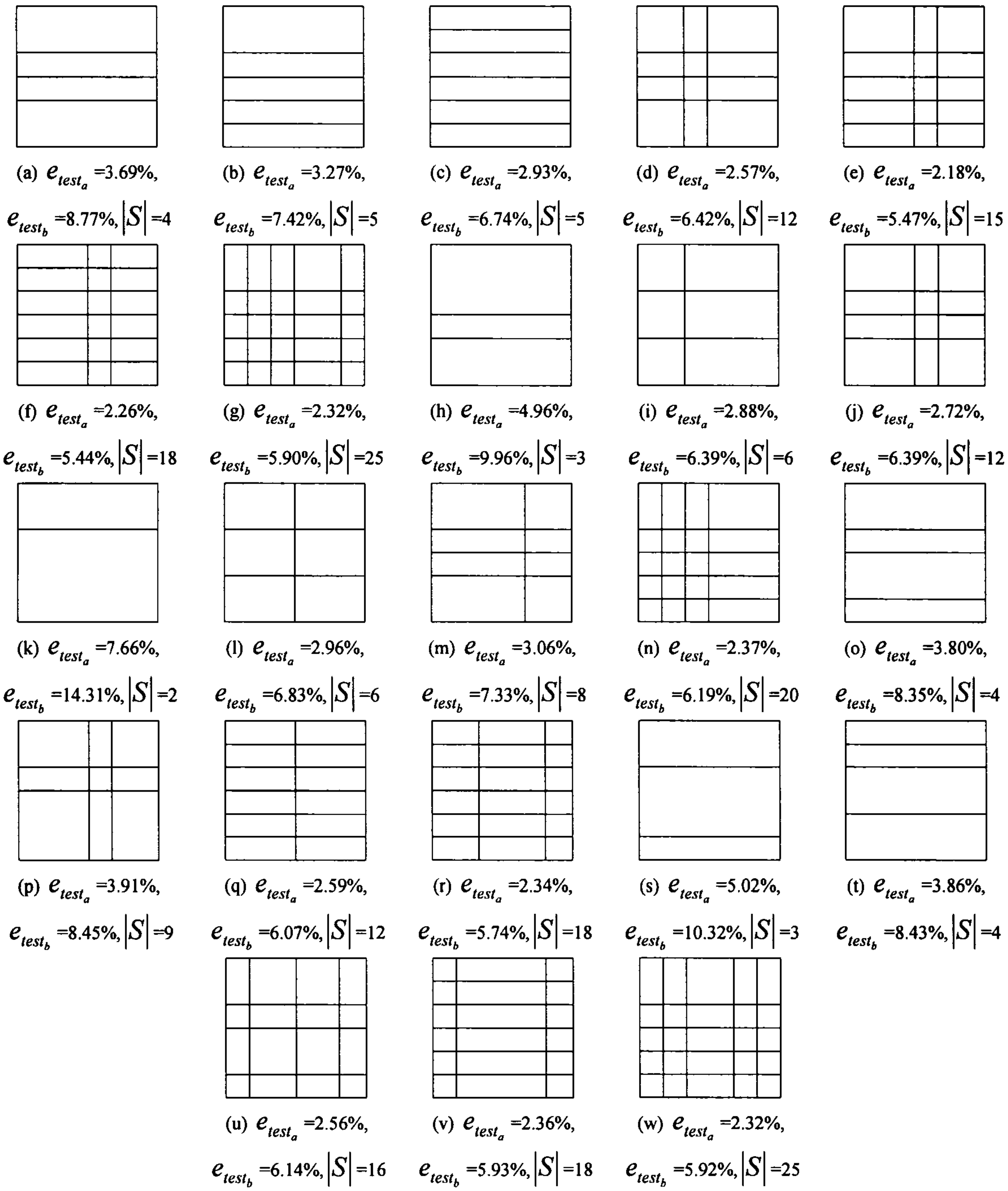

(a) e_{test_a} =3.69%, e_{test_b} =8.77%, $|S|$ =4

(b) e_{test_a} =3.27%, e_{test_b} =7.42%, $|S|$ =5

(c) e_{test_a} =2.93%, e_{test_b} =6.74%, $|S|$ =5

(d) e_{test_a} =2.57%, e_{test_b} =6.42%, $|S|$ =12

(e) e_{test_a} =2.18%, e_{test_b} =5.47%, $|S|$ =15

(f) e_{test_a} =2.26%, e_{test_b} =5.44%, $|S|$ =18

(g) e_{test_a} =2.32%, e_{test_b} =5.90%, $|S|$ =25

(h) e_{test_a} =4.96%, e_{test_b} =9.96%, $|S|$ =3

(i) e_{test_a} =2.88%, e_{test_b} =6.39%, $|S|$ =6

(j) e_{test_a} =2.72%, e_{test_b} =6.39%, $|S|$ =12

(k) e_{test_a} =7.66%, e_{test_b} =14.31%, $|S|$ =2

(l) e_{test_a} =2.96%, e_{test_b} =6.83%, $|S|$ =6

(m) e_{test_a} =3.06%, e_{test_b} =7.33%, $|S|$ =8

(n) e_{test_a} =2.37%, e_{test_b} =6.19%, $|S|$ =20

(o) e_{test_a} =3.80%, e_{test_b} =8.35%, $|S|$ =4

(p) e_{test_a} =3.91%, e_{test_b} =8.45%, $|S|$ =9

(q) e_{test_a} =2.59%, e_{test_b} =6.07%, $|S|$ =12

(r) e_{test_a} =2.34%, e_{test_b} =5.74%, $|S|$ =18

(s) e_{test_a} =5.02%, e_{test_b} =10.32%, $|S|$ =3

(t) e_{test_a} =3.86%, e_{test_b} =8.43%, $|S|$ =4

(u) e_{test_a} =2.56%, e_{test_b} =6.14%, $|S|$ =16

(v) e_{test_a} =2.36%, e_{test_b} =5.93%, $|S|$ =18

(w) e_{test_a} =2.32%, e_{test_b} =5.92%, $|S|$ =25

Figure 49 Zoning strategies associated to individual classifiers in the PD EoC *SE* in Table VIII

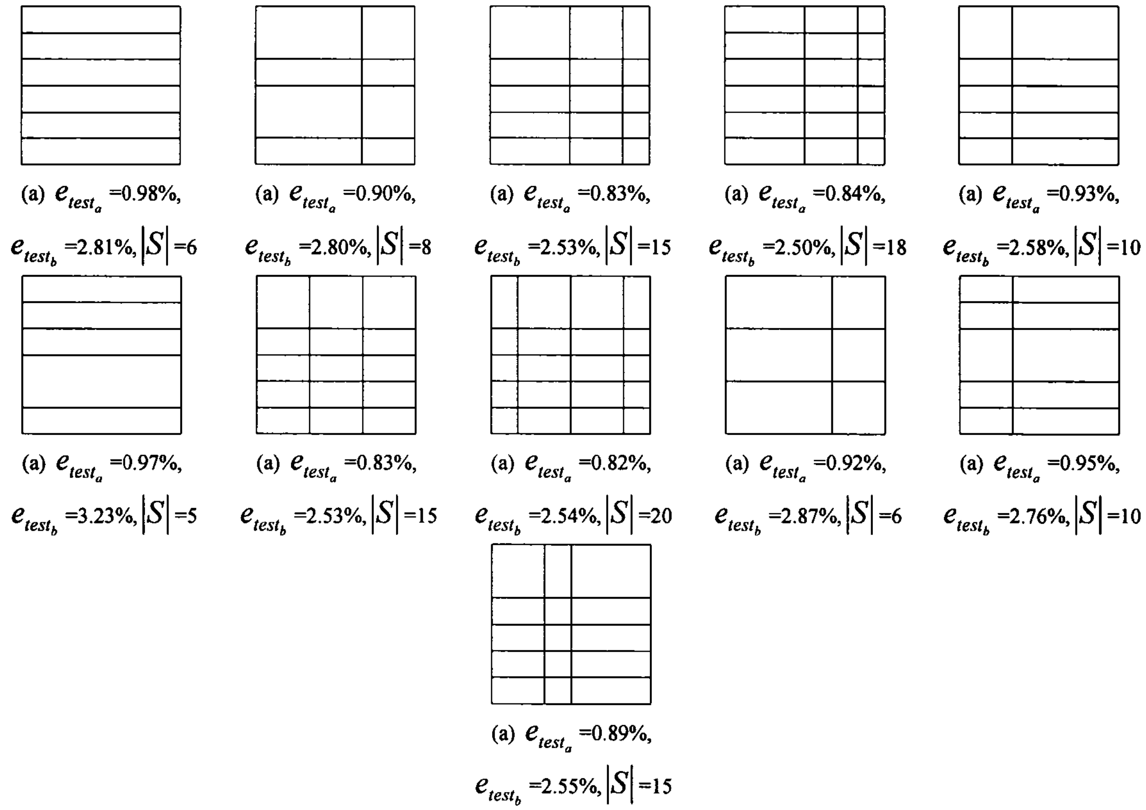

(a) e_{test_a} =0.98%, e_{test_b} =2.81%, $|S|$ =6

(a) e_{test_a} =0.90%, e_{test_b} =2.80%, $|S|$ =8

(a) e_{test_a} =0.83%, e_{test_b} =2.53%, $|S|$ =15

(a) e_{test_a} =0.84%, e_{test_b} =2.50%, $|S|$ =18

(a) e_{test_a} =0.93%, e_{test_b} =2.58%, $|S|$ =10

(a) e_{test_a} =0.97%, e_{test_b} =3.23%, $|S|$ =5

(a) e_{test_a} =0.83%, e_{test_b} =2.53%, $|S|$ =15

(a) e_{test_a} =0.82%, e_{test_b} =2.54%, $|S|$ =20

(a) e_{test_a} =0.92%, e_{test_b} =2.87%, $|S|$ =6

(a) e_{test_a} =0.95%, e_{test_b} =2.76%, $|S|$ =10

(a) e_{test_a} =0.89%, e_{test_b} =2.55%, $|S|$ =15

Figure 50 Zoning strategies associated to individual classifiers in the MLP EoC *SE* in Table IX

SI_{MLP}. Table X details the solutions obtained in the FSS optimization experiment with the use of all validation strategies. In this table, *validation* is the validation strategy used, *zones* the number of active zones, *HN* the number of MLP hidden nodes, $|S|$ the representation cardinality (feature number) and e_{test_a} and e_{test_b} the error rates in the $test_a$ and $test_b$ data sets. The table also includes the baseline representation and the original SI_{MLP} representation optimized by IFE for comparison purposes.

FSS results also confirm the need for global validation in classification system optimization. Solutions selected with global validation are more accurate than those

Table X

FSS optimization results with the divider zoning operator – best values from a single replication

Validation	Solution	MOMA					NSGA-II				
		Zones	HN	$\lvert S\rvert$	e_{test_a}	e_{test_b}	**Zones**	HN	$\lvert S\rvert$	e_{test_a}	e_{test_b}
None	Baseline	6	60	132	0.91%	2.89%	6	60	132	0.91%	2.89%
	SI_{MLP}	15	132	330	0.82%	2.51%	15	132	330	0.82%	2.51%
	SF'	15	136	301	0.86%	2.56%	15	134	296	0.85%	2.64%
	SC	15	117	293	0.85%	2.59%	15	149	298	0.85%	2.61%
	SF	15	112	280	0.87%	2.59%	15	122	243	0.85%	2.55%
Last	SF'	15	123	307	0.82%	2.52%	15	134	296	0.85%	2.64%
	SC	15	171	285	0.89%	2.56%	15	149	298	0.85%	2.61%
	SF	15	148	269	0.86%	2.64%	15	122	243	0.85%	2.55%
Global	SF'	15	161	321	0.82%	2.46%	15	144	318	0.83%	2.51%
	SC	15	130	322	0.79%	2.53%	15	122	306	0.83%	2.54%
	SF	15	159	318	0.82%	2.47%	15	181	301	0.83%	2.44%

selected with other strategies. The two-level FSS approach produces a solution SF with a smaller feature set than SF', produced with the traditional single-level FSS approach. Both MOMA and NSGA-II produced a solutions SC, SF and SF' that are comparable in terms of accuracy, but NSGA-II produced smaller feature sets. Reducing complexity also improved accuracy on $test_b$, which is higher in comparison with that of SI_{MLP}. This improvement is associated with the higher generalization power of smaller representations. NSGA-II also reduced the SI cardinality from 330 features to 301 features in SF, a reduction of 8.79%. It can be said that IFE optimizes representations with a small number of correlated features, and thus FSS is not capable of removing a higher number of features, as these are actually required for classification. Neither algorithm optimized solutions with missing parts. All FSS solutions have 15 active zones as the original representation SI.

Considering this single run and the required processing time, NSGA-II is more adequate than MOMA to reduce feature set cardinality. The solutions obtained with NSGA-II and global validation are detailed in Table XI, comparing classification accuracy without rejection ($e_{\max}$) and with fixed error rates with rejection. Error-rejection curves for classifiers in Table XI are detailed in Fig. 51. The rejection strategy was proposed by Fumera in [92], which is further discussed in the Appendix 3. The error-rejection curve of the original solution SI is comparable to the solutions with reduced feature sets obtained with the NSGA-II (SC, SF and SF'). Thus, FSS solutions performance with the rejection Table XI is comparable to the original SI solution, attaining the goal to reduce feature set complexity while keeping classification accuracy. It was demonstrated in Fig. 48 that solution SI outperforms the baseline representation when using rejection, thus the same can be said for the solutions obtained through the FSS methodology.

6.2.3 Stopping Criterion Experimental Results

The last experiment uses the 30 IFE and EoC experimental replications to verify the proposed stopping criterion when using the global validation strategy. A set of 10 random replications is selected to verify at which generation the optimization algorithms have converged to a good approximation set considering the global validation strategy.

Table XI

MLP classifier FSS solutions obtained with NSGA-II and the divider zoning operator – classification accuracies measured with and without rejection

Solution	Zones	$\|S\|$	$test_a$				$test_b$			
			$e_{\max}$	0.5%	0.25%	0.1%	$e_{\max}$	1.5%	1%	0.5%
Baseline	6	132	99.09%	98.22%	96.72%	93.46%	97.11%	94.64%	92.90%	88.01%
SI	15	330	99.18%	98.54%	97.10%	94.41%	97.49%	96.14%	94.65%	91.26%
SC	15	306	99.17%	98.43%	96.43%	93.57%	97.49%	96.00%	94.40%	91.14%
SF	15	301	99.17%	98.55%	96.62%	94.03%	97.46%	96.28%	94.66%	91.77%
SF'	15	318	99.17%	98.46%	97.00%	94.17%	97.56%	96.12%	94.78%	91.32%

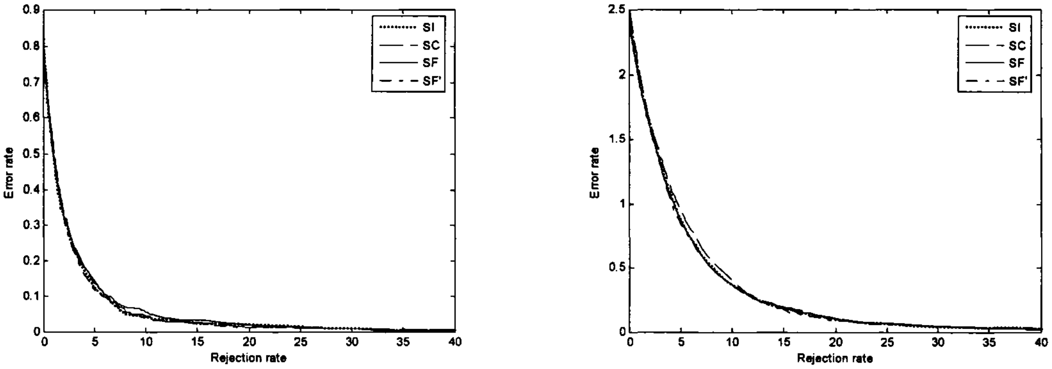

(a) $test_a$ (b) $test_b$

Figure 51 MLP classifier rejection rate curves of NSGA-II solutions obtained with global validation in Table XI

Based on this value, a w estimate is calculated. A simple relation was established between the problem complexity and w when $min_{ir} = 0$. Given binary string length L, it is sufficient to have $w = L/2$ to verify with $min_{ir} = 0$ that the algorithm stopped improving solutions. The remaining 20 replications are used to validate the selected w value. Table XII demonstrates w values for the optimized problems and the mean average stopping generation $\overline{t_{stop}}$ calculated for both NSGA-II and MOMA in these 20 replications. The table also includes the standard deviation associated to the t_{stop} values for these experiments.

The results in Tables VI and VII are the same when either the traditional stopping criterion (maximum generation count) or the proposed stopping criterion is used. The auxiliary archive S keeps good validated solutions, even when the population is over-fitted to the *optimization* data set. Therefore, the proposed stopping criterion is efficient in the context of classification system optimization and the global validation strategy. The stopping criterion may reduce processing time, as the optimization algorithm stops after it has converged to a good approximation set. The approach is efficient in this

Table XII

Divider zoning operator w values and calculated stopping generation (standard deviation values are shown in parenthesis)

Process	MOMA		NSGA-II	
	$w\ (L/2)$	$\overline{t_{stop}}$	$w\ (L/2)$	$\overline{t_{stop}}$
SI	5	11 (2.881)	5	11 (2.266)
SE_{PD}	41	904 (127.327)	5	12 (2.712)
SE'_{PD}	-	-	41	60 (14.552)
SE_{MLP}	41	627 (136.178)	5	13 (2.806)
SE'_{MLP}	-	-	41	125 (27.995)
SF'	165	1000	165	1000
SC	23	167	23	79
SF	161	1000	153	873

context because validated solutions are archived in S, thus the optimization algorithm may over-fit solutions during some generations with no loss of solution quality.

The stopping criterion is also validated with the FSS experiments, and the results are indicated in Table XII. Standard deviation values for the FSS experiments are not provided as they were performed only once. The coarse grain FSS optimization is the smaller problem, with a 45-bit binary string to encode the solution, and both MOMA and NSGA-II converge earlier than the maximum set generations ($mg = 1000$). By contrast, the fine grain FSS optimization is a considerably larger problem, with binary strings ranging between 306 and 330 bits. We observe that the optimization algorithms do not converge before the maximum number of generations mg, except for SF optimized by NSGA-II (which has the smaller bit string). These results indicate the need for larger populations or a higher mg value for the fine grain FSS problem. Results in Table X are also the same with the traditional stopping criterion (maximum generation count) or with the proposed stopping criterion based on solution improvement. Hence the estimated value $w = L/2$ is validated on a set of unseen PR approaches based on MOGAs with binary encoded individuals.

6.2.4 Experimental Results Discussion

On all optimization problems, it was observed that MOMA explored a higher number of unique solutions, as it optimizes the complete decision frontier and uses a local search approach to better explore solutions. This approach allowed MOMA to find a better RS_{IFE} set with the IFE methodology. The drawback is that MOMA uses more processing time, and NSGA-II offers a better compromise between solution quality and processing time for the EoC and FSS methodologies. Another observation is that tracking the improvement rate indicated the need to adjust the optimization parameters in the FSS problems, which is usually overlooked when stopping the optimization algorithm based solely on the maximum number of generations. Finally, solutions obtained with the proposed approach to optimize classification systems outperformed the baseline representation with the divider zoning operator.

6.3 Hierarchical Zoning Experimental Results

The same test set is repeated with the hierarchical zoning operator, thus, this section is also divided in four subsections. First the results for the IFE and EoC optimization are detailed, followed by a subsection that presents results for the FSS optimization. The third subsection verifies the proposed stopping criterion on the experimental data. Finally, the last subsection presents conclusions related to the results obtained with the hierarchical zoning operator on handwritten digits.

6.3.1 IFE and EoC Experimental Results

The first experimental set performed with the hierarchical zoning operator optimizes the IFE and EoC methodologies in 30 replications, as indicated in Fig. 43. The most accurate solution is selected in each run according to the validation strategy used. Figs. 52 and 53 detail the error rate dispersion obtained in these experiments for the PD and MLP classifiers respectively. Mean values and standard deviations for these experiments are detailed in Tables XIII and XIV. In both tables, *validation* indicates the validation strategy used, *zones* the solution zone number, *HN* the number of nodes in the MLP hidden layer (MLP classifier results only), $|S|$ the solution cardinality in features or aggregated classifiers, and e_{test_a} and e_{test_b} the error rates in the $test_a$ and $test_b$ data sets. The baseline representation is included in both tables for reference.

Unlike the divider zoning operator, the IFE with the hierarchical zoning operator was not able to outperform the baseline representation with both PD and MLP classifiers. Thus, the IFE using the divider zoning operator is more powerful to optimize representations for single classifier systems as it was able to outperform a solution

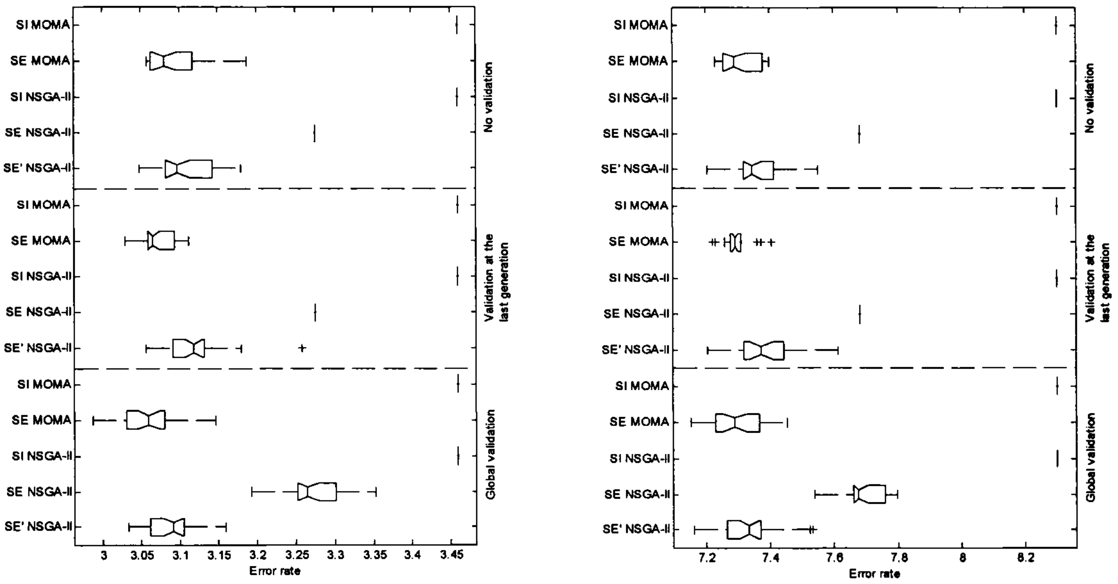

(a) $test_a$

(b) $test_b$

Figure 52 PD error rate dispersion on 30 replications with the hierarchical zoning operator – each solution set relates to one validation strategy tested: no validation, validation at the last generation and global validation

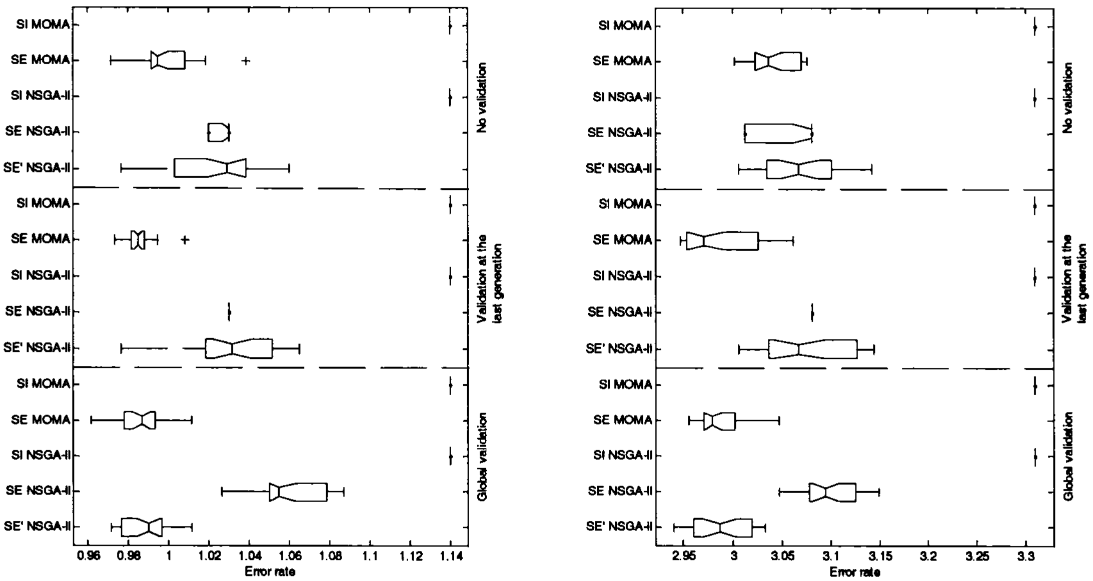

(a) $test_a$ (b) $test_b$

Figure 53 MLP error rate dispersion on 30 replications with the hierarchical zoning operator – each solution set relates to one validation strategy tested: no validation, validation at the last generation and global validation

defined by a human expert. We will see later that the use of a rejection strategy will improve performance, however, with high rejection rates, whereas the divider zoning operator performed better with lower rejection rates. The optimized EoCs are comparable to the original baseline representation, and the use of a rejection strategy later will improve performance, especially for the PD EoC. However, their computational cost is much higher than a single classifier for the baseline representation. Therefore, the first conclusion in this section is that the divider zoning operator performed better than the hierarchical zoning operator with isolated handwritten digits.

Considering the validation strategies, the hierarchical zoning operator results indicate that this zoning operator is less prone to over-fit than the divider zoning operator. For both MOMA and NSGA-II the IFE produced the same representation in all 30 runs, regardless of the validation strategy used. Mean error rates for EoCs optimized by

Table XIII

PD optimization results with the hierarchical zoning operator – mean values on 30 replications and standard deviation values (shown in parenthesis)

Validation	Solution	MOMA				NSGA-II			
		Zones	$\|S\|$	e_{test_a}	e_{test_b}	Zones	$\|S\|$	e_{test_a}	e_{test_b}
	Baseline	6	132	2.96%	6.83%	6	132	2.96%	6.83%
None	SI_{PD}	11	242	3.46% (0)	8.30% (0)	11	242	3.46% (0)	8.30% (0)
	SE_{PD}	-	16.97	3.09% (0.037)	7.31% (0.058)	-	8	3.28% (0)	7.68% (0)
	SE'_{PD}	-	-	-	-	-	12.77	3.12% (0.021)	7.39% (0.084)
Last	SI_{PD}	11	242	3.46% (0)	8.30% (0)	11	242	3.46% (0)	8.30% (0)
	SE_{PD}	-	15.47	3.07% (0.021)	7.3% (0.042)	-	8	3.28% (0)	7.68% (0)
	SE'_{PD}	-	-	-	-	-	12.77	3.12% (0.040)	7.39% (0.099)
Global	SI_{PD}	11	242	3.46% (0)	8.30% (0)	11	242	3.46% (0)	8.30% (0)
	SE_{PD}	-	14.46	3.06% (0.036)	7.3% (0.082)	-	7.33	3.27% (0.046)	7.7% (0.064)
	SE'_{PD}	-	-	-	-	-	13.7	3.09% (0.034)	7.33% (0.102)

MOMA in Tables XIII and XIV are significantly lower with validation at the last generation and the global validation strategy, as indicated by the statistical tests in the Appendix 2. The same tests indicate that EoCs optimized by NSGA-II and RS_{IFE} obtained with MOMA have significantly lower error rates when global validation is used, following the trend observed with the divider zoning operator in the previous section. This confirms the conclusion in the previous section that when the impact of over-fit is not known *a priori*, it is better to use the global validation strategy as it provides better results on over-fit prone problems. When the problem is not prone to over-fit, it has been demonstrated that global validation produces comparable solutions. Thus, the remainder of this section will consider solutions using the global validation for analysis of single classifiers and EoCs. Whereas the hierarchical zoning operator was unable to outperform the baseline representation, the results still indicate accuracy improvements when optimizing EoCs.

Table XIV

MLP optimization results with the hierarchical zoning operator – mean values on 30 replications and standard deviation values (shown in parenthesis)

Validation	Solution	MOMA					NSGA-II				
		Zones	HN	$\|S\|$	e_{test_a}	e_{test_b}	Zones	HN	$\|S\|$	e_{test_a}	e_{test_b}
	Baseline	6	60	132	0.91%	2.89%	6	60	132	0.91%	2.89%
None	SI_{MLP}	11	134	242	1.14% (0)	3.21% (0)	11	134	242	1.14% (0)	3.21% (0)
	SE_{MLP}	-	-	13.64	1% (0.017)	3.04% (0.026)	-	-	4.6	1.03% (0.005)	3.06% (0.032)
	SE'_{MLP}	-	-	-	-	-	-	-	7.83	1.02% (0.025)	3.07% (0.041)
Last	SI_{MLP}	11	134	242	1.14% (0)	3.21% (0)	11	134	242	1.14% (0)	3.21% (0)
	SE_{MLP}	-	-	50.79	0.99% (0.009)	2.98% (0.038)	-	-	7	1.03% (0)	3.08% (0)
	SE'_{MLP}	-	-	-	-	-	-	-	7	1.03% (0.026)	3.07% (0.046)
Global	SI_{MLP}	11	134	242	1.14% (0)	3.21% (0)	11	134	242	1.14% (0)	3.21% (0)
	SE_{MLP}	-	-	28.18	0.99% (0.012)	2.99% (0.023)	-	-	5.13	1.06% (0.017)	3.1% (0.027)
	SE'_{MLP}	-	-	-	-	-	-	-	22.86	0.99% (0.012)	2.99% (0.030)

Error rates obtained with EoCs are significantly lower than when using the single classifier *SI* (for more details, see Appendix 2). The zoning strategy associated to *SI* (regardless of the validation strategy used) is detailed in Fig. 54, with 11 zones (242 features). As with the divider zoning operator, the NSGA-II was able to optimize a better EoC when using the RS_{IFE} optimized by MOMA (producing SE'), which confirms the need for a high degree of classifier diversity to properly optimize an EoC. As with the divider zoning operator, experimental results indicate that the global validation strategy is the best approach for both the IFE and EoC methodologies. Again, it was also observed that it is better to use MOMA to optimize the IFE in order to obtain a diverse set RS_{IFE} to optimize EoCs using the NSGA-II. Selecting the best solutions with this configuration produces the results in Tables XV and XVI. Both tables details classification accuracy without rejection ($e_{\max}$) and with fixed error rates obtained

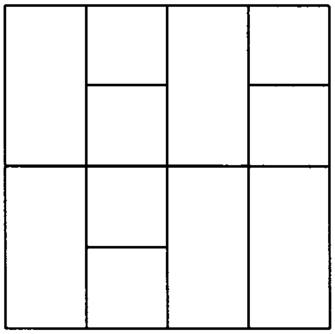

Figure 54 Solution SI_{PD} / SI_{MLP} (11 active zones) selected with either validation strategies in the IFE optimization with the hierarchical zoning operator (the individual is encoded as the patterns *04454*)

Table XV

IFE and EoC best results obtained in 30 replications with the PD classifier (handwriten digits and using the hierarchical zoning operator) – Classification accuracies measured with and without rejection

Solution	**Zones**	$\lvert S \rvert$	$test_a$				$test_b$			
			$e_{\max}$	**1.5%**	**1%**	**0.5%**	$e_{\max}$	**3%**	**2%**	**1%**
Baseline	6	132	97.04%	92.67%	85.15%	63.78%	93.17%	85.31%	77.69%	61.64%
SI_{PD}	11	242	96.54%	88.47%	80.72%	59.86%	91.70%	78.51%	68.88%	49.58%
SE_{PD}	-	19	96.97%	95.47%	94.02%	89.29%	92.78%	88.31%	85.50%	77.72%

Table XVI

IFE and EoC best results obtained in 30 replications with the MLP classifier (handwriten digits and using the hierarchical zoning operator) – classification accuracies measured with and without rejection

Solution	**Zones**	$\lvert S \rvert$	$test_a$				$test_b$			
			$e_{\max}$	**0.5%**	**0.25%**	**0.1%**	$e_{\max}$	**1.5%**	**1%**	**0.5%**
Baseline	6	132	99.09%	98.22%	96.72%	93.46%	97.11%	94.64%	92.90%	88.01%
SI_{MLP}	11	242	98.86%	97.49%	96.05%	91.40%	96.69%	93.70%	91.90%	86.98%
SE_{MLP}	-	25	99.03%	98.34%	96.93%	94.56%	97.05%	95.11%	93.50%	89.84%

through rejection. Details for the rejection strategies applied are discussed in the Appendix 3. The divider zoning operator in the previous section had MLP EoCs with lower cardinality than PD EoCs. The hierarchical zoning operator reverse the roles, and the best PD EoC has a lower cardinality value, which is confirmed by mean values in Tables XIII and XIV.

Concerning the single classifier SI, it has lower performance than the baseline representation with both the PD and MLP classifiers, even when using rejection. On the other hand, the PD EoC SE_{PD} outperforms the baseline representation with rejection. The MLP EoC SE_{MLP} is comparable to the baseline representation with rejection on $test_a$, and performs better than the baseline representation on $test_b$. However, this outperformance comes with a high processing time cost, thus the IEF and EoC methodologies are not able to outperform the baseline representation with the hierarchical zoning operator. Figures 55 and 56 demonstrate the error-rejection curve for solutions in Tables XV and XVI, further confirming this analysis.

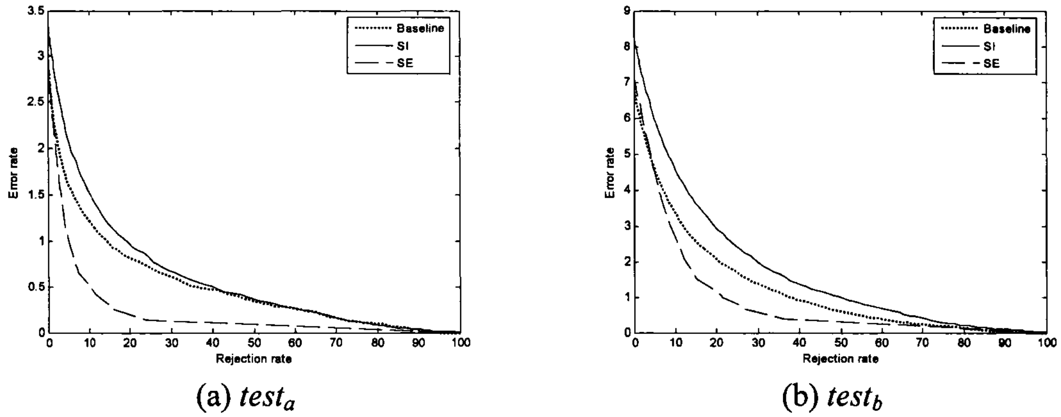

(a) $test_a$ (b) $test_b$

Figure 55 PD classifier rejection rate curves of solutions in Table XV (IFE with hierarchical zoning operator)

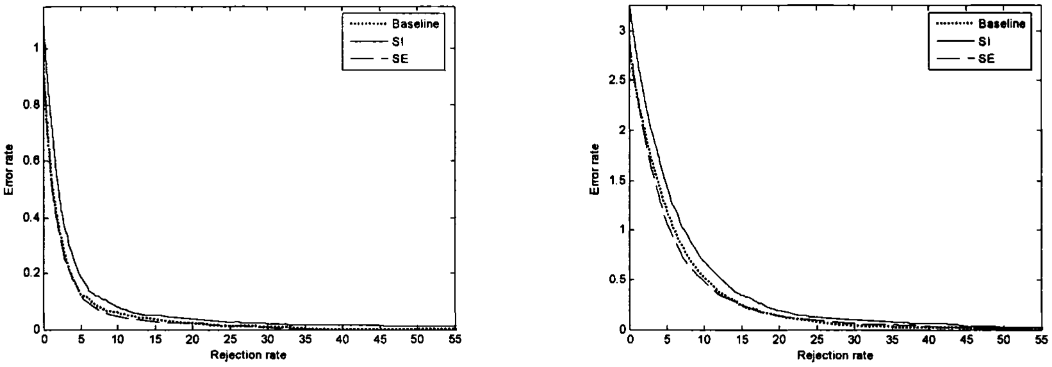

(a) $test_a$ (a) $test_b$

Figure 56 MLP classifier rejection rate curves of solutions in Table XVI (IFE with hierarchical zoning operator)

The EoCs in Tables XV and XVI are composed by a set of classifiers. The individual classifiers for each EoC SE are detailed in Figs. 57 and 58, for the PD and MLP classifiers respectively, where $|S|$ indicates the number of zones for the zoning strategy. Again, we have that not only accurate classifiers compose each EoC, classifiers with lower accuracies contribute positively to the overall EoC. This confirms the claim that classifier diversity is a key issue for EoC optimization. However, as classifiers obtained with the IFE using the hierarchical zoning operator are not as accurate as when using the divider zoning operator, the EoCs obtained are worse.

6.3.2 FSS Experimental Results

FSS optimization results are detailed in Table XVII. As with the divider zoning operator, accuracy was not improved and only the feature set dimensionality was reduced. Unlike the IFE and EoC optimization, the validation strategy matters with the FSS optimization and the global validation produced best results. With the hierarchical zoning operator, the coarse grain FSS did not reduced the feature set dimensionality, and the two level FSS is equivalent to a traditional FSS optimization and $SF = SF'$. Feature set dimensionality is practically the same as the original representation SI, which reinforces

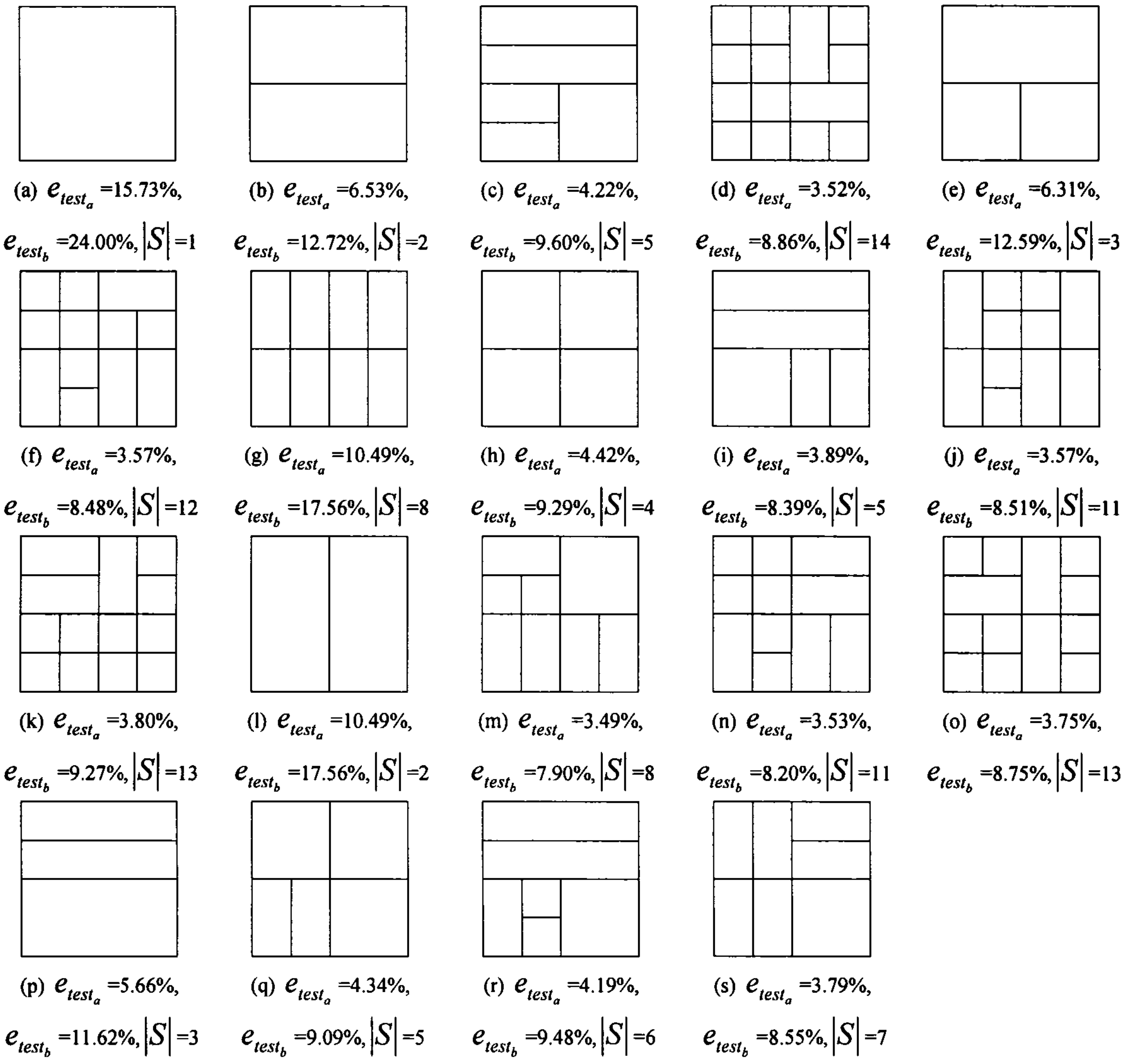

(a) e_{test_a}=15.73%, e_{test_b}=24.00%, $|S|$=1

(b) e_{test_a}=6.53%, e_{test_b}=12.72%, $|S|$=2

(c) e_{test_a}=4.22%, e_{test_b}=9.60%, $|S|$=5

(d) e_{test_a}=3.52%, e_{test_b}=8.86%, $|S|$=14

(e) e_{test_a}=6.31%, e_{test_b}=12.59%, $|S|$=3

(f) e_{test_a}=3.57%, e_{test_b}=8.48%, $|S|$=12

(g) e_{test_a}=10.49%, e_{test_b}=17.56%, $|S|$=8

(h) e_{test_a}=4.42%, e_{test_b}=9.29%, $|S|$=4

(i) e_{test_a}=3.89%, e_{test_b}=8.39%, $|S|$=5

(j) e_{test_a}=3.57%, e_{test_b}=8.51%, $|S|$=11

(k) e_{test_a}=3.80%, e_{test_b}=9.27%, $|S|$=13

(l) e_{test_a}=10.49%, e_{test_b}=17.56%, $|S|$=2

(m) e_{test_a}=3.49%, e_{test_b}=7.90%, $|S|$=8

(n) e_{test_a}=3.53%, e_{test_b}=8.20%, $|S|$=11

(o) e_{test_a}=3.75%, e_{test_b}=8.75%, $|S|$=13

(p) e_{test_a}=5.66%, e_{test_b}=11.62%, $|S|$=3

(q) e_{test_a}=4.34%, e_{test_b}=9.09%, $|S|$=5

(r) e_{test_a}=4.19%, e_{test_b}=9.48%, $|S|$=6

(s) e_{test_a}=3.79%, e_{test_b}=8.55%, $|S|$=7

Figure 57 Zoning strategies associated to classifiers in the PD EoC SE in Table XV

the conclusion in the previous section that the IFE produces solutions adapted to the selected feature extraction operator. The global validation strategy produced the best results, as indicated by Table XVII.

Considering this single run and the required processing time to perform FSS, NSGA-II is more adequate than MOMA to reduce feature set cardinality. The solutions obtained

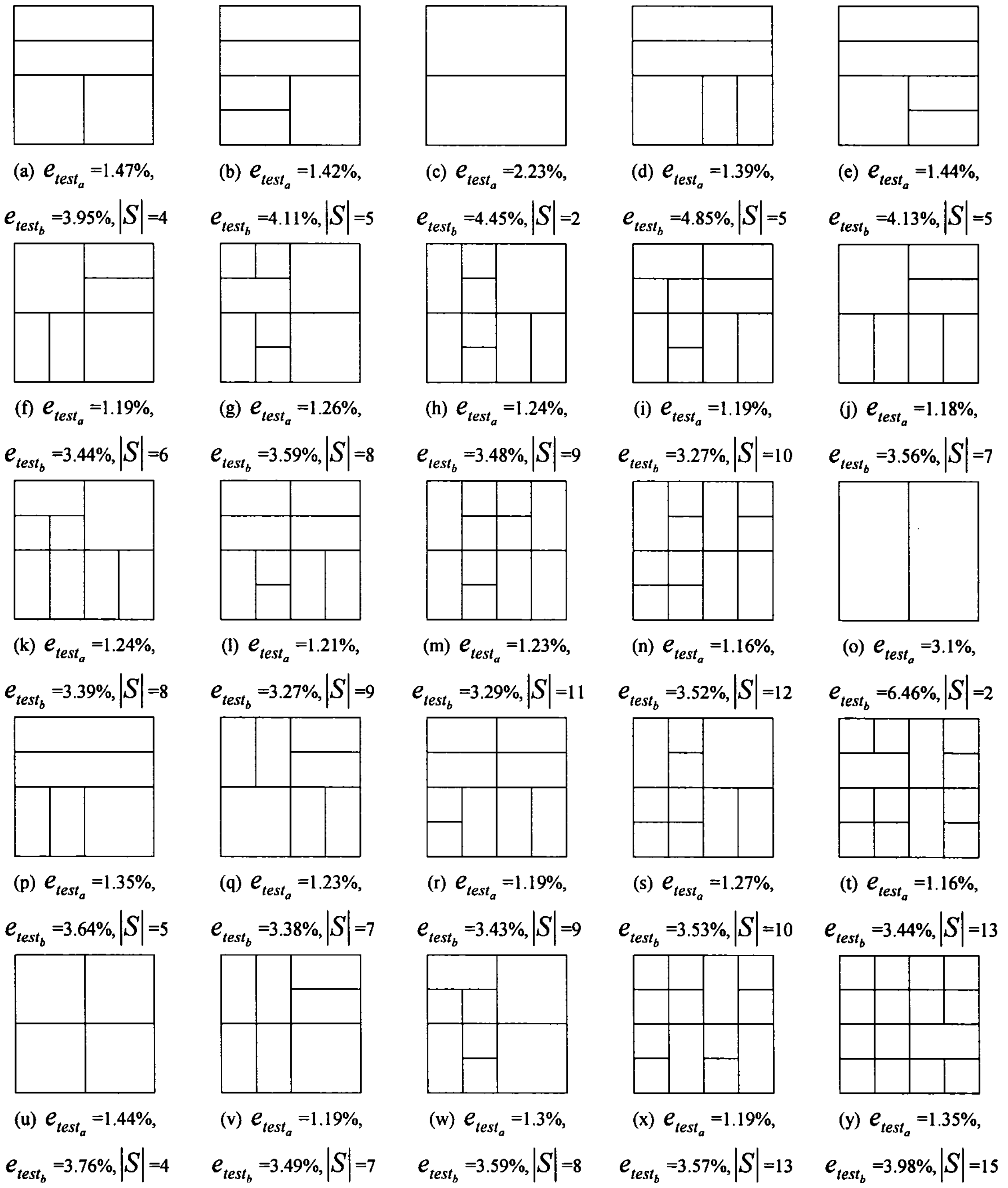

(a) e_{test_a} =1.47%, e_{test_b} =3.95%, $|S|$ =4

(b) e_{test_a} =1.42%, e_{test_b} =4.11%, $|S|$ =5

(c) e_{test_a} =2.23%, e_{test_b} =4.45%, $|S|$ =2

(d) e_{test_a} =1.39%, e_{test_b} =4.85%, $|S|$ =5

(e) e_{test_a} =1.44%, e_{test_b} =4.13%, $|S|$ =5

(f) e_{test_a} =1.19%, e_{test_b} =3.44%, $|S|$ =6

(g) e_{test_a} =1.26%, e_{test_b} =3.59%, $|S|$ =8

(h) e_{test_a} =1.24%, e_{test_b} =3.48%, $|S|$ =9

(i) e_{test_a} =1.19%, e_{test_b} =3.27%, $|S|$ =10

(j) e_{test_a} =1.18%, e_{test_b} =3.56%, $|S|$ =7

(k) e_{test_a} =1.24%, e_{test_b} =3.39%, $|S|$ =8

(l) e_{test_a} =1.21%, e_{test_b} =3.27%, $|S|$ =9

(m) e_{test_a} =1.23%, e_{test_b} =3.29%, $|S|$ =11

(n) e_{test_a} =1.16%, e_{test_b} =3.52%, $|S|$ =12

(o) e_{test_a} =3.1%, e_{test_b} =6.46%, $|S|$ =2

(p) e_{test_a} =1.35%, e_{test_b} =3.64%, $|S|$ =5

(q) e_{test_a} =1.23%, e_{test_b} =3.38%, $|S|$ =7

(r) e_{test_a} =1.19%, e_{test_b} =3.43%, $|S|$ =9

(s) e_{test_a} =1.27%, e_{test_b} =3.53%, $|S|$ =10

(t) e_{test_a} =1.16%, e_{test_b} =3.44%, $|S|$ =13

(u) e_{test_a} =1.44%, e_{test_b} =3.76%, $|S|$ =4

(v) e_{test_a} =1.19%, e_{test_b} =3.49%, $|S|$ =7

(w) e_{test_a} =1.3%, e_{test_b} =3.59%, $|S|$ =8

(x) e_{test_a} =1.19%, e_{test_b} =3.57%, $|S|$ =13

(y) e_{test_a} =1.35%, e_{test_b} =3.98%, $|S|$ =15

Figure 58 Zoning strategies associated to individual classifiers in the MLP EoC *SE* in Table XVI

Table XVII

FSS optimization results with the hierarchical zoning operator – best values from a single replication

Validation	Solution	MOMA					NSGA-II				
		Zones	**HN**	$\|S\|$	e_{test_a}	e_{test_b}	**Zones**	**HN**	$\|S\|$	e_{test_a}	e_{test_b}
	Baseline	6	60	132	0.91%	2.89%	6	60	132	0.91%	2.89%
	SI_{MLP}	11	134	242	1.14%	3.31%	11	134	242	1.14%	3.31%
None	SC	11	120	218	1.28%	3.58%	11	120	218	1.28%	3.58%
	SF / SF'	11	115	209	1.24%	3.61%	11	90	200	1.23%	3.51%
Last	SC	11	125	226	1.23%	3.42%	11	120	218	1.28%	3.58%
	SF / SF'	11	105	209	1.23%	3.55%	11	90	200	1.23%	3.51%
Global	SC	11	134	242	1.14%	3.31%	11	134	242	1.14%	3.31%
	SF / SF'	11	131	238	1.17%	3.33%	11	120	240	1.16%	3.30%

with NSGA-II and the global validation strategy have their accuracy compared to the baseline representation in Table XVIII, which details classification accuracy on both $test_a$ and $test_b$ without rejection ($e_{\max}$) and with fixed error rates using rejection (see Appendix 3 for details on the rejection strategy). Solution SC is the same as SI_{MLP}, thus the equality between results (the coarse grain FSS was unable to eliminate features). The solutions SF and SF' are also equal, and their performance with rejection is very close to the original representation SI_{MLP}.

Table XVIII

MLP classifier FSS solutions obtained with NSGA-II and the hierarchical zoning operator – classification accuracies measured with and without rejection

Solution	**Zones**	$\|S\|$	$test_a$				$test_b$			
			$e_{\max}$	**0.5%**	**0.25%**	**0.1%**	$e_{\max}$	**1.5%**	**1%**	**0.5%**
Baseline	6	132	99.09%	98.22%	96.72%	93.46%	97.11%	94.64%	92.90%	88.01%
SI	11	242	98.86%	97.49%	96.05%	91.40%	96.69%	93.70%	91.90%	86.98%
SC	11	242	98.86%	97.49%	96.05%	91.40%	96.69%	93.70%	91.90%	86.98%
SF / SF'	11	240	98.84%	97.45%	95.95%	91.90%	96.70%	93.74%	91.84%	86.99%

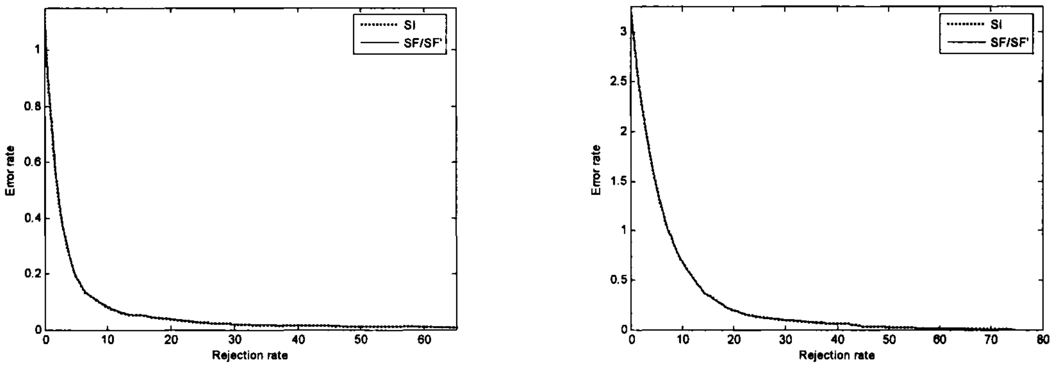

(a) *test$_a$* (b) *test$_b$*

Figure 59 MLP classifier rejection rate curves of NSGA-II solutions obtained with global validation in Table XVIII

The error-rejection curves in Fig. 59 confirm that solutions with reduced feature sets are comparable to the original representation SI_{MLP}. As the original representation SI_{MLP} does not outperform the baseline representation (even with rejection), it can also be said that solutions with reduced feature sets does not outperform the baseline representation.

6.3.3 Stopping Criterion Experimental Results

The last experiment uses the 30 IFE and EoC experimental replications to verify the proposed stopping criterion when using the global validation strategy. The procedure used with the divider zoning operator is repeated, selecting a set of 10 random replications to verify at which generation the optimization algorithms have converged to a good approximation set when using the global validation strategy. Based on this value, an estimate of w is calculated and a relation was established between the problem complexity and w when $min_{ir} = 0$. Again, given the binary string length L, it is sufficient to have $w = L/2$ to verify algorithm convergence when $\min_{ir} = 0$. The remaining 20 replications are then used to validate the selected w value. Table XIX demonstrates w values for the optimized problems and the mean average stopping generation $\overline{t_{stop}}$ calculated for both NSGA-II and MOMA in these 20 replications. The table also includes the standard deviation values for $\overline{t_{stop}}$ when experiments are replicated several times. Again, results in Tables XIII and XIV are the same when either the traditional stopping criterion (maximum generation count) or the proposed stopping criterion is used. The stopping criterion reduces processing time, as the optimization algorithm stops after it has converged to a good approximation set.

Table XIX

Hierarchical zoning operator values and calculated stopping generation (standard deviation values are shown in parenthesis)

Process	**MOMA**		**NSGA-II**	
	$w\ (L/2)$	$\overline{t_{stop}}$	$w\ (L/2)$	$\overline{t_{stop}}$
SI	8	44 (13.302)	8	25 (8.86)
SE_{PD}	36	724 (173.761)	5	14 (4.02)
SE'_{PD}	-	-	36	217 (63.33)
SE_{MLP}	36	653 (230.924)	5	11 (1.85)
SE'_{MLP}	-	-	36	125 (48.74)
SC	17	119	17	57
SF / SF'	121	1000	121	1000

As with the divider zoning operator, the stopping criterion is also validated with the FSS experiments and the results are indicated in Table XIX. Standard deviation values are not presented as the FSS experiments were performed once. The coarse grain FSS optimization (SC) is the smaller problem, with a 33-bit binary string to encode the solution, and both MOMA and NSGA-II converge earlier. On the other hand, the fine grain FSS optimization (SF) and the traditional FSS optimization (SF') is a considerably larger problem, with a 242-bit binary string. As with the divider zoning operator, the optimization algorithms does not converge before the maximum number of generations mg. Results in Table XVII are also the same with the traditional stopping criterion (maximum generation count) or with the proposed stopping criterion based on solution set improvement. Hence the estimated value $w = L/2$ is confirmed for the stopping criterion.

6.3.4 Experimental Results Discussion

It was also observed with the hierarchical zoning operator that MOMA explored a higher number of unique solutions, as it optimizes the complete decision frontier and uses a local search approach to explore solutions. This approach allowed MOMA to find a better RS_{IFE} set with the IFE methodology to optimize EoCs. The drawback is that MOMA uses more processing time, and NSGA-II offers a better compromise between solution quality and required processing time for the EoC and FSS methodologies. The hierarchical zoning operator was unable to outperform the baseline representation, unlike the divider zoning operator. A single classifier obtained with the IFE using the hierarchical zoning operator was comparable to the baseline representation only with a high rejection rate. The EoCs obtained had similar performance to the baseline representation, and the use of rejection strategies improved their performance. However, their computational costs are higher than that of a single classifier, and a similar performance to the baseline representation is not enough to justify this operator. Thus, it can be said that the hierarchical zoning operator has not the representational power to create discriminating feature sets for this classification problem.

6.4 Discussion

This chapter assessed the proposed classification system optimization approach. Tests were performed on isolated handwritten digits to verify zoning operators and improvements against a baseline representation defined by a human expert. Results demonstrated that the divider zoning operator provided better results when optimizing classification systems, outperforming the baseline representation. The hierarchical zoning operator was unable to optimize solutions better than the baseline representation.

Comparing results obtained with both zoning operators (with and without rejection), it is clear that the divider zoning operator outperformed the hierarchical zoning operator on these experiments.

Concerning the impact of over-fit, experiments indicate that over-fit is problem dependant as discussed in [48]. This situation is mostly observed with the hierarchical zoning operator. Also, it was observed that global validation guarantees that good solutions found are preserved regardless of the over-fit impact. Thus, it is concluded that it is safer to use global validation, as the impact of over-fit is not known *a priori*.

The optimization algorithms were also compared, and it was found that global validation allows both MOMA and NSGA-II to perform similarly in the IFE task, but MOMA produces a more diverse representation set RS_{IFE} to optimize EoCs. MOMA optimizes the entire decision frontier, keeping a set of max_{S^l} solutions for each feature set dimensionality, and it was expected that its RS_{IFE} set had higher representation diversity. On the other hand, NSGA-II performed similar to MOMA to optimize EoCs (using RS_{IFE} optimized by MOMA) and to reduce feature set dimensionality through FSS. The NSGA-II advantage over MOMA is the smaller processing time required to optimize good solutions, which makes this algorithm more suitable for both EoC and FSS optimization tasks.

Comparing results obtained in Tables VIII and IX with the divider zoning operator to other representations in the literature, we have the following scenario. Milgram *et al.* experimented with isolated handwritten digits in [93]. Using the same baseline representation they obtained error rates of 1.35% on $test_a$ with a NN classifier and 0.63% on $test_a$ with a SVM (one against all). Correia [94] used an MLP classifier to obtain an error rate of 1.12% on $test_a$ and 3.32% on $test_b$. Liu and Sako [95] using the PD classifier obtained an error rate of 8.11%, but on a different NIST-SD19 data set partitioning. The results obtained by Milgram with SVM are the most interesting, as they outperform the solutions optimized by the proposed approach, however, with a different classifier. It has been known that SVM classifier are more discriminating than MLP classifiers, and future works shall experiment with SVM classifiers to obtain higher accuracies.

The next chapter will use the analysis performed in this chapter to experiment the approach to optimize classification systems with isolated handwritten uppercase letters. Based on results presented in this chapter, experiments with isolated handwritten uppercase letters in the next chapter will use the following configuration. All experiments will use the global validation to guarantee generalization power on selected solutions. The IFE will use the divider zoning operator for its higher performance observed with handwritten digits. MOMA will be used to optimize the IFE to produce a diverse RS_{IFE} set, while the NSGA-II will be used for EoC and FSS optimization. Finally, the FSS optimization process will use the proposed two-level FSS as it produced better results with the divider zoning operator.

CHAPTER 7

EXPERIMENTS ON ISOLATED HANDWRITTEN UPPERCASE LETTERS

Chapter 6 assessed the proposed approach to optimize classification systems with isolated handwritten digits. These experiments were verified the most performing zoning operator for the IFE, the best validation strategy and the use of optimization algorithms. To verify the system's robustness on an unknown problem, an experiment with uppercase letters is performed. This chapter discusses the experimental protocol for these tests, presents the results and discusses them, comparing to a baseline representation defined by a human expert.

7.1 Experimental Protocol

The tests with uppercase letters are performed as indicated in Fig. 60. Chapter 6 determined the best configuration to optimize the classification optimization system. Unlike the experiments detailed in Chapter 6, experiments with handwritten letters only aim to validate the classification system optimization approach, not the validation strategies, zoning operators or optimization algorithms. Thus, experiments with uppercase letters are performed using the following configuration:

- Global validation to select solutions through generations.
- Two-level FSS to reduce representation cardinality.
- MOMA to optimize the IFE.
- NSGA-II to optimize EoCs and FSS.
- Divider zoning operator.

The IFE methodology is applied first to obtain the representation set RS_{IFE} (the auxiliary archive S) with MOMA. This set is then used to train the classifier sets K_{PD}

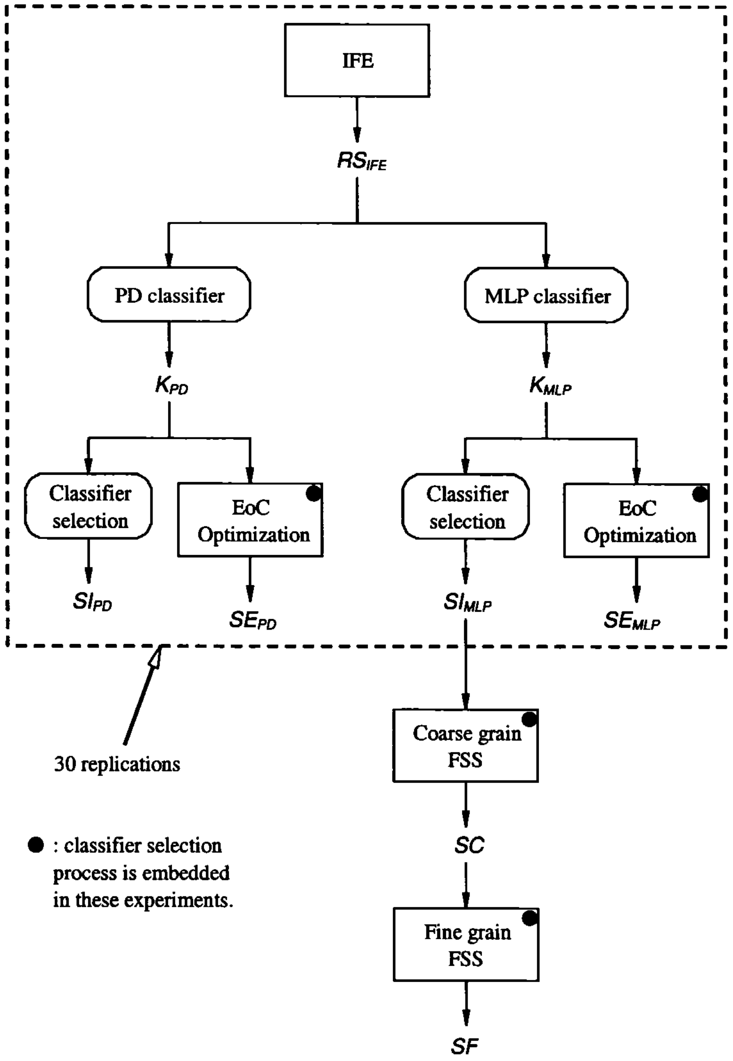

Figure 60 Experimental overview – the classification system optimization approach is tested in two stages, the IFE and the EoC methodologies are replicated 30 times for statistical analysis, experimentation on FSS is performed once, due to the processing time required (the PD classifier is tested only during the first stage, whereas the MLP classifier is tested in both stages)

and K_{MLP} using the PD and MLP classifiers. The most accurate classifiers $SI_{PD}, SI_{PD} \in K_{PD}$ and $SI_{MLP}, SI_{MLP} \in K_{MLP}$ are selected for a single classifier system. EoCs are then optimized using the NSGA-II with K_{PD} and K_{MLP}, producing SE_{PD} and SE_{MLP}. These tests are performed 30 times for meaningful statistical analysis. The FSS approach further refines solution SI_{MLP}, reducing representation cardinality in order to speed up the classification process. As with handwritten digits, the processing time required for each FSS stage limits this stage to a single run using the NSGA-II.

Experiments are performed with the disjoint data sets in Table XX, which are isolated handwritten uppercase letters extracted from NIST-SD19. The protocol to train, validate and test classifiers is the same as in Chapter 6. MLP hidden nodes are optimized as feature set cardinality fractions in the set $f = \{0.4, 0.45, 0.5, 0.55, 0.6\}$. MLP and PD classifier training is performed with the *training* data set. The *validation* data set is used to adjust the classifier parameters (MLP hidden nodes and PD hyper planes). The wrapper approach is performed with the *optimization* data set, and the *selection* data set is used to validate candidate solutions with global validation. Solutions are compared with the *test* data set, unknown to the resulting solutions.

Table XX

Handwritten uppercase letters data sets extracted from NIST-SD19

Database	Size	Origin	Sample range
training	43160	hsf_0123	1 to 43160
validation	3980	hsf_4	1 to 3980
optimization	3980	hsf_4	3981 to 7960
selection	3980	hsf_4	7961 to 11940
test	12092	hsf_7	1 to 12092

The parameters used with MOMA are the following: the crossover probability is set to $p_c = 80\%$, and mutation probability is set to $p_m = 1/L$, where L is the length of the mutated binary string [90]. The local search operator will look for $n = 1$ neighbors during $NI = 3$ iterations, with deviation $a = 0\%$. Each slot in the archive S is allowed to store $max_{S^l} = 5$ solutions. These parameters were determined empirically during the preliminary experiments detailed in Chapter 3. The same parameters

($p_c = 80\%, p_m = 1/L$) are used for NSGA-II. The maximum number of generations for both algorithms is dynamically determined with the proposed stopping criterion, using $w = L/2$, $min_{ir} = 0$ and $mg = 1000$, which stops the algorithm when it detects that solutions cannot be improved, or at most in 1000 generations.

Population size is problem dependent. To optimize the zoning operator, the population size is $m = 64$, while to optimize FSS, we use $m = 100$ for the coarse grain FSS and $m = 150$ for the fine grain FSS. The later value is based on previous results obtained with handwritten digits that indicated that a larger population is required for fine grain FSS. For EoC optimization, $m = 166$ is used. Individual initialization is performed in two steps in all optimization processes. The first step creates one individual for each possible cardinality value. For IFE and FSS optimization, one individual associated with each possible number of zones is added, while for EoC optimization, one individual is added for each possible EoC cardinality. The second step completes the population with individuals initialized with a Bernoulli distribution.

As with handwritten digits, experiments are conducted on a Beowulf cluster. The cluster has 25 nodes using Athlon XP 2500+ processors with 1GB of PC-2700 DDR RAM (333MHz FSB). The optimization algorithms were implemented using LAM MPI v6.5 in master-slave mode with a simple load balance. PD vote and MLP output calculations were performed once in parallel using a load balance strategy, and results were stored in files to be loaded into memory for the EOC optimization process.

7.2 Experimental Results

This section presents and discusses results obtained for handwritten uppercase letters using the divider zoning operator, and the algorithms selected in Chapter 6. The first subsection details results for the IFE and EoC optimization, followed by a subsection that presents results for the FSS optimization. The third subsection verifies the proposed stopping criterion on the experimental data.

7.2.1 IFE and EoC Experimental Results

The first stage optimizes the IFE and EoC methodologies in 30 replications, using both the PD and MLP classifiers. For each replication, solutions are validated using global validation and the best solution found in each replication is used for comparisons. Figures 61 and 62 indicate the *test* error rate dispersion of selected *SI* and *SE* solutions for the PD and MLP classifiers. Mean error rate and standard deviation values are detailed in Tables XXI and XXII. In both tables, *zones* indicates the solution zone number, *HN* the number of nodes in the MLP hidden layer (MLP classifier results only), $|S|$ the solution cardinality in features or aggregated classifiers, and e_{test} the error rate in the *test* data set. The baseline representation is included in both tables for comparison purposes.

Solution SI_{PD} and SI_{MLP} are the same on all 30 replications, thus mean error rate values in Tables XXI and XXII are the actual error rate for these solutions. The zoning strategies for these solutions are detailed in Fig. 63. Mean error rates in Tables XXI and XXII demonstrate the accuracy improvement over the baseline representation defined by a human expert. For a single PD classifier (SI_{PD}), the IFE methodology reduced the error rate by 21.84%. For a PD EoC (SE_{PD}) the error rate was reduced by 30.11% based on mean values. For a single MLP classifier (SI_{MLP}), the IFE methodology improved accuracy by 14.2%, and for an MLP EoC (SE_{MLP}), improvements based on mean values are of 19.60%.

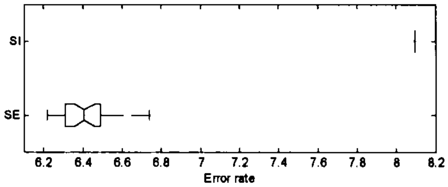

Figure 61 Uppercase letters PD error rate dispersion on 30 replications – each solution set relates to one optimization problem: IFE (SI) and EoC (SE) optimization

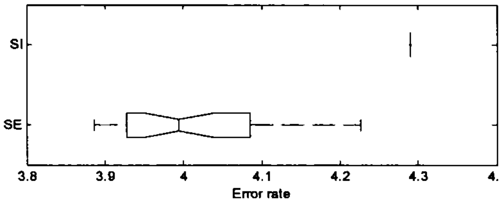

Figure 62 Uppercase letters MLP error rate dispersion on 30 replications – each solution set relates to one optimization problem: IFE (SI) and EoC (SE) optimization

Table XXI

Uppercase letters PD optimization results – mean values on 30 replications and standard deviation values (shown in parenthesis)

Solution	**Zones**	$\|S\|$	e_{test}
Baseline	6	132	9.20%
SI_{PD}	16	352	7.19% (0)
SE_{PD}	-	14.41	6.43% (0.131)

Selecting the best solutions in Tables XXI and XXII produces the results in Tables XXIII and XXIV, detailing classifier accuracy without rejection ($e_{\max}$) and with fixed error rates with the use of a rejection mechanism. As indicated by mean values

Table XXII

Uppercase letters MLP optimization results – mean values on 30 replications and standard deviation values (shown in parenthesis)

Solution	Zones	HN	$\|S\|$	e_{test}
Baseline	6	80	132	5.00%
SI_{MLP}	10	88	220	4.29% (0)
SE_{MLP}	-	-	5.23	4.02% (0.093)

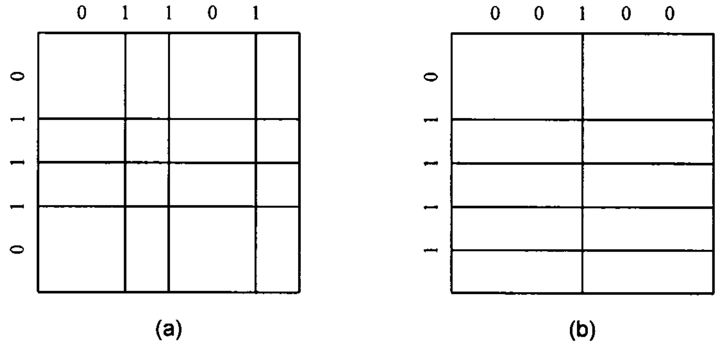

Figure 63 Solutions SI_{PD} (a) and SI_{MLP} (b), with 16 and 10 active zones respectively, selected with the global validation strategy in the IFE optimization

previously discussed in Tables XXI and XXII, EoC cardinality with the divider zoning operator is lower for the MLP EoC, an effect also observed with handwritten digits in the previous chapter. For further details on the rejection strategies used, see the Appendix 3.

Solutions obtained with the IFE and EoC methodologies outperform the baseline representation with and without the use of rejection strategies. PD and MLP classifier results in Tables XXIII and XXIV are significantly better with the proposed IFE and

Table XXIII

IFE and EoC best results obtained in 30 replications with the PD classifier (handwritten letters and using the divider zoning operator) – accuracies measured with and without rejection

Solution	Zones	$\|S\|$	*test*			
			e_{max}	4%	2%	1%
Baseline	6	132	90.80%	66.56%	34.30%	16.47%
SI_{PD}	16	352	91.81%	81.44%	50.46%	21.94%
SE_{PD}	-	12	93.78%	91.01%	83.47%	75.75%

Table XXIV

IFE and EoC best results obtained in 30 replications with the MLP classifier (handwritten uppercase letters using the divider zoning operator) – Accuracies measured with and without rejection

Solution	Zones	$\|S\|$	*test*			
			e_{max}	1.5%	1%	0.5%
Baseline	6	132	95.00%	89.07%	86.30%	82.20%
SI_{MLP}	10	220	95.71%	90.54%	88.65%	82.51%
SE_{MLP}	-	5	96.11%	93.07%	90.64%	85.58%

EoC approaches. For both the PD and MLP classifier, EoCs are better than single classifiers, justifying once again the use of the multiple classifier approach. Figures 64 and Figure 65 depict the error-rejection curve for these solutions, confirming this analysis.

The EoCs in Tables XXIII and XXIV are composed by the classifier sets detailed in Figs. 66 and 67, for the PD and MLP classifiers respectively, where $|S|$ indicates the zone number associated to the representation. Figures 66.c and 67.c indicate that one

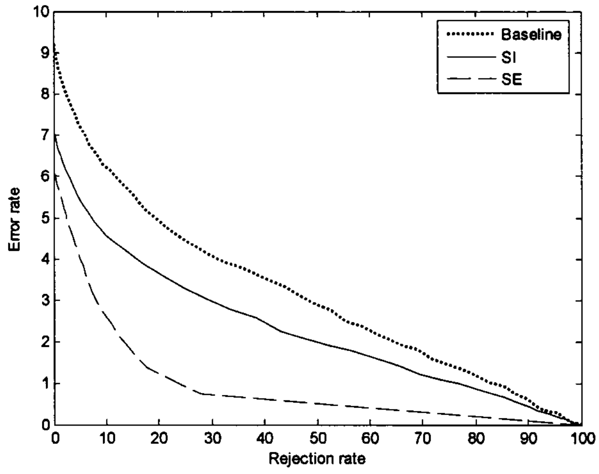

Figure 64 PD classifier rejection rate curves of solutions in Table XXIII (IFE with divider zoning operator)

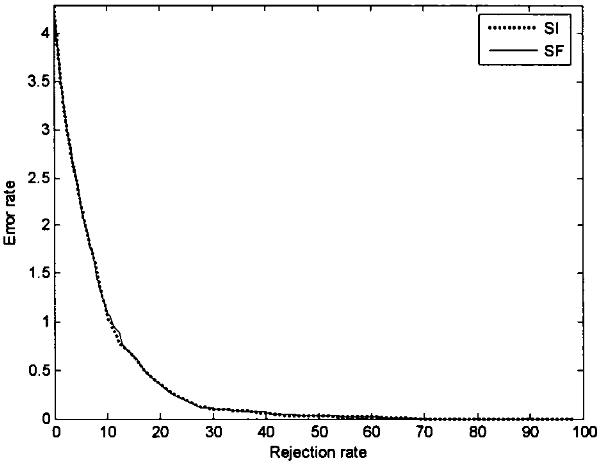

Figure 65 MLP classifier rejection rate curves of solutions in Table XXIV (IFE with divider zoning operator)

solution selected in the EoC have higher accuracy than SI_{PD} and SI_{MLP}. We verified solutions selected with validation at the last generation and with no validation, only to find out that SI_{PD} and SI_{MLP} obtained with global validation have the highest accuracy on the *test* data set. We believe that the solutions in Figs. 66.c and 67.c were not found due to the size of the *selection* data set used to validate optimized solutions. Thus, it can be said that whereas the global validation performs better than the other validation strategies tested, the *selection* data set size will impact in the global validation strategy performance.

Again, we have that not only accurate classifiers compose each EoC, and classifiers with lower accuracies contribute to the overall EoC performance. This follows the trend observed with handwritten digits in the previous chapter, indicating that classifier diversity is a key issue for EoC optimization. The PD EoC included the baseline representation, whereas the MLP EoC included the representation SI optimized by the IFE.

7.2.2 FSS Experimental Results

The next stage refines solution SI_{MLP} through FSS, where the goal is to reduce representation complexity while keeping the accuracy comparable to the original SI_{MLP}. Table XXV details the solutions obtained with the proposed two level FSS approach, detailing the original classification accuracy (without rejection, $e_{\max}$) and with the use of rejection to obtain fixed error rates (see details in the Appendix 3). In this table, *zones* is the number of active zones, *HN* the number of MLP hidden nodes, $|S|$ the representation cardinality (feature number) and *test* the accuracy in the *test* data set, regarding the rejection strategies or with 0 rejection. The table also includes the baseline representation and the original SI_{MLP} representation optimized by the IFE for comparison purposes.

It was observed with handwritten digits in Table X that the two level FSS was not able to remove a large number of features (reducing less than 10%). The conclusion was that

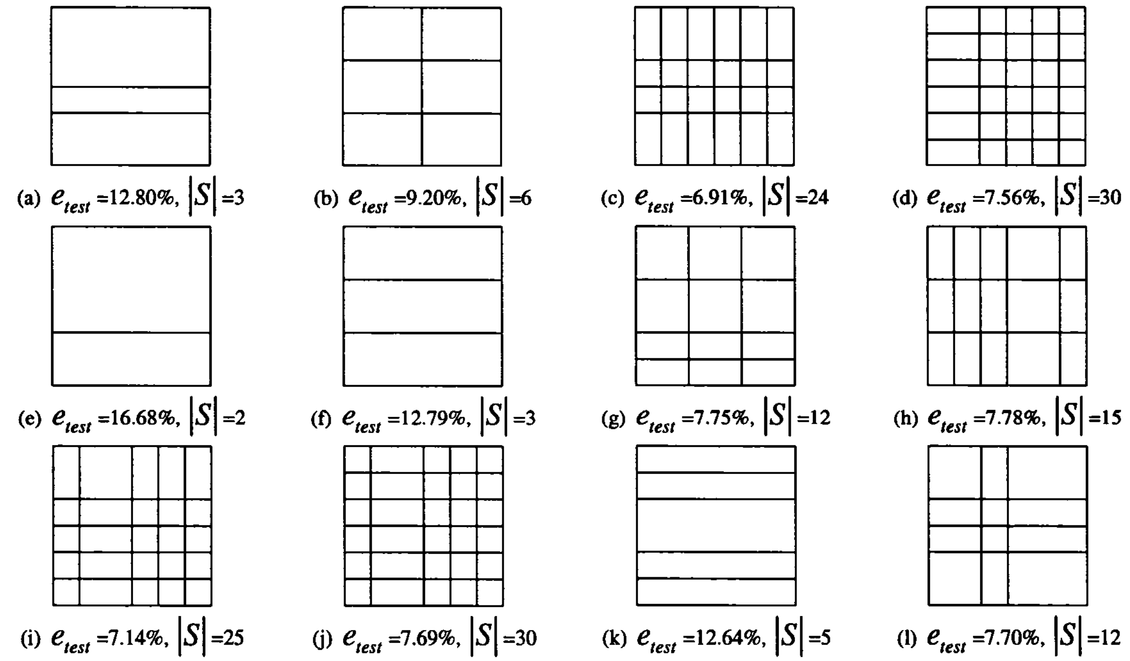

(a) e_{test} =12.80%, $|S|$=3 (b) e_{test} =9.20%, $|S|$=6 (c) e_{test} =6.91%, $|S|$=24 (d) e_{test} =7.56%, $|S|$=30

(e) e_{test} =16.68%, $|S|$=2 (f) e_{test} =12.79%, $|S|$=3 (g) e_{test} =7.75%, $|S|$=12 (h) e_{test} =7.78%, $|S|$=15

(i) e_{test} =7.14%, $|S|$=25 (j) e_{test} =7.69%, $|S|$=30 (k) e_{test} =12.64%, $|S|$=5 (l) e_{test} =7.70%, $|S|$=12

Figure 66 Zoning strategies associated to individual classifiers in the PD EoC *SE* in Table XXIII

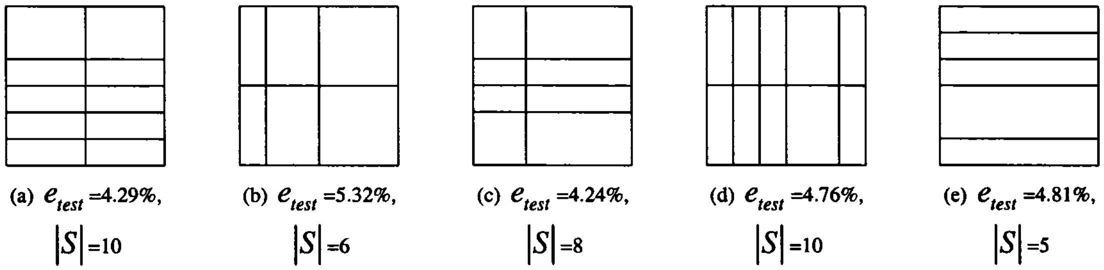

(a) e_{test} =4.29%, $|S|$=10 (b) e_{test} =5.32%, $|S|$=6 (c) e_{test} =4.24%, $|S|$=8 (d) e_{test} =4.76%, $|S|$=10 (e) e_{test} =4.81%, $|S|$=5

Figure 67 Zoning strategies associated to individual classifiers in the MLP EoC *SE* in Table XXIV

the IFE optimized a solution SI_{MLP} with few correlated features. This effect is also observed with handwritten uppercase letters, and it is stronger than with handwritten digits. The coarse grain FSS is unable to remove feature transformations, keeping the original 220 features ($SC = SI_{MLP}$), whereas the fine grain FSS removes only two features. These results further justify the claim that the IFE finds a zoning strategy adapted to the feature vector.

Table XXV

Uppercase letters FSS optimization results, best values from a single replication (classification accuracies are measured with and without rejection)

Solution	**Zones**	**HN**	$\|S\|$	*test*			
				e_{max}	**1.5%**	**1%**	**0.5%**
Baseline	6	80	132	95.00%	89.07%	86.30%	82.20%
SI_{MLP}	10	88	220	95.71%	90.54%	88.65%	82.51%
SC	10	88	220	95.71%	90.54%	88.65%	82.51%
SF	10	98	218	95.73%	90.49%	88.24%	84.01%

Figure 68 demonstrates the similarity of SI_{MLP} and SF through their error-rejection. This is depicted by the nearly equal error-rejection curves, implying that their performance (SI and SF) is equivalent when using a rejection strategy. However, it must be noted that SF has only two less features than SI and that it is expected for both classifiers to have similar performance.

7.2.3 Stopping Criterion Experimental Results

The stopping criterion is able to reduce processing time, as indicated in Table XXVI. Again, the fine grain FSS process stops at the maximum number of generations ($mg = 1000$), regardless of the increased population size ($m = 150$) in comparison to the experiments in Chapter 6. This further exposes the complexity associated to the fine grain FSS process, which in consequence requires the exploration of a larger number of candidate solutions for complete convergence. For the remaining optimization processes, the stopping criterion stops the optimization process at a generation $t_{stop}, t_{stop} < mg$. The results presented in Tables XXI and XXII provide similar improvements to those obtained in Chapter 6, thus confirming the stopping criterion on an unknown problem. Standard deviation values for $\overline{t_{stop}}$ are not provided for the FSS experiments as they are performed only once.

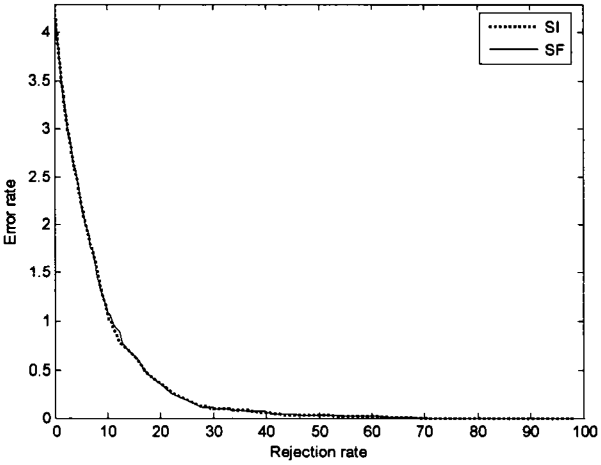

Figure 68 MLP classifier rejection rate curves of solutions in Table XXV

Table XXVI

w values and calculated stopping generation for the uppercase letters experiments (standard deviation values are shown in parenthesis)

Process	w $(L/2)$	$\overline{t_{stop}}$
SI	5	10 (2.687)
SE_{PD}	41	204 (68.240)
SE_{MLP}	41	124 (28.524)
SC	15	142
SF	110	1000

7.3 Discussion

This chapter assessed the approach to optimize classification systems with isolated handwritten uppercase letters, an unknown problem to the approach to optimize classification systems and the configuration selected in Chapter 6. Whereas the goal in

Chapter 6 was to find the best combination of zoning operator, optimization algorithms and validation strategies, this chapter used the best configuration to optimize a classification system for uppercase letters.

The main goal of the proposed approach to optimize classification systems is to adapt classification systems to other problems. In this context, a classification system based on the baseline representation is adapted to uppercase letters. As expected, representations optimized for this problem are different than representations found for handwritten digits in Chapter 6, justifying once again the approach to optimize classification systems.

Solutions found outperformed the baseline representation, originally defined for handwritten digits, and the optimized EoCs further improved accuracy. One aspect noticed in both experiments with digits and uppercase letters is that EoC improvements are higher with the PD classifier. One possible explanation is that the IFE produces solutions based on the PD classifier, and solution diversity is not as high when training the MLPs. However, this statement cannot be verified as the processing time required to optimize the IFE with MLPs renders this test unfeasible.

The two level FSS was not able to reduce the representation SI_{MLP} complexity. The FSS experiments with digits in Chapter 6 did not reduce a significant amount of features with the divider zoning operator, and with the hierarchical zoning operator the results are similar to those presented in this chapter. Thus, it can be said that the IFE selects a zoning strategy adapted to the feature extraction operator, producing a representation with few correlated features that FSS is not able to reduce to speedup the classification stage.

Comparing the results in Tables XXIII and XXIV, we obtain the following results. Milgram *et al.* used the same *test* data set and the baseline representation in [93], obtaining error rates of 7.60% with a 3-NN classifier and 3.17% with a SVM classifier (one against all). The result with the SVM classifier indicates that a more discriminating classifier may improve accuracy, as the baseline representation was outperformed by the proposed approach with the MLP classifier. A direct comparison to other works in the literature is difficult, due to differences in the experimental protocol to test classifiers. Thus, error rates are listed to illustrate typical accuracies with uppercase letters, not as comparable values to the presented experimental results. Koerich in [33] used an MLP classifier to classify handwritten letters from NIST-SD19 (both uppercase and lowercase), obtaining an error rate of 11.90%. Oh and Suen in [25] used a modular neural network to experiment with uppercase letters extracted from NIST-SD19, obtaining an error rate of 9.94%.

CONCLUSIONS

This thesis proposed and assessed an approach to optimize and adapt classification systems based on multi-objective genetic algorithms. This difficult problem has been traditionally solved by human experts, whereas the proposed semi-automatic approach uses the expert's domain knowledge to create a representation set to optimize and adapt classification systems. We have seen that this problem is difficult since the over-fit to the optimization stage plays an important role, which is often overlooked in similar methodologies. The choice of a suitable validation strategy was the key to find performing solutions with good generalization power to unseen data.

A serie of experimental tests was performed to evaluate the methodologies for optimizing classification systems with both the PD and MLP classifiers. It was observed that IFE outperformed the traditional human expert based approach and produced a set of diverse classifiers, which can be aggregated into an EoC for higher accuracy than a single classifier. IFE also prototypes solutions using a computationally efficient wrapper with the PD classifier. This wrapper approach reduces processing time and turns IFE into a feasible approach for genetic optimization. The proposed two-level FSS methodology outperformed the traditional one-level FSS with handwritten digits and the divider zoning operator, producing an accurate and less complex classifier. Solutions obtained in the FSS context had no missing parts and all zones were active. From this statement, we conclude that missing parts are not a key issue for FSS optimization, and that representation complexity can be measured through the feature set cardinality on future experiments.

This thesis also demonstrated that, similar to learning algorithms, methodologies to optimize classification systems using a wrapped classifier are prone to solution over-fit. Validation strategies to overcome this challenge have been discussed and tested. It was observed in some problems that the global validation is not significantly better than validation at the last generation. However, since the impact of over-fit on solutions obtained is unknown *a priori*, it is safer to use global validation as it guarantees solution quality once the optimization process has been completed in all situations.

It was also demonstrated that MOMA outperforms NSGA-II for the IFE methodology when the classification system targets EoCs. This effect is associated with the exploratory mechanism in MOMA and its archiving strategy. The drawback is that MOMA requires more processing power to complete the optimization process. When a single classifier solution is desired, then NSGA-II can be used in place of MOMA. The EoC methodology results indicate no significant advantage in accuracy for either algorithm, and thus it was concluded that the NSGA-II is the most appropriate optimization algorithm considering the required processing time.

As for the FSS approach, results for both MOMA and NSGA-II are comparable in accuracy. It was also seen that the proposed two-level FSS approach may provide better solutions in some situations. One conclusion from the experimental data is that the IFE already produces a solution SI with few correlated features, adapted to the selected feature extraction operator. This was better observed with uppercase letters, where the FSS operation removed no more than 2 features. Considering the restrictions imposed by the limited experimental data, it can be also said that NSGA-II is preferable to MOMA in terms of required processing power. A more significant statistical analysis to verify these statements is required, however, the processing time required currently makes this analysis not feasible.

Finally, the experimental data were used to validate a stopping criterion adapted to classification system optimization in the context of the global validation. The novelty of this stopping criterion is that it takes into account not only the maximum generation count, but the algorithm improvement rate as well. A relation between the encoded binary string and the w parameter was empirically determined with handwritten digits to monitor improvement in that context. The stopping criterion discussed is capable of detecting convergence and halts the algorithm before the set maximum number of generations, thereby reducing processing time while keeping solution quality. The stopping criterion also helped verify the need to revise the population size or maximum number of generations with the fine grain FSS optimization.

Even thought this thesis successfully proposed and tested the approach, obtaining significant improvements in both classification accuracy and in understanding the over-fit issue, some aspects where not developed owing to time and scope constraints. Here we outline future directions we believe worthy of investigation:

- Evaluate different zoning operators, most specifically operators that allow zones to overlap and do not necessarily cover the entire image.
- Optimize classification systems for other zoning based classification problems, such as signature verification, which could benefit from the proposed semi-automatic approach.
- Compare the MOGA based approach to other optimization algorithms, aiming to find a better compromise between solution quality and required processing time.
- Investigate the stopping criterion with other multi-objective optimization problems outside the pattern recognition domain, also aiming real coded individuals, rather than working only with binary coded individuals.

APPENDIX 1

Fast elitist non-dominated sorting genetic algorithm – NSGA II

The *Fast Elitist Non-Dominated Sorting Genetic Algorithm* (NSGA-II) introduced by Deb *et al.* in [63], is a second generation MOGA (as classified by Coello in [55]). This particular algorithm is chosen as this thesis baseline MOGA, owing its known efficiency to solve MOOPs in the literature [96, 97, 98]. The NSGA-II has also been used as a baseline MOGA for problem specific algorithms comparison [99, 100] and in general MOGA studies [101, 102, 103], which further justifies this choice. The main advantage of NSGA-II lies on its elite and diversity preservation mechanisms.

The NSGA-II procedure is outlined in Fig. 69, evolving a population P of constant size m. The offspring population $Q^t, |Q^t| = m$ is created from the parent population $P^t, |P^t| = m$. Both Q^t and P^t populations are combined to create population $R^t, |R^t| = 2m$. A non-dominated sorting is applied on R^t and the new population P^{t+1} is filled by solutions of different non-dominated fronts $F^i, F^i \in R^t$. The process is performed from the best to the worse front, until $|F^i \cup P^{t+1}| > m$. At this point a diversity metric is used to sort individuals in F^i and individuals are copied to P^{t+1} until $|F^i \cup P^{t+1}| = m$. Remaining solutions in R^t are rejected. This process is algorithmically detailed in Algorithm 9.

Diversity preservation is achieved through the use of the *crowding distance*. Given solution i, the crowding distance measures the perimeter of the cuboid described by the two nearest solutions to i. The crowding distance favors solutions isolated in the objective function space to help the algorithm to exploit that area. One advantage of using the crowding distance is its parameter free nature, allowing the metric self adaptation to the current population. The crowding distance assignment in Algorithm 9 is detailed in Algorithm 10. For every solution in the front F we initially assign a 0 diversity value. Next for each objective function m we rank solutions from the lowest to

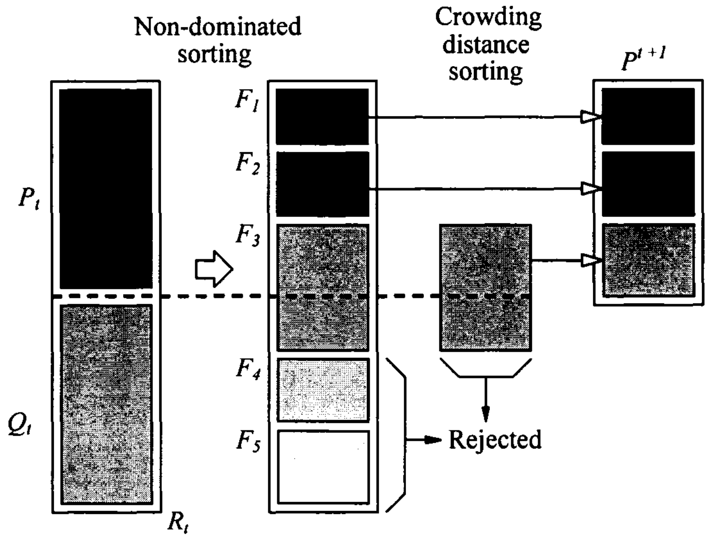

Figure 69 NSGA-II procedure

Algorithm 9: NSGA-II algorithm

```
Result : Population $P$
Creates initial population $P^1$ with $m$ individuals
$t = 1$;
while $t < mg$ do
        $R^t = P^t \cup Q$;
        $F$ =fast-non-dominated-sort$\left(R^t\right)$;
        while $\left|P^{t+1}\right| + \left|F^i\right| \leq m$ do
                $P^{t+1} = P^{t+1} \cup F^i$;
                crowding-distance-assignement$\left(F^i\right)$;
                $i = i + 1$;
        end
        $Sort\left(F^i, \prec_n\right)$;
        $P^{t+1} = P^{t+1} \cup F^i\left[1 : \left(N - \left|P^{t+1}\right|\right)\right]$;
        $Q^{t+1}$=make-new-pop$\left(P^{t+1}\right)$;
        $t = t + 1$;
end
```

Algorithm 10: Crowding distance assignment

```
**Data**: Front $F$
**Result** : Crowding-distance vector $d_I$
$\forall i \in F, d^i = 0$;
**for** objective function $m = 1, \dots, M$ **do**
    Sort $F$ in worse order of $f_m$ or find the sorted indices vector $I_m = sort(f_m, >)$;
    $l = |F|$;
    $d_{I_l^m} = d_{I_l^m} = \infty$ (set a large distance to boundary solutions);
    **for** $j = 2, \dots, l-1$ **do**
        $d_{I_j^m} = d_{I_j^m} + \frac{f_m^{I_{j+1}} - f_m^{I_{j-1}}}{f_m^{\max} - f_m^{\min}}$;
    **end**
**end**
```

the highest values, assigning to the boundary solutions a high diversity value (∞). The remaining solutions are assigned a value calculated with the average value of the cuboid perimeter for that objective function. Once the procedure is done, the most isolated solutions have high diversity values, whereas close solutions have lower diversity values.

Crossover and mutation genetic operations to create Q^t are performed as usual on the mating pool M. Selection is performed differently, using a crowded tournament selection. This selection assumes that each solution in P^t has two properties, the non-dominated rank r_i in the population and the local crowding distance d_i. It creates the mating pool M from P^t by taking pairs of solutions i and j and selecting the best, based on both the non-dominated rank and the local crowding distance. The crowded tournament selection is performed as in Algorithm 11.

Algorithm 11: Crowded tournament selection operator

```
Data: population $P^t$
Result : Mating pool $M$
repeat
        Select solutions $i, j \in P^t$, such as that both $i$ and $j$ have not yet participated two times in tournaments;
        if $r_i < r_j$ then
                $M = M \cup \{i\}$;
        else
                if $r_i > r_j$ then
                        $M = M \cup \{j\}$;
                else
                        if $d_i > d_j$ then
                                $M = M \cup \{i\}$;
                        else
                                $M = M \cup \{j\}$;
                        end
                end
        end
until $|M| = m$;
```

APPENDIX 2

Statistical analysis

To compare solutions obtained in Chapters 6 and 7, a non-parametric multiple comparison procedure with Dunn-Sidak correction is performed. The null hypothesis, in this context, states that there is no significant statistical difference between the mean error rates of samples obtained from different experiments. The alternative hypothesis is that mean error rates are different. The null hypothesis is verified with a confidence level of 95% ($\alpha = 0.05$). For handwritten digits, the first goal is to determine what the best validation strategy is. Next, the tests compare results provided by both optimization algorithms to verify which is the most suitable for each optimization stage. Finally, the tests are also used to verify improvements obtained with EoCs in comparison to a single classifier based approach. These tests are performed for both zoning operators (divider and hierarchical), using both the NSGA-II and MOMA algorithms.

The best combination of optimization algorithms, zoning operators and validation strategies is determined with digits. Thus, multiple comparison tests with handwritten uppercase letters are used strictly to compare the improvement obtained with EoCs in comparison to the single classifier approach.

All figures used to compare results (Figs. 8 to 13) indicate the statistical difference between mean values.

All figures used to compare results (Figs. 70 to 82) indicate the statistical difference between mean values. Each experiment is represented by a line segment, where values in the x axis are the ranking in the multiple comparison (not actual error rates). Overlaping line segments indicate comparable mean values, whereas non-overlaping line segments indicate significantly different results.

2.1 Handwritten Digits

This section is divided in four subsections. The first two details the tests performed with the divider zoning operator, followed by the tests using the hierarchical zoning operator.

Each subsection pair discusses the tests and their results for each classifier, which complements the analysis discussed in Chapter 6.

2.1.1 Divider Zoning Operator and PD Classifier

The first multiple comparison test verifies the impact of validation strategies, which is detailed in Figs. 70 and 71, for the MOMA and NSGA-II optimization algorithms respectively. Using $max_{S'} = 5$ with MOMA to optimize the IFE, there is no relevant difference between validation at the last generation and global validation, as indicated in Figs. 70.a and 70.b. The same parameter is used to optimize EoCs. Regarding $test_a$ in Fig. 70.c, the global validation performs better. However, with $test_b$ in Fig. 70.d both validation at the last generation and global validation are not significantly different. These results indicate that validation at the last generation with MOMA is sensible to the $max_{S'}$ parameter, and a low value may produce suboptimal solutions. To guarantee solution quality regardless of the $max_{S'}$ value, global validation is selected as the most performing for MOMA.

The same tests are performed with the NSGA-II, verifying the impact of validation strategies on all optimization problems. Unlike MOMA, which has an auxiliary archive to store solutions for validation at different performance levels, NSGA-II always provide better results when using the global validation as demonstrated in Fig. 71.

Once the global validation is selected as the most performing validation strategy, algorithms are tested to verify which is better for each optimization stage. Results for this test are presented in Fig. 72. It is verified for both test data sets ($test_a$ and $test_b$) that MOMA and NSGA-II are not significantly different to optimize the IFE, thus either algorithm may be used when the target is a single classifier based system. As for EoCs,

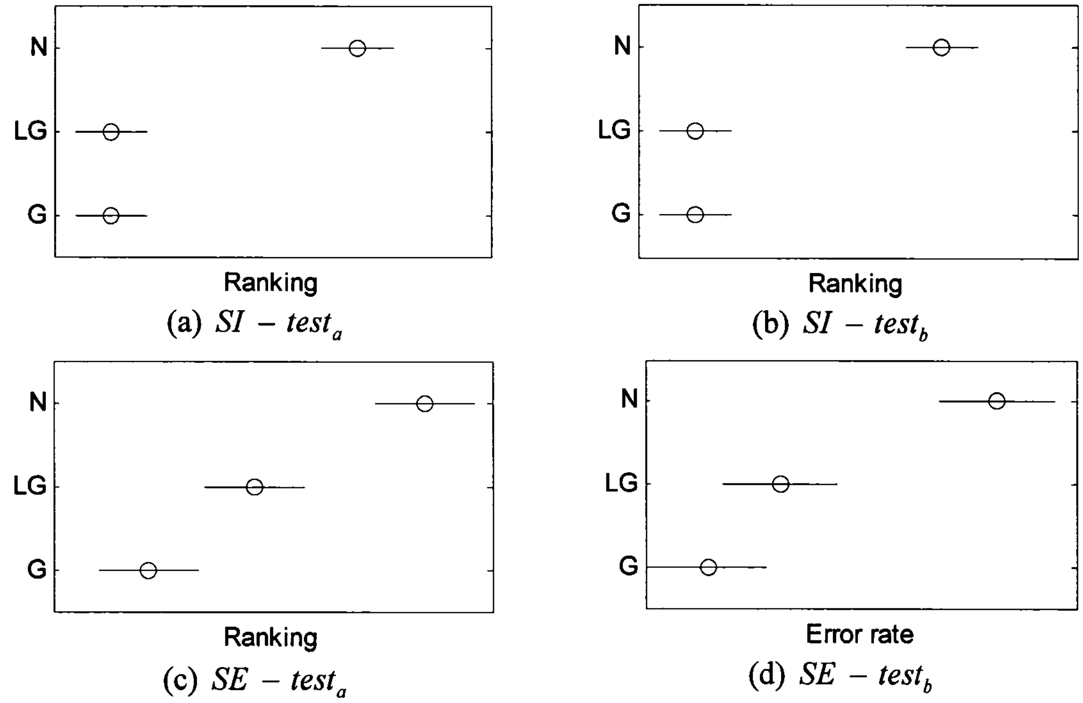

(a) $SI - test_a$

(b) $SI - test_b$

(c) $SE - test_a$

(d) $SE - test_b$

Figure 70 MOMA multiple comparison results for the validation strategies in each optimization problem with the PD classifier and the divider zoning operator – strategies tested are: no validation (N), validation at the last generation (LG) and global validation (G)

the best results are obtained when using RS_{IFE} optimized by MOMA, as solution SE optimized by NSGA-II is not even significantly different from SI. When using RS_{IFE} obtained with MOMA to optimize EoCs (SE for MOMA and SE' for NSGA-II),there is no significant difference in the accuracy obtained with both algorithms.

With these results, it is concluded that when considering EoC optimization, MOMA is better to optimize the IFE in order to create a more diverse set RS_{IFE}. If the target is a single classifier based system, then NSGA-II is better as it requires less processing time. To optimize EoCs the results indicate that NSGA-II is better for its smaller processing time.

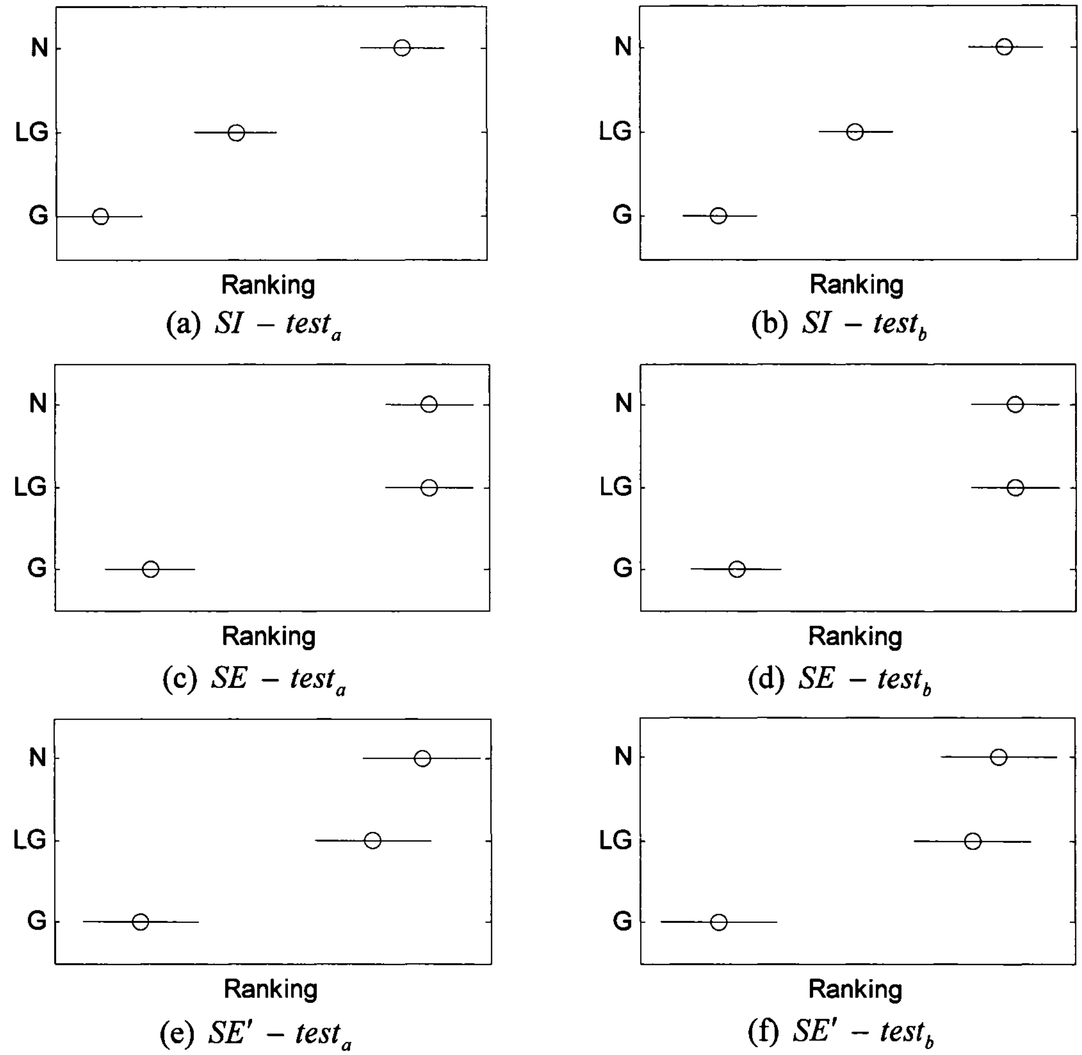

(a) *SI* – $test_a$

(b) *SI* – $test_b$

(c) *SE* – $test_a$

(d) *SE* – $test_b$

(e) *SE'* – $test_a$

(f) *SE'* – $test_b$

Figure 71 NSGA-II multiple comparison results for the validation strategies in each optimization problem with the PD classifier and the divider zoning operator – strategies tested are: no validation (N), validation at the last generation (LG) and global validation (G)

2.1.2 Divider Zoning Operator and MLP classifier

As with the PD classifier, the first test verifies the impact of validation strategies. Results are detailed in Figs. 73 and 74, for the MOMA and NSGA-II optimization

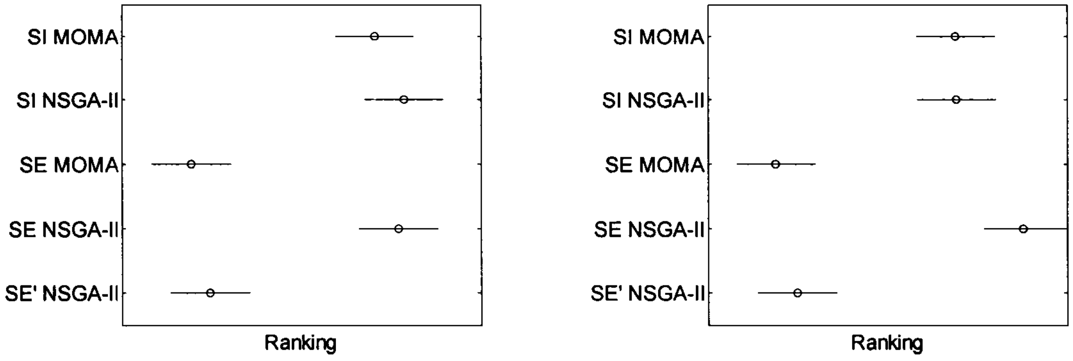

(a) $test_a$ (b) $test_b$

Figure 72 PD classification system optimization approaches multiple comparison using global validation and the divider zoning operator

algorithms respectively. Again, there is no relevant difference between validation at the last generation and global validation when using $max_{S'} = 5$ with MOMA to optimize the IFE. This statement is supported by Figs. 73.a and 73.b. The same parameter is used to optimize EoCs, but unlike PD EoCs, both validation at the last generation and global validation are not significantly different when optimizing MLP EoCs. As the impact of over-fit is not known *a priori*, it is safer to use the global validation strategy.

These tests are also performed with the NSGA-II, to verify the impact of validation strategies on all optimization problems. The results in Fig. 74 are similar to those obtained with the PD classifier in the previous section. Again, NSGA-II provides better results when using the global validation strategy.

Results with the MLP classifier indicate that the global validation is also the most performing validation strategy. Next, algorithms are tested to verify which is better for each optimization stage using global validation. Results for this test are presented in Fig. 75. It is verified for both test data sets ($test_a$ and $test_b$) that MOMA and NSGA-II are not significantly different to optimize the IFE, thus either algorithm may be used when

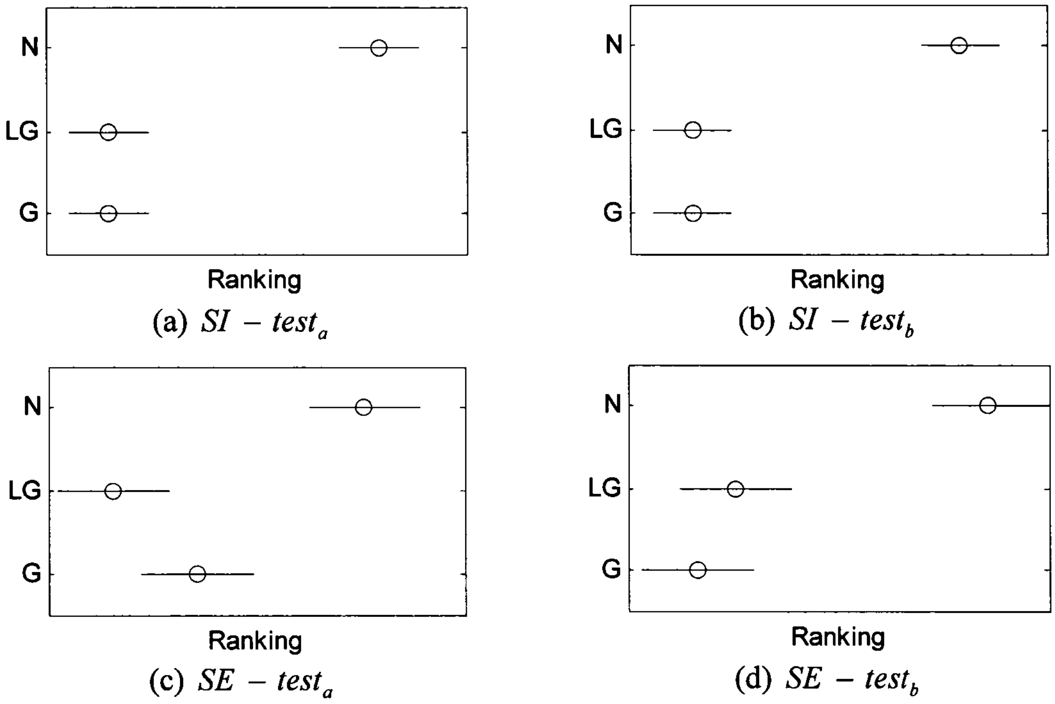

(a) $SI - test_a$

(b) $SI - test_b$

(c) $SE - test_a$

(d) $SE - test_b$

Figure 73 MOMA multiple comparison results for the validation strategies in each optimization problem with the MLP classifier and the divider zoning operator – strategies tested are: no validation (N), validation at the last generation (LG) and global validation (G)

the target is a single classifier based system. As for EoCs, the best results are obtained when using RS_{IFE} optimized by MOMA and the NSGA-II algorithm. When using RS_{IFE} obtained with MOMA to optimize EoCs (SE for MOMA and SE' for NSGA-II),there is no significant difference in the accuracy obtained with both algorithms.

Similar to the results obtained with the PD classifiers, these results also indicate that MOMA is better to optimize the IFE if the goal is EoC optimization (to create a more diverse set RS_{IFE}). If the target is a single classifier based system, then NSGA-II is better as it requires less processing time. To optimize EoCs, the results discussed in this section also indicate that NSGA-II using RS_{IFE} optimized by MOMA is better for its smaller processing time.

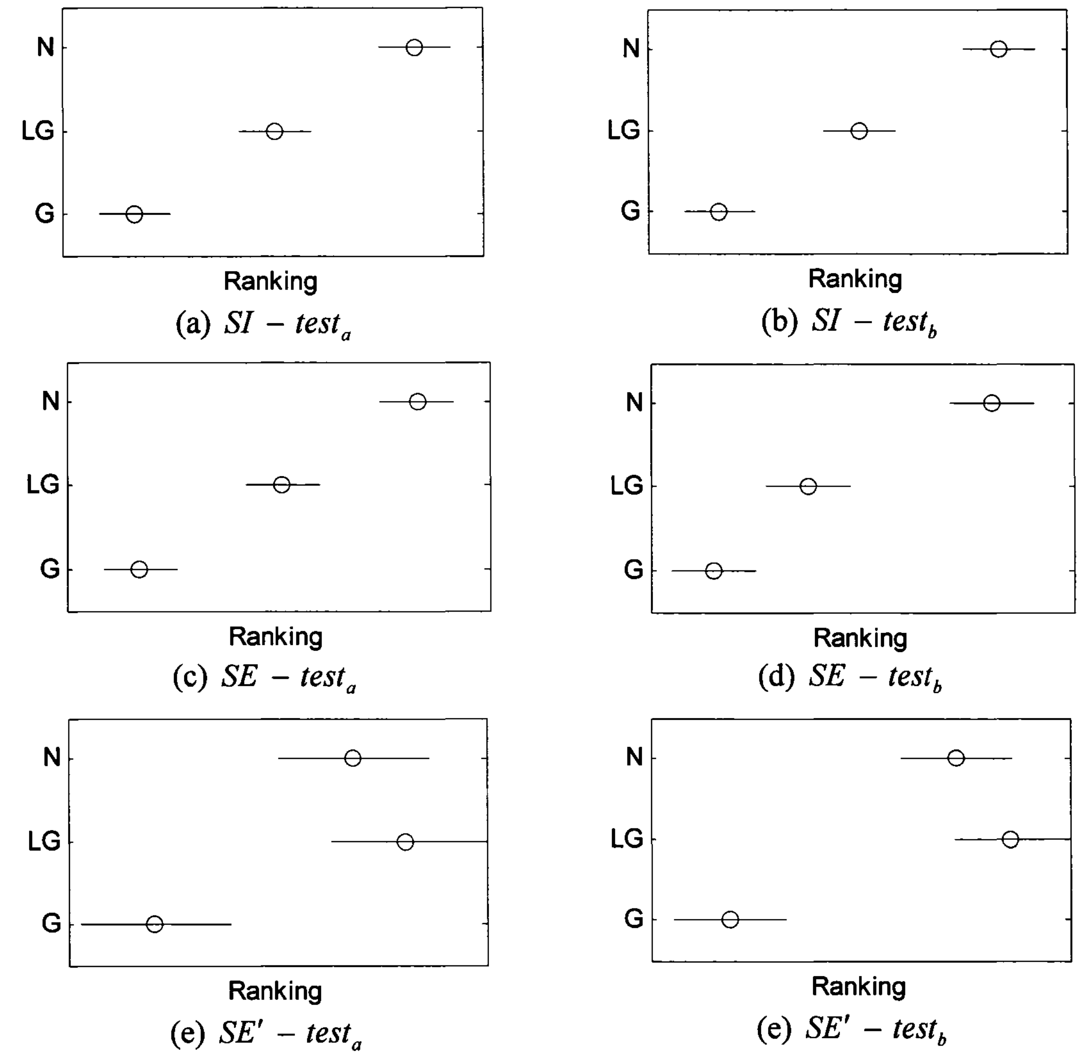

(a) *SI* – *test*$_a$

(b) *SI* – *test*$_b$

(c) *SE* – *test*$_a$

(d) *SE* – *test*$_b$

(e) *SE'* – *test*$_a$

(e) *SE'* – *test*$_b$

Figure 74 NSGA-II multiple comparison results for the validation strategies in each optimization problem with the MLP classifier and the divider zoning operator – strategies tested are: no validation (N), validation at the last generation (LG) and global validation (G)

2.1.3 Hierarchical Zoning Operator and PD Classifier

All experiments discussed in the two previous sections are repeated once again for the hierarchical zoning operator. To compare validation strategies, the first multiple

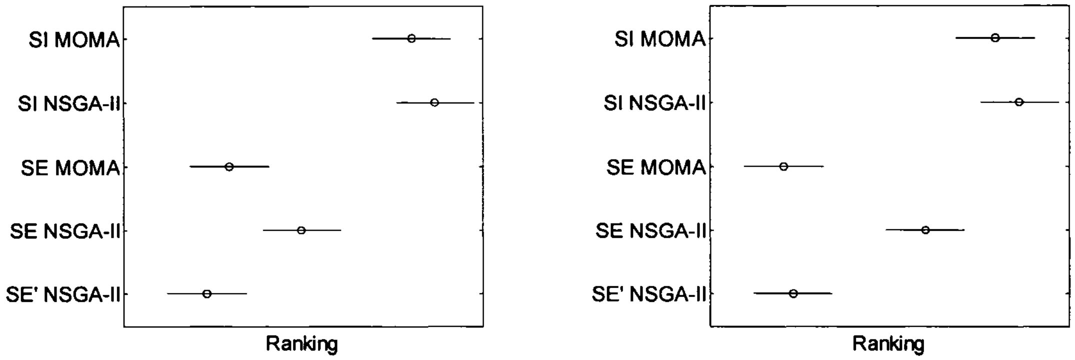

Figure 75 MLP classification system optimization approaches multiple comparison using global validation and the divider zoning operator

comparison test verifies their impact and results are detailed in Figs. 76 and 77, for the MOMA and NSGA-II optimization algorithms respectively. Again, when using $max_{S^l} = 5$ with MOMA to optimize the IFE, there is no relevant difference between validation at the last generation and global validation, as indicated in Figs. 70.a and 70.b. However, unlike in previous comparisons, solutions selected with all validation strategies are the same. The same happens to NSGA-II, thus it can be said that the proposed hierarchical zoning operator is not affected by over-fit. However, when optimizing EoCs it is observed that validation strategies produces different outcomes regarding $test_a$ in Figs. 76.c and Figure 77.c. In both situations global validation produced the most significantly different results. Thus, as the impact of over-fit is unknown on each unknown problem, the global validation strategy is the best approach as it is able to select good solutions in all situations.

Comparing optimization algorithms in Fig. 78 with global validation further confirms the conclusions in the previous section. MOMA and NSGA-II have the same performance to optimize the IFE, thus, for single classifier approaches the NSGA-II is the best choice for its lower processing time. Considering EoCs, it is observed again that

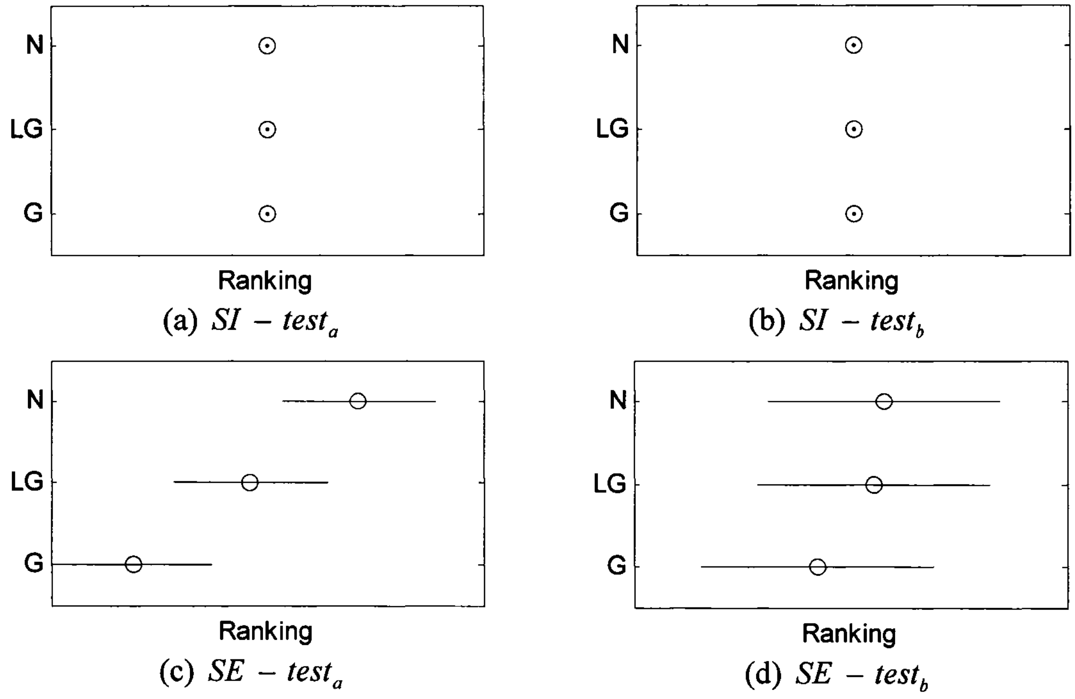

(a) $SI - test_a$

(b) $SI - test_b$

(c) $SE - test_a$

(d) $SE - test_b$

Figure 76 MOMA multiple comparison results for the validation strategies in each optimization problem with the PD classifier and the hierarchical zoning operator – Strategies tested are: no validation (N), validation at the last generation (LG) and global validation (G)

SE' optimized by NSGA-II using RS_{IFE} obtained with MOMA is the best choice. Its performance surpasses that of SE optimized by NSGA-II and is equivalent to SE optimized by MOMA, which requires more processing time. Thus, for EoC based approaches the most performing configuration is to use MOMA top optimize IFE and NSGA-II to select the best EoC configuration.

2.1.4 Hierarchical Zoning Operator and MLP classifier

Results obtained with the MLP classifier are similar to those obtained in the previous section with the PD classifier. Figure 79 details the validation strategy comparison results obtained with MOMA, whereas Fig. 80 does the same for NSGA-II. With both

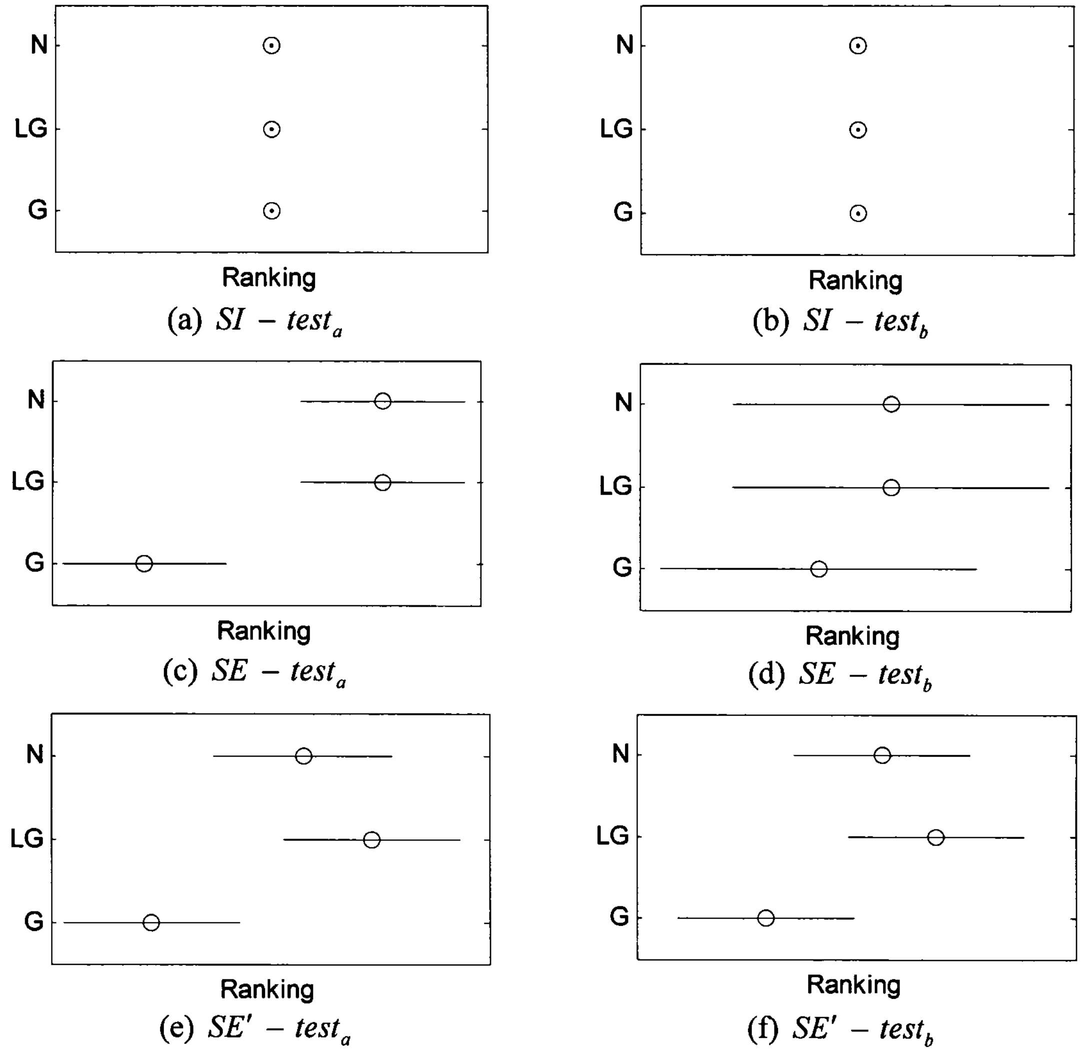

(a) $SI - test_a$

(b) $SI - test_b$

(c) $SE - test_a$

(d) $SE - test_b$

(e) $SE' - test_a$

(f) $SE' - test_b$

Figure 77 NSGA-II multiple comparison results for the validation strategies in each optimization problem with the PD classifier and the hierarchical zoning operator – strategies tested are: no validation (N), validation at the last generation (LG) and global validation (G)

optimization algorithms, the single best classifier SI selected from RS_{IFE} is the same, regardless of the validation strategy used. Thus, over-fit was not an issue to optimize the IFE using the hierarchical zoning operator. On the other hand, EoC optimization is different. With MOMA, Figures 79.b and 79.d indicate that global validation and validation at the last generation are significantly different from no validation. As in other

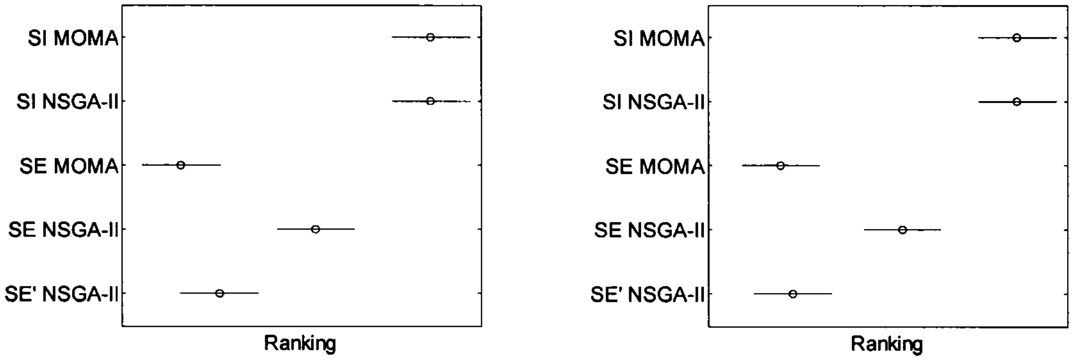

(a) $test_a$ (b) $test_b$

Figure 78 PD classification system optimization approaches multiple comparison using global validation and the hierarchical zoning operator

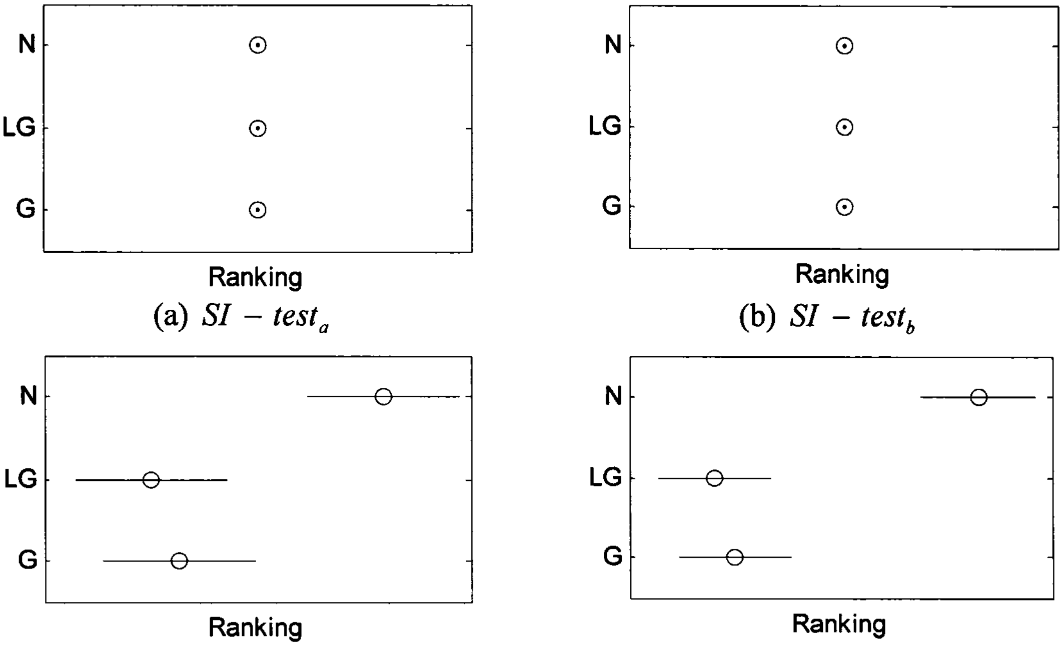

(a) $SI - test_a$ (b) $SI - test_b$

(c) $SE - test_a$ (d) $SE - test_b$

Figure 79 MOMA multiple comparison results for the validation strategies in each optimization problem with the MLP classifier and the hierarchical zoning operator – strategies tested are: no validation (N), validation at the last generation (LG) and global validation (G)

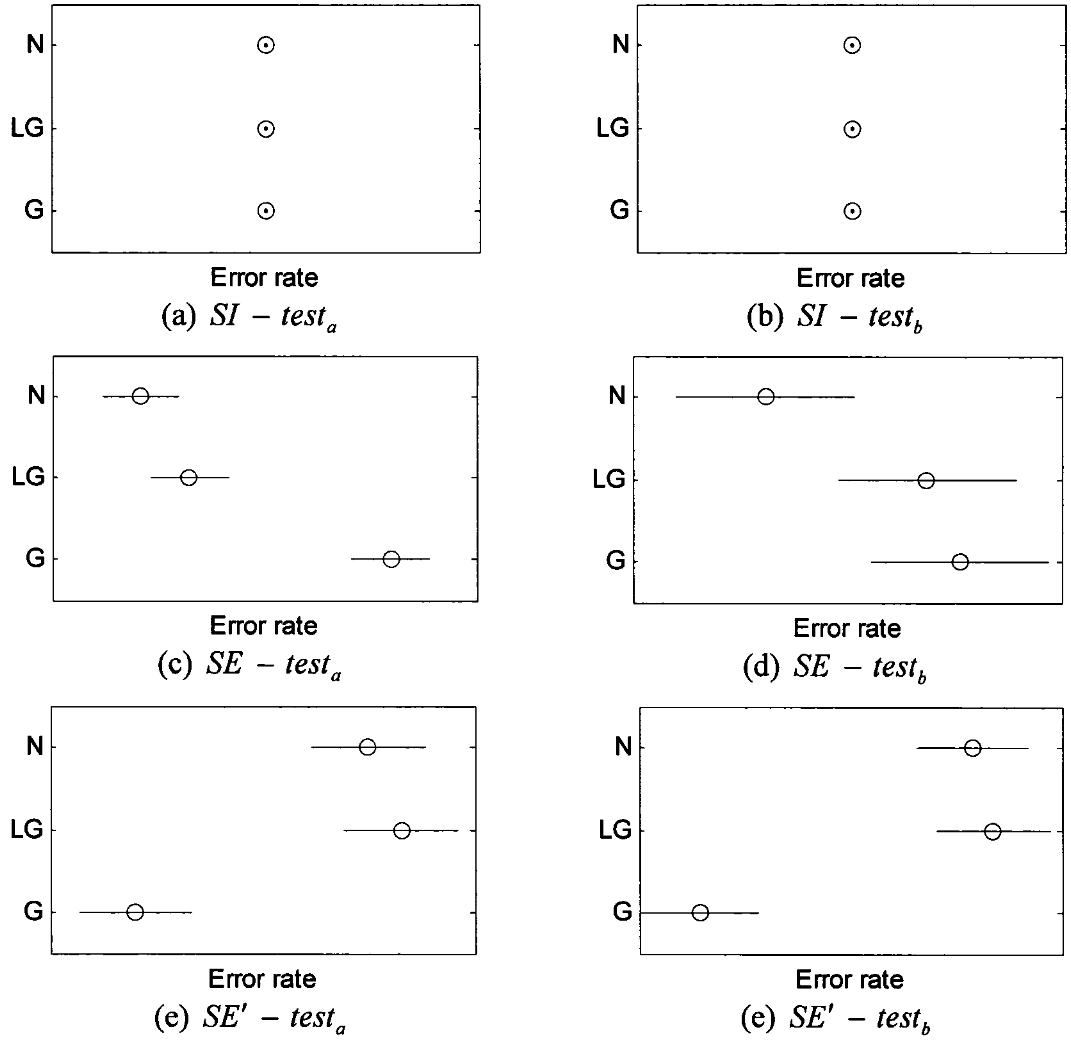

(a) $SI - test_a$

(b) $SI - test_b$

(c) $SE - test_a$

(d) $SE - test_b$

(e) $SE' - test_a$

(e) $SE' - test_b$

Figure 80 NSGA-II multiple comparison results for the validation strategies in each optimization problem with the MLP classifier and the hierarchical zoning operator – strategies tested are: no validation (N), validation at the last generation (LG) and global validation (G)

situations, validation at the last generation has similar performance to global validation, and both strategies perform significantly better than no validation. Both global validation and validation at the last generation are not significantly different because of the archive defined in MOMA. Other $max_{S'}$ values may produce different results, therefore it is better to use global validation. Considering EoCs optimized by NSGA-II in Fig. 80 (SE and SE'), it is observed that for SE' the validation strategies play an important role, and that global validation produces better results.

Comparing algorithms in Fig. 81 yields similar results to those in previous sections. NSGA-II produces results to MOMA with the IFE, thus it is preferable to use it when a single classifier approach is targeted. As for EoCs, NSGA-II and MOMA provide comparable results when using the same IFE solution set RS_{IFE} produced by MOMA.

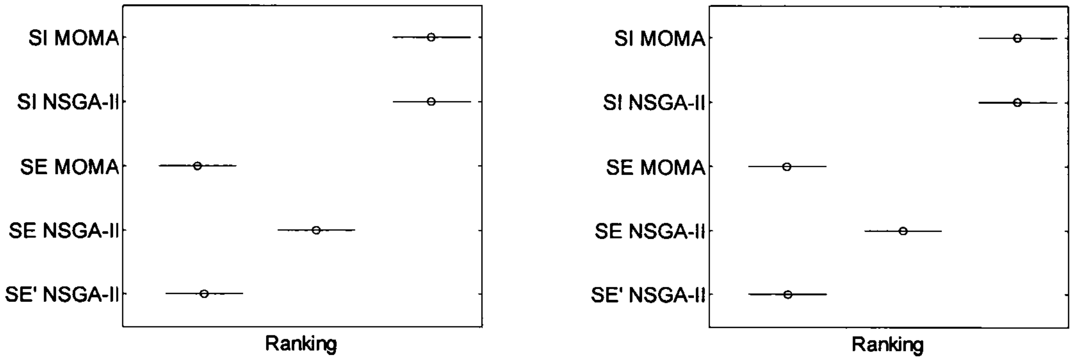

(a) $test_a$ (b) $test_b$

Figure 81 MLP classification system optimization approaches multiple comparison using global validation and the hierarchical zoning operator

Again, when targeting EoC based classification systems it is better to use MOMA to optimize the IFE to have a higher solution diversity, and NSGA-II for its reduced processing time.

2.2 Handwritten Uppercase Letters

The tests in Section 2.1 indicated the best configuration to optimize classification systems, thus this section compare results obtained with handwritten uppercase letters with this configuration. Results detailed in Fig. 82 demonstrate the improvement

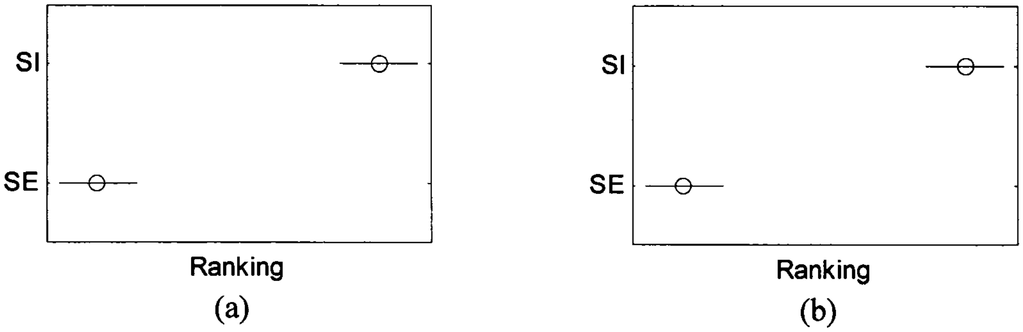

Figure 82 Uppercase letters multiple comparison for PD (a) and MLP (b) classification system optimization, error rates measured on the *test* data set

obtained when optimizing an EoC *SE* in comparison to the best single classifier *SI* selected. The tests confirmed that optimizing an EoC improves results with both classifiers.

APPENDIX 3

Rejection strategies

Given an unknown observation x, a classifier tries to determine to which class C_i the observation x belongs to. The classification procedure calculates for each known class C_i the posterior probability $\hat{P}(C_i \mid x)$, indicating the probability that x belongs to C_i. One strategy to reduce classification error is to reject observations that are likely to be misclassified, so that they can be handled by more efficient means, such as human verification.

Fumera proposed in [92] a method for classifier rejection using multiple thresholds based on posterior probabilities. The MLP classifier outputs posterior probabilities for each class, and the same applies to MLP EoCs. However, the PD classifier outputs distances to hyper planes for each class C_i, whereas the PD EoC outputs vote counts. Thus, the first step to apply rejection is to have all classifiers outputs converted to posterior probabilities for each class. This section first describes how the PD classifier outputs (single classifier and EoC) are converted to posterior probabilities, describing next Fumera's method with multiple thresholds for rejection.

3.1 PD Classifier

The PD classifier outputs for each class a distance to a hyperplane. Thus, a rejection strategy must first calculate the posterior probabilities to establish thresholds for rejection. One commonly used function to create posterior probabilities for a classifier as the PD is the *softmax* function. This neural transfer function converts the distance values to values between 0 and 1 that sum up to 1.

For an unknown observation x, the distance $d_i(x)$ to the hyper plane associated to class C_i (with n classes), the estimate of the posterior probability $\hat{P}(C_i \mid x)$ of x belonging to class C_i is calculated as in (3.1).

$$\hat{P}(C_i \mid x) = \frac{e^{d_i(x)}}{\sum_{j=1}^{n} e^{d_j(x)}}, \qquad (3.1)$$

Hensen's method [104] is used to calculate posterior probabilities from PD EoC votes. Given a PD EoC with N classifiers, the unknown observation x and $v(i \mid x)$ the vote number for class C_i, we have that the estimate of the posterior probability $\hat{P}(C_i \mid x)$ for PD EoCs is calculated as

$$\hat{P}(C_i \mid x) = \frac{v(I(x) \mid x)}{N}, \qquad (3.2)$$

where $I(x)$ is calculated as

$$I(x) = \arg \max_{j=1}^{n} v(i \mid x). \qquad (3.3)$$

3.2 Rejection With Multiple Thresholds

For a classification problem with n classes, the classifier will select the class C_i the observation x belongs to as the highest posterior probability $\hat{P}(C_i \mid x)$. A traditional single threshold rejection strategy [105] will reject observation x if

$$\max_{j=1}^{n} \hat{P}(C_j \mid x) = \hat{P}(C_i \mid x) < T, \qquad (3.4)$$

and it will accept observation x if

$$\max_{j=1}^{n} \hat{P}(C_j \mid x) = \hat{P}(C_i \mid x) \geq T, \tag{3.5}$$

where T is the threshold to decide if x is accepted or not after classification.

Fumera demonstrated in [92] that using *class-related thresholds* (CRT) yields higher accuracies than using a single threshold T. With the CRT, observation x will be rejected if

$$\max_{j=1}^{n} \hat{P}(C_j \mid x) = \hat{P}(C_i \mid x) < T_i, \tag{3.6}$$

and it will be accepted if

$$\max_{j=1}^{n} \hat{P}(C_j \mid x) = \hat{P}(C_i \mid x) \geq T_i. \tag{3.7}$$

An iterative process is used to calculate the threshold T_i for each class C_i, based on a desired error rate e during the classification stage. This iterative process has to systematically test different T_i values until it finds a threshold that yields the desired error rate e. This process is repeated for each class C_i, until all thresholds are calculated for the classification stage. As the error rate e is used to optimize all thresholds, the overall classification error when all classes are combined is also e. This statement is easily verified for any given data set D with n classes such as that $D = \{X_1, \ldots, X_n\}$, where X_i are the observations belonging to class C_i. For an error rate e, the number of misclassified observations mo is $mo = e|D|$. This can be expanded to $mo = e(|X_1| + \ldots |X_n|)$, which is equivalent to $mo = e|X_1| + \ldots + e|X_n|$. This guarantees that searching for each threshold T_i independently with a fixed error rate e will yield an overall error rate e for the complete data set D.

Algorithm Algorithm 12 details an algorithm version of the iterative process, calculating the threshold T_i for the observation set X_i belonging to all classes C_i. The process requires a threshold increment a to systematically test threshold values. a should be a small value to allow a more accurate calculation to the threshold T_i. The algorithm starts with the threshold $T_i = 0$, accepting all $\hat{P}(C_i \mid x)$. It then increments its value until it achieves the desired error rate e and stopping the procedure.

Algorithm 12: Algorithm used to calculate the rejection thresholds given the desired error rate e

```
**Data**: desired error rate $e$, threshold increment $a$, data set $D$
**Result** : The thresholds $T_1, \ldots, T_n$
$\forall i \in F, d' = 0$;
**for** $i = 1$ **to** $n$ **do**
        $T_i = 0$;
        **repeat**
                $T_i = T_i + a$;
                Calculate $error$, the classification error rate of $X_i$ using the threshold $T_i$;
        **until** $error \geq e$;
**end**
```

During the classification stage, observations are rejected according to (3.6) or accepted if (3.7) is true. This procedure was used in Chapters 6 and 7 to create error-rejection curves and evaluate classifier accuracy with fixed error rates.

BIBLIOGRAPHY

[1] J. H. Holland, Adaptation in Natural and Artificial Systems. MIT Press, 1975.

[2] C. M. Bishop, *Neural Networks for Pattern Recognition.* Oxford University Press, 1995

[3] C. Cortes and V. Vapnik, "Support-vector networks", *Machine Learning*, vol. 20, no. 3, pp. 273–297, 1995.

[4] C. J. C. Burges, "A tutorial on support vector machines for pattern recognition", *Data Mining and Knowledge Discovery*, vol. 2, no. 2, pp. 121–167, 1998.

[5] T. G. Dietterich, "Ensemble Learning", in *The Handbook of Brain Theory and Neural Networks*, 2nd ed., M. A. Arbib, Ed. MIT Press, 2002.

[6] J. Kittler, M. Hatef, R. P. W. Duin, and J. Matas, "On combining classifiers", *IEEE Transactions on Pattern Analysis and Machine Intelligence*, vol. 20, no. 3, pp. 226–239, 1998.

[7] A. Lemieux, C. Gagné, and M. Parizeau, "Genetical Engineering of Handwriting Representation", in *Proceedings of the Eigth International Workshop on Frontiers in Handwriting Recognition – IWFHR-8*. Ontario, Canada: IEEE Computer Society, 2002, pp. 145–150.

[8] A. Teredesai, J. Park, and V. Govindaraju, "Active Handwritten Character Recognition using Genetic Programming", in *Proceedings of the European Conference on Genetic Programming – EuroGP*, 2001, pp. 371–380.

[9] C. Emmanouilidis, A. Hunter, and J. MacIntyre, "A multiobjective evolutionary setting for feature selection and a commonality-based crossover operator", in *Proceedings of the 2000 Congress on Evolutionary Computation – CEC00*, California, USA, IEEE Press, 2000, pp. 309–316.

[10] L. S. Oliveira, R. Sabourin, F. Bortolozzi, and C. Y. Suen, "A Methodology for Feature Selection Using Multi-Objective Genetic Algorithms for Handwritten DigitString Recognition", *International Journal of Pattern Recognition and Artificial Intelligence*, vol. 17, no. 6, pp. 903–929, 2003.

[11] D. Ruta and B. Gabrys, "Classifier Selection for Majority Voting", *Information Fusion*, vol. 6, pp. 63–81, 2005.

[12] L. I. Kuncheva and L. C. Jain, “Design classifier fusion systems by genetic algorithms”, *IEEE Transactions on Evolutionary Computation*, vol. 4, no. 4, pp. 327–336, 2000.

[13] G. Tremblay, R. Sabourin, and P. Maupin, “Optimizing nearest neighbour in random subspaces using a multi-objective genetic algorithm”, in *17th International Conference on Pattern Recognition – ICPR2004*, Cambridge, U.K.: IEEE Computer Society, August 2004, pp. 208–211.

[14] S. D. Bay, “Combining nearest neighbor classifiers through multiple feature subsets”, in *Proc. 15th International Conf. on Machine Learning*, Morgan Kaufmann, San Francisco, CA, 1998, pp. 37–45.

[15] T. K. Ho, “Nearest neighbors in random subspaces”, in *Proceedings of the 2nd Int'l Workshop on Statistical Techniques in Pattern Recognition*, Sydney, Australia, August 1998, pp. 640–648.

[16] P. J. Grother, NIST Special Database 19 – Handprinted forms and characters database, National Institute of Standards and Technoloy NIST, 1995, database, CD documentation.

[17] P. V. W. Radtke, L. S. Oliveira, R. Sabourin, and T. Wong, “Intelligent Zoning Design Using Multi-Objective Evolutionary Algorithms”, in *Proceedings of the 7th International Conference on Document Analysis and Recognition – ICDAR2003*. Edinburg, Scotland: IEEE Computer Society, August 2003, pp. 824–828.

[18] P. V.W. Radtke, T.Wong, and R. Sabourin, “A Multi-Objective Memetic Algorithm for Intelligent Feature Extraction”, in *Proceedings of the Third International Conference on Evolutionary Multi-Criterion Optimization – EMO 2005*. Berlin: Springer-Verlag, 2005, pp. 767–781.

[19] P. V. W. Radtke, R. Sabourin, and T. Wong, “Intelligent feature extraction for ensemble of classifiers”, in *Proceedings of the 8th International Conference on Document Analysis and Recognition – ICDAR 2005*. IEEE Computer Society, 2005, pp. 866–870.

[20] P. V. W. Radtke, T. Wong, and R. Sabourin, “Classification system optimization with multi-objective genetic algorithms”, in *Proceedings of the 10th International Workshop on Frontiers in Handwriten Recognition – IWFHR 2006*. IAPR, 2006, *in press*.

[21] P. V. W. Radtke, T. Wong, and R. Sabourin, "An evaluation of over-fit control strategies for multi-objective evolutionary optimization", in *Proceedings of the International Joint Conference on Neural Networks – IJCNN 2006*.IEEE Computer Society, 6359–6366, 2006.

[22] Øivind Dur Trier, A. K. Jain, and T. Taxt, "Feature Extraction Methods for Character Recognition – A Survey", *Pattern Recognition*, vol. 29, no. 4, pp. 641–662, 1996.

[23] R. R. Bailey and M. Srinath, "Orthogonal Moment Features for use with Parametric and Non-Parametric Classifiers", *IEEE Transactions on Pattern Analysis and Machine Intelligence*, vol. 18, no. 4, pp. 389–399, 1996.

[24] P. D. Gader, "Automatic Feature Generation for Handwritten Digit Recognition", *IEEE Transactions on Pattern Analysis and Machine Intelligence*, vol. 18, no. 12, pp. 1256–1261, 1996.

[25] I.-S. Oh and C. Y. Suen, "Distance features for neural network-based recognition of handwritten characters", *International Journal on Document Analysis and Recognition*, vol. 2, no. 1, pp. 873–885, 1998.

[26] L. Heutte, T. Paquet, J. Moreau, Y. Lecourtier, and C. Olivier, "A structural/statistical feature based vector for handwritten character recognition", *Pattern Recognition Letters*, vol. 19, no. 7, pp. 629–641, 1998.

[27] V. di Lecce, G. Dimauro, A. Guerriero, S. Impedovo, G. Pirlo, and A. Salzo, "Zoning Design for Hand-Written Numeral Recognition", in *Proceedings of the Seventh International workshop on Frontiers in Handwriting Recognition – IWFHR-7*, 2000, pp. 583–588.

[28] R. Sabourin, M. Cheriet, and G. Genest, "An Extended-Shadow-Code Based Approach for Off-Line Signature Verification", in *Proceedings of The Second IAPR Conf. on Document Analysis and Recognition*, Tsukuba, Japan, 1993, pp. 1–5.

[29] R. Sabourin, G. Genest, and F. J. Prêteux, "Off-line signature verification by local granulometric size distributions", *IEEE Transactions on Pattern Analysis and Machine Intelligence*, vol. 19, no. 9, pp. 976–988, 1997.

[30] L. S. Oliveira, R. Sabourin, F. Bortolozzi, and C. Y. Suen, "Feature Selection Using Multi-Objective Genetic Algorithms for Handwritten Digit Recognition", in *Proceedings of the 16th IAPR International Conference on Pattern Recognition*. IEEE Computer Society, 2002, pp. 568–571.

[31] G. F. Houle, D. B. Aragon, R. W. Smith, M. Shridhar, and D. Kimura, "Multi-Layered Corroboration-Based Check Reader", in *Proceedings of The International Association for Pattern Recognition Workshop on Document Analysis Systems – DAS'96*, 1996, pp. 495–546.

[32] Z.-C. Li and C. Y. Suen, "The partition-combination method for recognition of handwritten characters", *Pattern Recognition Letters*, vol. 21, no. 8, pp. 701–720, 2000.

[33] A. L. Koerich, "Large Vocabulary Off-Line HandwrittenWord Recognition", Ph.D. dissertation, École de Technologie Supérieure – ETS – Université du Québec, Montreal, Québec, Canada, 2002.

[34] C.-L. Liu, H. Sako, and H. Fujisawa, "Performance evaluation of pattern classifiers for handwritten character recognition", *International Journal on Document Analysis and Recognition*, vol. 3, no. 4, pp. 191–204, 2002.

[35] M. Kudo and J. Sklansky, "Comparison of algorithms that select features for pattern classifiers", *Pattern Recognition*, vol. 33, no. 1, pp. 25–41, 2000.

[36] A. W. Whitney, "A Direct Method of Non-Parametric Measurement Selection, *IEEE Transactions on Computers*, vol. 20, no. 9, pp. 1100–1103, 1971.

[37] P. Pudil, J. Novovicova;, and J. Kittler, "Floating search methods in feature selection", *Pattern Recogn. Letters*, vol. 15, no. 11, pp. 1119–1125, 1994.

[38] P. Narendra and K. Fukunaga, "A branch and bound algorithm for feature subset selection", *IEEE Transactions on Computers*, vol. 26, no. 9, pp. 1917–1922, 1977.

[39] D. E. Goldberg, *Genetic Algorithms in Search, Optimization and Machine Learning. New York*, NY, USA: Addison Wesley, 1989.

[40] H. Yuan, S.-S. Tseng,W. Gangshan, and Z. Fuyan, "A Two-phase Feature Selection Method using both Filter and Wrapper", in *Proceedings of the IEEE International Conference on Systems, Man and Cybernetics – SMC'99*, vol. 2, 1999, pp. 132–136.

[41] L. Breiman, "Bagging predictors", *Machine Learning*, vol. 24, no. 2, pp. 123–140, 1996.

[42] R. Schapire, *The boosting approach to machine learning: An overview*, 2001. [Online]. Available: http://www.research.att.com/ schapire/boost.html

[43] L. S. Oliveira, R. Sabourin, F. Bortolozzi, and C. Y. Suen, “A methodology for feature selection using multi-objective genetic algorithms for handwritten digit string recognition”, *International Journal of Pattern Recognition and Artificial Intelligence – IJPRAI*, vol. 17, no. 6, pp. 903–929, 2003.

[44] L. S. Oliveira, M. Morita, R. Sabourin, and F. Bortolozzi, “Multi-Objective Genetic Algorithms to Create Ensemble of Classifiers”, in *Proceedings of the Third International Conference on Evolutionary Multi-Criterion Optimization – EMO 2005*. Berlin: Springer-Verlag, 2005, pp. 592–606.

[45] L. S. Oliveira, R. Sabourin, F. Bortolozzi, and C. Y. Suen, “Feature selection for ensembles : A hierarchical multi-objective genetic algorithm approach”, in *Proceedings of the 7th International Conference on Document Analysis and Recognition – ICDAR2003*, Edinburg, Scotland, August 2003, pp. 676–680.

[46] J. Reunanen, “Overfitting in making comparisons between variable selection methods”, *Journal of Machine Learning Research*, no. 3, pp. 1371–1382, 2003.

[47] J. Loughrey and P. Cunningham, “Overfitting in wrapper-based feature subset selection: The harder you try the worse it gets”, in *Proceedings of International Conference on Innovative Techniques and Applications of Artificial Intelligence*, 2004, pp. 33–43.

[48] J. Loughrey and P. Cunningham , “Using early-stopping to avoid overfitting in wrapper-based feature subset selection employing stochastic search”, Department of Computer Science, Trinity College, Tech. Rep. TCD-CS-2005-37, 2005.

[49] X. Llorà, D. Goldberg, I. Traus, and E. B. i Mansilla, “Accuracy, parsimony, and generality in evolutionary learning systems via multiobjective selection”, in *International Workshop in Learning Classifier Systems*, 2002, pp. 118–142.

[50] E. B. i Mansilla, X. Llorà, and I. Traus, “Multiobjective learning classifier systems”, *Studies in Computational Intelligence*, vol. 16, pp. 261–288, 2006.

[51] L. S. Oliveira, R. Sabourin, F. Bortolozzi, and C. Y. Suen, “Automatic Recognition of Handwritten Numerical Strings: A Recognition and Verification Strategy”, *IEEE Trans. on Pattern Analysis and Machine Intelligence*, vol. 24, no. 11, pp. 1438–1454, 2002.

[52] S. Bandyopadhyay, S. K. Pal, and B. Aruna, “Multiobjective GAs, Quantitative Indices, and Pattern Classification”, *IEEE Transactions on System, Man, and Cybernetics – Part B: Cybernetics*, vol. 34, no. 5, pp. 2088–2099, 2004.

[53] K. Deb, *Multi-Objective Optimization using Evolutionary Algorithms*. Baffins Lane, Chichester, West Sussex, PO19 1UD ,England: John Wiley & Sons, LTD, 2001.

[54] J. D. Schaffer, "Multiple objective optimization with vector evaluated genetic algorithms", in *Proceedings of the First International Conference on Genetic Algorithms – ICGA*, J. J. Grefenstette, Ed. Lawrence Erlbaum Associates, 1985, pp. 93–100.

[55] C. A. C. Coello, "Evolutionary multi-objective optimization: a historical view of the field", *IEEE Computational Intelligence Magazine*, vol. 1, no. 1, pp. 28–36, 2006.

[56] N. Srinivas and K. Deb, "Multiobjective optimization using nondominated sorting in genetic algorithms", *Evolutionary Computation*, vol. 2, no. 3, pp. 221–248, 1994.

[57] K. Deb and T. Goel, "Controlled elitist non-dominated sorting genetic algorithms for better convergence", in *Proceedings of the First International Conference on Evolutionary Multi-Criterion Optimization – EMO 2001*, E. Zitzler, K. Deb, L. Thiele, C. A. C. Coello, and D. Corne, Eds. Berlin: Springer-Verlag, 2001, pp. 67–81.

[58] E. Zitzler, M. Laumanns, and L. Thiele, "SPEA2: Improving the strength pareto evolutionary algorithm for multiobjective optimization", in *Evolutionary Methods for Design Optimization and Control with Applications to Industrial Problems*, K. C. Giannakoglou, D. T. Tsahalis, J. PÈriaux, K. D. Papailiou, and T. Fogarty, Eds. Athens, Greece: International Center for Numerical Methods in Engineering – Cmine, 2001, pp. 95–100.

[59] W. M. Spears, *The role of mutation and recombination in evolutionary algorithms*, Ph.D. dissertation, George Mason University, Fairfax, Virginia, USA, 1998.

[60] H. Ishibuchi and K. Narukawa, "Recombination of Similar Parents in EMO Algorithms", in *Proceedings of the Third International Conference on Evolutionary Multi-Criterion Optimization – EMO 2005*. Berlin: Springer-Verlag, 2005, pp. 265–279.

[61] D. A. V. Veldhuizen and G. B. Lamont, "Multiobjective Evolutionary Algorithms: Analyzing the State-of-the-Art", *IEEE Transactions on Evolutionary Computation*, vol. 2, no. 8, pp. 125–147, 2000.

[62] E. Zitzler, K. Deb, and L. Thiele, "Comparison of Multiobjective Evolutionary Algorithms: Empirical Results", *Evolutionary Computation Journal*, vol. 2, no. 8, pp. 125–148, 2000.

[63] K. Deb, S. Agrawal, A. Pratab, and T. Meyarivan, "A Fast Elitist Non-Dominated Sorting Genetic Algorithm for Multi-Objective Optimization: NSGA-II", in *Proceedings of the Parallel Problem Solving from Nature VI Conference*, Paris, France, 2000, pp. 849–858.

[64] E. Cantú-Paz, *Efficient and Accurate Parallel Genetic Algorithms*. Norwell, Massachussets 02061 USA: Kluwer Academic Publishers, 2000.

[65] Dubreuil, M., Gagné, C., Parizeau, M., "Analysis of a Master-Slave Architecture for Distributed Evolutionary Computations", IEEE Transactions on Systems, Man and Cybernetics, vol. 36, no. 1, pp. 229–235, 2006.

[66] E. Cantú-Paz, "A survey of parallel genetic algorithms", Calculateurs Paralleles, Reseaux et Systems Repartis, vol. 10, no. 2, pp. 141–171, 1998.

[67] T. Hiroyasu, M. Miki, and M. Masaki, "A new model of distributed genetic algorithm for cluster systems: Dual individual DGA", in *Proceedings of High Performance Computing Conference* - Lecture Notes in Computer Science 1940. Springer Verlag, 2000, pp. 374–383.

[68] T. Hiroyasu, M. Miki, and S. Watanabe, "Divided Range Genetic Algorithms in Multiobjective Optimization Problems", in *Proceedings of the International Workshop on Emergent Synthesis – IWES'99*, 1999, pp. 57–66.

[69] Z.-Y. Zhu and K.-S. Leung, "Asynchronous Self-Adjustable Island Genetic Algorithm for Multi-Objective Optimization Problems", in *Proceedings of the Congress on Evolutionary Computation*. IEEE, 2002, pp. 837–842.

[70] F. Streichert, H. Ulmer, and A. Zell, "Parallelization of multi-objective evolutionary algorithms using clustering algorithms", in *Proceedings of the Third International Conference on Evolutionary Multi-Criterion Optimization – EMO 2005*. Berlin: Springer-Verlag, 2005, pp. 92–107.

[71] J. Knowles, "On Metrics for Comparing nondominated Sets", in *Proceedings of the 2002 Conference on Evolutionary Computation – CEC'2002*. Honolulu, Hawaii, USA: IEEE, 2002, pp. 711–716.

[72] E. Zitzler, L. Thiele, M. Laumanns, C. M. Fonseca, and V. G. Fonseca, "Performance Assesment of Multiobjective Optimizers: An Analysis and Review", *IEEE Transactions on Evolutionary Computation*, vol. 7, no. 2, pp. 117–132, 2003.

[73] E. Zitzler, *Evolutionary algorithms for multiobjective optimization: Methods and applications*, Ph.D. dissertation, Swiss Federal Institute of Technology Zurich, 1999.

[74] E. Zitzler and L. Thiele, "Multiobjective Optimization Using Evolutionary Algorithms – A Comparative Case Study", in *Parallel Problem Solving from Nature – PPSVN V.* Springer Verlag, 1998, pp. 292–301.

[75] L. Heutte, J. Moreau, B. Plessis, J. Plagmaud, and Y. Lecourtier, Handwritten numeral recognition based on multiple feature extractors", in *Proceedingss of 2nd ICDAR*, 1993, pp. 167–170.

[76] G. Dimauro, S. Impedovo, G. Pirlo, and A. Salzo, "Zoning design for handwritten numeral recognition", in *ICIA (2)*, 1997, pp. 592–599.

[77] G. H. John, R. Kohavi, and K. Pfleger, "Irrelevant features and the subset selection problem", in *International Conference on Machine Learning*, 1994, pp. 121–129.

[78] K. Chen and H. Liu, "Towards an evolutionary algorithm: A comparison of two feature selection algorithms", in *1999 Congress on Evolutionary Computation*, 1999, pp. 1309–1313.

[79] F. Kimura, S. Inoue, T. Wakabayashi, S. Tsuruoka, and Y. Miyake, "Handwritten Numeral Recognition using Autoassociative Neural Networks", in *Proceedings of the International Conference on Pattern Recognition*, 1998, pp. 152–155.

[80] A. El-Yacoubi, M. Gilloux, R. Sabourin, and C. Y. Suen, "Objective Evaluation of the Discriminant Power of Features in an HMM-basedWord Recognition System", in *Proceedings of the 1997 Brazilian Symposium on Documents and Image Analysis – BSDIA'97*, Curitiba, PR, Brazil, 1997, pp. 60–73.

[81] L. S. Oliveira, N. Benahmed, R. Sabourin, F. Bortolozzi, and C. Y. Suen, "Feature subset selection using genetic algorithms for handwritten digit recognition", in *Proceedings of the 14th Brazilian Symposium on Computer Graphics and Image Processing*. Florianópolis-Brazil: IEEE Computer Society, 2001, pp. 362–369.

[82] J. Moody and J. Utans, “Principled architecture selection for neural networks: Application to corporate bond ratings predictions”, in *Advances in Neural Information Processing Systems*, J. Moody, S. Hanson, and R. P. Lippman, Eds. Morgan Kauffman, 2001, vol. 4, pp. 683–690.

[83] T. Murata, H. Nozawa, Y. Tsujimura, M. Gen, and H. Ishibuchi, “Effect of Local Search on the Performance of Cellular Multi-Objective Genetic Algorithms for Designing Fuzzy Rule-based Classification Systems”, in *Proceedings of the 2002 Conference on Evolutionary Computation - CEC'2002*, 2002, pp. 663–668.

[84] H. Ishibuchi, T. Yoshida, and T. Murata, “Balance Between Genetic Search and Local Search in Memetic Algorithms for Multiobjective Permutation Flowshop Scheduling”, *IEEE Transactions on Evolutionary Computation*, vol. 7, no. 2, pp. 204–223, 2003.

[85] J. D. Knowles and D. Corne, “Memetic algorithms for multiobjective optimization: issues, methods and prospects”, in *Recent Advances in Memetic Algorithms*. Springer Verlag, 2004, pp. 313–352.

[86] N. Krasnogor and J. Smith, “A tutorial for competent memetic algorithms: Model, taxonomy, and design issues”, *IEEE Transactions on Evolutionary Computation*, vol. 9, no. 5, pp. 474–488, 2005.

[87] A. Jaszkiewicz, “Do Multiple-Objective Metaheuristics Deliver on Their Promise? A Computational Experiment on the Set-Covering Problem”, *IEEE Transactions on Evolutionary Computation*, vol. 7, no. 2, pp. 133–143, 2003.

[88] G. Parks, L. Jianping, M. Balazs, and I. Miller, “An Empirical Investigation of Elitism in Multiobjective Genetic Algorithms”, *Foundations of Computing and Decision Sciences*, vol. 26, no. 1, pp. 51–74, 2001.

[89] J. W. Pepper, B. L. Golden, and E. A. Wasil, “Solving the traveling salesman problem with annealing-based heuristics: A computationa study”, *IEEE Trans. On Systems, Mand and Cybernetics – Part A: Systems and Humans*, vol. 32, no. 1, pp. 72–77, 2002.

[90] Ágoston Endre Eiben, R. Hinterdind, and Z. Michalewicz, “Parameter control in evolutionary algorithms”, *IEEE Transactions on Evolutionary Computation*, vol. 3, no. 2, pp. 124–141, 1999.

[91] R. F. Gunst and R. L. Mason, *How to Construct Fractional Factorial Experiments – ASQC basic references on quality control: v. 14*. 611 East Wisconsin Avenue, Milwaukee, Wisconsin 53202, USA: American Society for Quality Control – Statistics Division, 1991.

[92] G. Fumera, F. Roli, and G. Giacinto, "Reject option with multiple thresholds", *Pattern Recoginition*, vol. 33, no. 12, pp. 2099–2101, 2000.

[93] J. Milgram, R. Sabourin, and M. Cheriet, "Estimating posterior probabilities with support vector machines: A case study on isolated handwritten character recognition", submitted to the *IEEE Transactions on Neural Networks*, 2006.

[94] S. E. N. Correia, *Reconhecimento de caracteres manuscritos usando wavelets*, Master dissertation, Campina Grande, Paraíba, Brazil, 2005.

[95] C.-L. Liu and H. Sako, "Class-specific feature polynomial classifier for pattern classification and its application to handwritten numeral recognition", *Pattern Recognition*, vol. 39, no. 4, pp. 669–681, 2006.

[96] G. L. Pappa, A. A. Freitas, and C. A. A. Kaestner, "Multi-objective algorithms for attribute selection in data mining", in *Applications of Multi-Objective Evolutionary Algorithms*, C. C. Coello and G. Lamont, Eds. World Scientific, December 2004, pp. 603–626.

[97] F. Schlotmann, A. Mitschele, and D. Seese, "A Multi-Objective Approach to Integrated Risk Management", in *Proceedings of the Third International Conference on Evolutionary Multi-Criterion Optimization – EMO 2005*. Berlin: Springer-Verlag, 2005, pp. 692–706.

[98] B. de la Iglesia, A. Reynolds, and V. J. Rayward-Smith, "Developments on a Multi-objective Metaheuristic (MOMH) Algorithm for Finding Interesting Sets of Classification Rules", in *Proceedings of the Third International Conference on Evolutionary Multi-Criterion Optimization – EMO 2005*. Berlin: Springer-Verlag, 2005, pp. 826–840.

[99] R. O. Day and G. B. Lamont, "Extended Multi-objective fast messy Genetic Algorithm Solving Deception Problems", in P*roceedings of the Third International Conference on Evolutionary Multi-Criterion Optimization – EMO 2005*. Berlin: Springer-Verlag, 2005, pp. 296–310.

[100] L. Jourdan, D. Corne, D. Savic, and G. Walters, "Preliminary Investigation of the 'Learnale Evolution Model' for Faster/Better Multiobjective Water Systems Design", in *Proceedings of the Third International Conference on Evolutionary Multi-Criterion Optimization – EMO 2005*. Berlin: Springer-Verlag, 2005, pp. 841–855.

[101] Y. Nojima, K. Narukawa, S. Kaige, and H. Ishibuchi, "Effects of Removing Overlapping Solutions on the Performance of the NSGA-II Algorithm", in *Proceedings of the Third International Conference on Evolutionary Multi-Criterion Optimization – EMO 2005*. Berlin: Springer-Verlag, 2005, pp. 341–354.

[102] J. B. Kollat and P. M. Reed, "The Value of Online Adaptative Search: A Performance Comparison of NSGA-II, ε-NSGA-II and ε-MOEA", in *Proceedings of the Third International Conference on Evolutionary Multi-Criterion Optimization – EMO 2005*. Berlin: Springer-Verlag, 2005, pp. 386–398.

[103] D. Greiner, G. Winter, J. M. Emperador, and B. Galván, "Gray Coding in Evolutionary Multicriteria optimization: Application in Frame Structural Optimum Design", in *Proceedings of the Third International Conference on Evolutionary Multi-Criterion Optimization – EMO 2005*. Berlin: Springer-Verlag, 2005, pp. 576–591.

[104] L. K. Hensen, C. Liisberg, and P. Salamon, "The error-reject tradeoff", *Open Systems & Information Dynamics*, vol. 4, no. 2, pp. 159–184, 1997.

[105] C. K. Chow, "On optimium error and reject tradeoff", *IEEE Transactions on Information Theory*, vol. 16, no. 1, pp. 41–46, 1970.